

AUS Repository

Polyaniline-based flexible implantable electrodes for neural sensing/stimulation applications

Item Type	Thesis
Authors	Almufleh, Nader Lutfi
Download date	2026-06-08 03:05:49
Link to Item	http://hdl.handle.net/11073/21499

POLYANILINE-BASED FLEXIBLE IMPLANTABLE ELECTRODES FOR
NEURAL SENSING/STIMULATION APPLICATIONS

by
Nader Lutfi Almufleh

A Thesis Presented to the Faculty of the
American University of Sharjah
College of Engineering
In Partial Fulfillment
for the Degree of

Master of Science in
Biomedical Engineering

Sharjah, United Arab Emirates
March 2021

Declaration of Authorship

I declare that this thesis is my own work and, to the best of my knowledge and belief, it does not contain material published or written by a third party, except where permission has been obtained and/or appropriately cited through full and accurate referencing.

Signed..... Nader Lutfi Nader Almufleh

Date.....13/04/21.....

The Author controls copyright for this report.
Material should not be reused without the consent of the author. Due
acknowledgement should be made where appropriate.

Approval Signatures

We, the undersigned, approve the Master's Thesis of Nader Lutfi Almufleh

Thesis Title: Polyaniline-based flexible implantable electrodes for neural sensing/stimulation applications.

Date of Defense: 18/03/2021

Name, Title and Affiliation

Signature

Dr. Amani Al-Othman
Associate Professor, Department of Chemical Engineering
Thesis Advisor

Dr. Hasan Awad Moh'd Al Nashash
Professor, Department of Electrical Engineering
Thesis Co-Advisor

Dr. Mohammed Hussein Al-Sayah
Professor, Department of Biology, Chemical and Environmental Science
Thesis Co-Advisor

Dr. Yassir Makkawi
Professor, Department of Chemical Engineering
Thesis Committee Member

Dr. Paul Nancarrow
Associate Professor, Department of Chemical Engineering
Thesis Committee Member

Dr. AbdulRahim Shamayleh
Program Coordinator
Biomedical Engineering Program

Dr. Lotfi Romdhane
Associate Dean for Graduate Affairs and Research
College of Engineering

Dr. Sameer Al-Asheh
Interim Dean
College of Engineering

Dr. Mohamed El-Tarhuni
Vice Provost for Graduate Studies
Office of Graduate Studies.

Acknowledgment

I would like to thank my advisors Dr. Al-Othman, Dr. Al-Nashash and Dr. Al-Sayah for providing knowledge, guidance, support, and motivation throughout my research stages. I'm deeply beholden for their great assistance, worthy discussion and suggestions.

I would like to thank the professors of the Engineering department who taught me the master level courses with mighty teaching methods and skills. I am really appreciative of their dignified advices and motivation.

I would also like to thank the American University of Sharjah for granting me the graduate assistantship during my study.

Dedication

To my family...

Abstract

Implantable bioelectrodes have the potential to advance neural sensing and muscle stimulation, mainly in patients with peripheral nerve injuries. The current emerging prostheses rely on the use of conductive and capacitive materials to assist the nerve recovery process, which is often slow. Therefore, implantable electrodes are used to stimulate and restore muscle function after injury. The function of implantable electrodes is to work as an interface between the damaged nerve and the muscle which is controlled by that nerve. There are conventional implantable electrodes that are fabricated from precious metals, such as platinum and gold. Aside from the cost, they have many disadvantages such as high impedance, toughness, and they make damage to the soft tissue. This thesis discusses the fabrication and characterization of novel, low-cost, flexible bioelectrodes based on silicone, and polyaniline (PANI), and polymethyl methacrylate (PMMA) in addition to their combinations. Implantable electrodes were fabricated from variant combinations of these polymers and their electrochemical and mechanical properties were evaluated. PANI was used as the main conducting components for fabrication. The characterization methods included conductivity, capacitive behaviour, cost, long term impedance, and their mechanical properties. The results of the fabricated PANI-silicone based samples displayed a bulk impedance of 600 Ω with an impedance of 1.6 k Ω at the frequency of 1 kHz and a modulus of elasticity of 75.312 MPa. The charge storage capacity of the fabricated sample was equal to 138.14 C/ Cm² which is the highest compared to the literature materials. The samples did not have any peaks so they were considered as stable samples. The mechanical test results of the fabricated batches were compared to those found in the literature such as PEDOT: PSS (poly 3,4-ethylenedioxythiophene): polystyrene sulfonate) and skin tissue. The young modulus of the fabricated samples (sample 1 and sample 9) were 0.1468 MPa and 75.312 MPa respectively, while the young modulus from the literature were 1.8 ± 0.2 GPa and 83.33 ± 4.9 MPa respectively. The results for the silicone with PANI showed promising electrochemical and mechanical characteristics with flexible and ductile properties.

Keywords --- Conductive polymers, Flexible electrodes, Implantable electrodes, Polyaniline implantable electrode.

Table of Contents

Abstract.....	6
List of Figures	9
List of Tables.....	11
List of Abbreviations	12
Chapter 1. Introduction.....	13
1.1 Overview and Problem Formulation.....	13
1.2 Thesis Objectives.....	14
1.3. Research Contribution.....	14
1.4 Thesis Organization	15
Chapter 2. Literature Review	16
2.1. The Nervous System.....	16
2.1.1. Functions of the nervous system.....	16
2.1.2. Structural classifications.	16
2.1.3. Functional classifications.	16
2.1.4. Nervous tissue.....	17
2.2. Neural Interfaces.....	20
2.3. Bioelectrodes	21
2.3.1. Types of bioelectrodes.	21
2.3.2. Implantable electrodes materials.	25
2.4. Electrical Stimulation.....	27
2.4.1. Neuromodulation	27
2.4.2. Functional electrical stimulation (FES).	28
2.5. Material for Neural Interface Design.....	29
Chapter 3. Methodology	34
3.1. PANI Preparation Materials	34
3.2. Samples Preparation.....	34
3.3. Samples Characterization using EIS.....	36
3.3.1. Electrochemical impedance spectroscopy.....	36
3.3.2. Cyclic voltammetry (CV).....	37
3.3.3. Mechanical testing.	38
3.4. Impedance with Time Test.....	38
3.5. ECG Test.....	39
Chapter 4. Results and Discussion	40
4.1. PANI-Silicone Electrodes Samples	40
4.1.1. EIS results.....	40
4.1.2. CV results	42
4.1.3. Mechanical testing results	45
4.2. PANI-Silicone-PMMA Electrodes Samples	46
4.2.1. EIS results.....	47
4.2.2. CV results	49
4.3. PANI-Silicone Electrodes Samples (Last batch).....	51
4.3.1. EIS results.....	51
4.3.2. CV results.....	53
4.3.3. Mechanical testing results	55

4.3.4. Long term impedance test results	56
4.4. Confidence Interval and ECG Test	59
4.4.1. Confidence intervals	59
4.4.2. ECG test results	60
Chapter 5. Conclusions and Future Work.....	63
References	65
Appendix A: Detailed Results.....	76
A.1. PANI Samples EIS Results	76
A.2. PANI Samples CV Results.....	80
A.3. PANI Samples Mechanical Testing Results.....	85
A.4. Confidence interval Test Results	87
A.5. ECG Test Results.....	87
A.6. MATLAB code for calculating the Charge Storage Capacity (CSC).....	88
Vita	89

List of Figures

Figure 2.1: Neuron structure [9].....	18
Figure 2.2: Impulse propagation due to a) unmyelinated sheath b) myelinated sheath [10].....	19
Figure 2.3: The axon regeneration process [9].....	19
Figure 2.4: Types of bioelectrodes interfacing with PNS [51].	22
Figure 2.5: (A) Schematic representation of a slowly penetrating interfascicular nerve electrode. (B) Cross-section of an implanted nerve electrode [50].	23
Figure 2.6: Examples of epineural electrode [50].....	23
Figure 2.7: Penetrating microelectrodes types [65].....	25
Figure 2.8: Block diagram of the FES system [2].....	28
Figure 2.9: The freehand is an implanted system [97].	29
Figure 3.1: The electrode sample [This work].	35
Figure 3.2: Experimental setup used to measure the characterization of my sample.	36
Figure 3.3: Equivalent circuit and its corresponding Nyquist plot.	37
Figure 3.4: Cyclic voltammetry output [113].	37
Figure 3.5: Mechanical tests performed for our sample [114].....	38
Figure 3.6: Stress-strain relationship [114].....	38
Figure 4.1: Nyquist plot for the sample 1.	41
Figure 4.2: Nyquist plot for sample 2.	42
Figure 4.3: Nyquist plot for the sample 3.	42
Figure 4.4: Cyclic voltammetry test for the sample 1.	43
Figure 4.5: The relationship between time and current.	43
Figure 4.6: Cyclic voltammetry test for sample 2.	43
Figure 4.7: Cyclic voltammetry test for sample 3.	44
Figure 4.8: Stress of the material VS strain for the sample 1.	45
Figure 4.9: Nyquist plot for sample 4.	48
Figure 4.10: Nyquist plot for sample 5.	48
Figure 4.11: Nyquist plot for sample 6.	48
Figure 4.11: Cyclic voltammetry test for sample 4.	49
Figure 4.13: Cyclic voltammetry test for sample 6.	50
Figure 4.14: Nyquist plot for sample 7.	52
Figure 4.15: Nyquist plot for sample 8.	52
Figure 4.16: Nyquist plot for sample 9.	53
Figure 4.17: Cyclic Voltammetry for sample 7.....	53
Figure 4.18: Cyclic Voltammetry for sample 8.....	54
Figure 4.19: Cyclic Voltammetry for sample 9.....	54
Figure 4.20: Stress of the material VS strain for the sample 9.	54
Figure 4.21: Change of samples weight over testing period.....	57
Figure 4.22: Change of bulk impedance in long-term samples pre/post CV test.....	57
Figure 4.23: Change of impedance at 1 kHz in long-term samples pre/post CV test.	57
Figure 4.24: Displays resulting voltammograms from performing cyclic voltammetry on prepared samples after immersion in PBS.	58
Figure 4.25: Displays the change of current density during the cyclic voltammetry test over 4 weeks of immersion.	58

Figure 4.26: Bioelectrode sample consists of (6 % PANI, 22 % Glycerol, and 72 % Silicone)	60
Figure 4.27: The relationship between the impedance and frequency at 1kHz for 20 Bioelectrode samples consists of (6% PANI, 22 % Glycerol, and 72% Silicone).....	60
Figure 4.28: ECG result using the standard Ag-Agcl Electrodes (The blue graph is without filtering and the orange is after the filtering).....	61
Figure 4.29: ECG result using the fabricated Electrodes (The blue graph is without filtering and the orange is after the filtering).....	61
Figure A.1: EIS of a bioelectrode for sample 1 (intercept with the x-axis).....	76
Figure A.2: Nyquist plot for sample 2.	76
Figure A.3: Nyquist plot for sample 3.	76
Figure A.4: Nyquist plot for sample 4.	77
Figure A.5: Nyquist plot for sample 5.	77
Figure A.6: Nyquist plot for sample 6.	77
Figure A.7: Nyquist plot for sample 7.	78
Figure A.8: Nyquist plot for sample 8.	78
Figure A.9: Nyquist plot for sample. 9	78
Figure A.10: Cyclic voltammetry test for the sample 1.....	80
Figure A.11: The relationship between time and current.	81
Figure A.12: Cyclic voltammetry test for the first sample 2.	81
Figure A.13: Cyclic voltammetry test for the first sample 3.	81
Figure A.14: Cyclic voltammetry test for sample 4.	82
Figure A.15: Cyclic voltammetry test for sample 5.	82
Figure A.16: Cyclic voltammetry test for sample 6.	82
Figure A.17: Cyclic voltammetry test for sample 7.	83
Figure A.18: Cyclic Voltammetry for sample 8.....	83
Figure A.19: Cyclic Voltammetry for sample 9.....	83
Figure A.20: Stress of the material VS strain of a bioelectrode sample 1.	85
Figure A.21: Stress of the material VS strain of a bioelectrode sample contained for sample 9.	85
Figure A.22: ECG result using the standard Ag-Agcl Electrodes.....	87
Figure A.23: ECG result using the fabricated Electrodes.....	88
Figure A.24: MATLAB code for calculating CSC	88

List of Tables

Table 2.1: Blends of conductive polymers.	30
Table 3.1: PANI preparation materials.	34
Table 3.2: Comparison between different prepared electrode mass compositions.	35
Table 4.1: Comparison between different prepared electrode mass compositions.	40
Table 4.2: A comparison table for charge density for the first batch of the prepared samples.	44
Table 4.3: Literature values for mechanical properties of conductive polymers.	46
Table 4.4: Comparison of prepared samples with different mass ratios.....	47
Table 4.5: A comparison table for charge density.....	50
Table 4.6: Comparison between different prepared electrode samples.	51
Table 4.7: A comparison table for charge density.....	54
Table 4.8: Literature values for mechanical properties of conductive polymers.	56
Table 4.9: Change of charge storage capacity in long-term PANI based samples.	58
Table A.1: Comparison between different prepared electrode samples.	79
Table A.2: Comparison of prepared samples with different ratios	79
Table A.3: Change of bulk impedance in long-term samples pre/post CV test.....	80
Table A.4: Change of impedance at 1 kHz in long-term samples pre/post CV test....	80
Table A.5: A comparison table for charge density.....	84
Table A.6: Change of charge storage capacity in long-term PANI based samples.....	84
Table A.9: literature values for mechanical properties of conductive polymers.	86

List of Abbreviations

CNS	Central Nervous System
CV	Cyclic Voltammetry
ECG	Electrocardiograph
EEG	Electroencephalograph
EIS	Electrochemical Impedance Spectroscopy
EMG	Electromyograph
EOG	Electrooculograph
FBR	Foreign Body Response
PANI	Polyaniline
PBS	Phosphate Buffer Solution
PDMS	Polydimethylsiloxane
PEDOT	3, 4-ethylene dioxythiophene
PI	Polyimide
PMMA	Polymethyl methacrylate
PNS	Peripheral Nervous System
PPy	Polypyrrole
PTh	Polythiophene

Chapter 1. Introduction

In this chapter, the introduction of implantable bioelectrode material is discussed, followed by a summary of the topics investigated in this study, along with a thesis contribution. The general organization of the thesis is finally provided.

1.1 Overview and Problem Formulation

Bioelectrodes act as a bridge between the human body and the instrumentation system, it acquires the electrical signal from the body or it can be used to trigger the nerve/muscle.

It is a sensor which works as an interface between the proximal end of the muscle and the injured nerve. Flexible bioelectrodes were among the most successful projects in the area of bioelectrodes. Since last decade, neuroprosthetic applications have demonstrated promising results for traumatic neural injuries, hence the demand for implantable electrodes has expanded [1, 2].

For decades, neural sensing, monitoring, and stimulating methods have received much interest [1]. Many of these methods have so far relied heavily on precious materials such as gold and platinum [2].

These materials caused damage to the soft tissue and had poor electrochemical properties. These, particularly, introduce more noise over the acquired signal and affect its durability. As a result, multiple attempts were conducted in the literature to create new flexible electrode materials that could solve the previously mentioned disadvantages.

These materials are based on conductive polymers such as Poly-aniline [3] and PEDOT: PSS [4]. In this thesis the synthesis and characterization of flexible implantable electrodes based on a combination of a conductive polymer (poly-aniline (PANI)), glycerol, and silicone were demonstrated.

For the conductive material to be prepared, the components are mixed and molded into a rectangular electrode shape. After that, the implantable electrodes were evaluated for their electrochemical and mechanical properties. In this thesis, the novel

bioelectrode material is presented and investigated. The fabricated bioelectrodes should be biocompatible, conductive, and flexible.

1.2 Thesis Objectives

This thesis aimed at producing a low-cost, flexible bioelectrode material that is biocompatible and stable over time in order to avoid a foreign body reaction during long-term implantation.

Furthermore, it should have electrical and mechanical properties that are similar to the stimulating units within the body, to be able to transmit the electrical impulses to the target muscle/nerve. Therefore, the electrodes were fabricated; they are made of a flexible composite mixture of silicone, glycerol, and PANI. To achieve this goal, the plan was to:

1) Fabricate electrodes with different combinations:

-Silicone + PANI.

-Silicone + PANI + Glycerol.

- Silicone + PANI + PMMA + Glycerol.

2) Conduct electrochemical, mechanical, stability, and biocompatibility testing protocols to determine the properties of the fabricated samples.

3) Based on the conducted results, adjust the electrodes performance, electrochemical characterization tests including electrochemical testing (including impedance spectroscopy (EIS) and cyclic voltammetry (CV)), and mechanical properties by varying the composition of the different components (PANI polymer, silicone) and observe the effect on the electrode properties.

4) Perform the long-term test for the electrode sample to investigate the effect of long-term implantation of the bioelectrode material properties and to know how long the electrode can be stayed within the body.

1.3. Research Contribution

Research has been conducted in the field of implantable electrodes [5-7], several materials used in producing the electrodes were studied including noble metallic materials such as gold and platinum [2], or conductive polymers such as PANI [3] and

PEDOT: PSS [4]. While it is practical, these materials still suffer from different limitations such as poor electrochemical properties and high impedance, high cost for manufacturing, and they make damage to the soft tissues. In this thesis, PANI and silicone are proposed to fabricate implantable electrodes. The combination of PANI within silicone and glycerol is examined for the first time in the literature. Silicone has commonly been used as a supporting material due to its biocompatibility and stability. The outcome of this work is the fabrication of functional and stable implantable electrodes at a potentially reduced cost to address multiple problems associated with the use of traditional electrodes, such as flexibility and high impedance.

1.4 Thesis Organization

The rest of this thesis is arranged as follows: Chapter 2 discusses the background of anatomy and physiology of the body's nervous system, followed by a discussion of bio electrodes types and materials. Chapter 3 explains the methodology of the preparation and characterization of the bioelectrode material in this thesis. Chapter 4 presents the experimental results, and finally, chapter 5 consists of the conclusion and future work to be done.

Chapter 2. Literature Review

In this section, the nervous system, structural classifications, anatomy and physiology of the nervous system, functional classifications of the peripheral nervous system, bioelectrodes, types of bioelectrodes, materials used in bioelectrode, the uses of implantable electrodes in medical applications, and materials used in neural interfaces were discussed.

2.1. The Nervous System

The nervous system is a complex collection of nerves and specialized cells (neurons); it is responsible for the main functions of the body. It is made up of the brain, spinal cord, and nerves which connect organs to the rest of the body [8]. It is a fast response system which response to internal or external changes by activating muscles or glands. It is a complex system that has a lot of classifications. These classifications are used to explain its functionality, as presented in the following sections. Figure.2.1 shows the nervous system parts; these parts were discussed in the structural classification of the nervous system.

2.1.1. Functions of the nervous system. The function of the nervous system is to transmit information to and from the brain and spinal cord to the rest of the body. The nervous system functions by communicating with the body using these parts of the control system; the receptors (sensory input) respond to the changes in the environment (stimuli). Then it will send information to the control centre (integration), which will determine the setpoint, then it analyzes the information and will determine the best response to this change. The effector (motor output) will provide a means for a response to the stimulus by activating muscles and glands.

2.1.2. Structural classifications. The nervous system is comprising of the Central Nervous System (CNS) which consists of the brain and the spinal cord, and the Peripheral Nervous System (PNS) which consists of the rest of the body (nerves outside the brain and the spinal cord). These two systems work together to enable the body to communicate with the outer environment [8].

2.1.3. Functional classifications. The PNS has two branches: the sensory nerves (Afferent) and motor nerves (Efferent) [8]. The sensory nerves transmit the

information from the body to the CNS. The motor nerves are divided into two sectors: the voluntary nervous system (somatic nervous system) which is responsible for the voluntary control of body movements, and the involuntary nervous system (autonomic nervous system) which sends the response (command) to the CNS and then to the body (activate muscles or glands). The CNS contains all the non-sensory neurons (somatic nervous system and the autonomic nervous system).

2.1.4. Nervous tissue. Nervous tissue is a group of ordered cells in the nervous system, it controls body movements, and it is responsible for sending and carrying information to and from body parts. The nervous tissue has two main parts: Neurons and neuroglia. The neuron's function is to transmit electrical impulses while the neuroglia has many functions such as supporting and protecting neurons [9].

2.1.4.1. Neuron structure. The main components of the neuron are cell body, axons, dendrites, and synapse. Each neuron consists of a nucleus surrounded by several cellular components such as Mitochondrion, Neurofibrils, Golgi Apparatus, Endoplasmic reticulum which are housed in a cell body.

The cell body controls all the cell functions, and it is connected to the dendrites, which are extended away from the cell body. The dendrite's function is to receive the information from another neuron and transmit it to the cell body [9]. The axon is a tube structure which is responsible for carrying the electrical impulse from dendrites or the cell to the end of the neuron. Axon terminals can pass the electrical impulse from one neuron to another.

The junction between the cell body and the axons is called Axon hillock. The synapse is the chemical junction between the axon terminal in one neuron and the dendrites from another neuron (it is a place where the chemical interactions can occur) as shown in Figure. 2.1.

One of the most critical internal structures of the cell body is the myelin sheaths, which are produced by Schwann cells (in PNS) and oligodendrocytes (in CNS). The myelin sheath works as an insulator; it increases the speed and the efficiency of the electrical impulse.

The myelin sheath is wrapped around the axon as several layers. The myelin sheath is not covering the axon fully; there are some spaces between each of the two

myelin sheaths, which are called the Node of Ranvier, and it works as a channel for sodium ions [9].

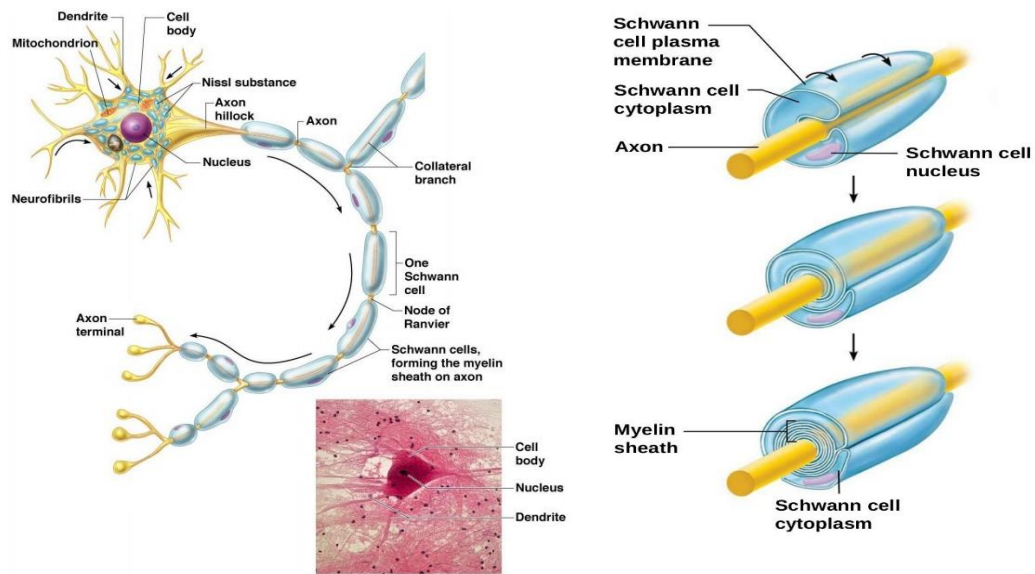


Figure 2.1: Neuron structure [9].

2.1.4.2. Neuron functional classification. Nerve cells are classified as sensory neurons and motor neurons based on the direction of the electrical impulse.

Sensory neurons (Afferent) are further classified into unipolar, bipolar, and multipolar shaped cells that conduct the action potential to or from the CNS.

They carry the autonomic and somatic nervous system signals. However, motor neurons (Efferent) are multipolar shaped cells that are responsible for conducting the action potential out from the CNS [8].

2.1.4.3. Nerve impulses. At resting state, the neuron axon in the cell membrane is polarized (has Na^+ ions and K^+ ions). When the cell membrane gets stimulated, it begins to depolarize, and an action potential will take place.

The action potential (depolarization) will move in one direction from one section to another while the previous section starts to return to its resting state [8,10]. As shown in (Figure 2.2), when the neurons have unmyelinated axon the transmission of the signal will be relatively slow because the axon membrane bears depolarization/repolarization. However, if the neurons have myelinated axon the

transmission of the signal will be extremely fast because of the presence of myelin sheath in a procedure called saltatory conduction [9].

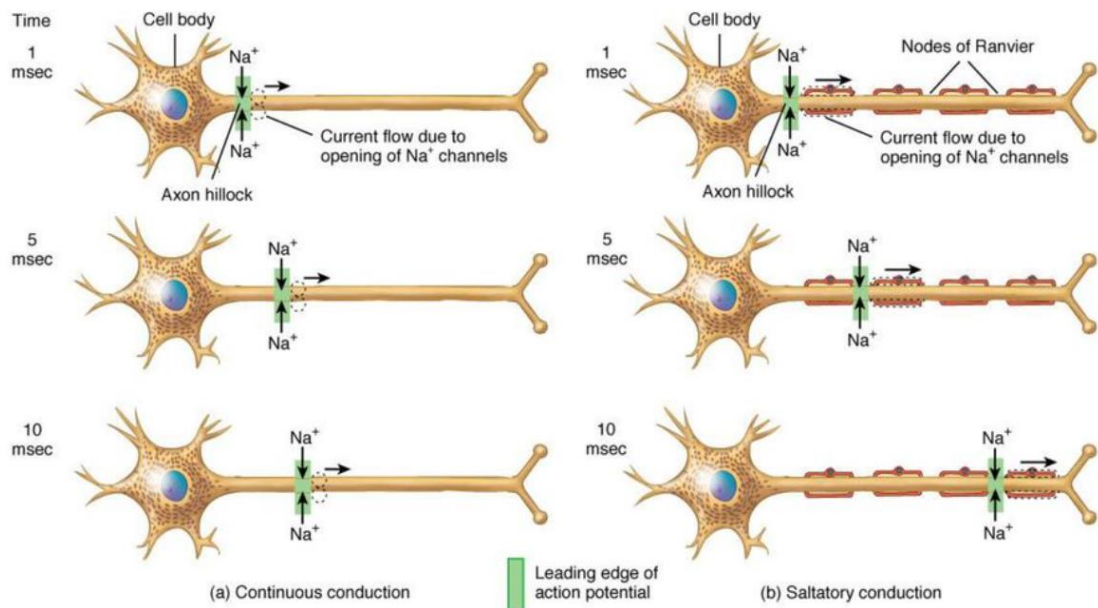


Figure 2.2: Impulse propagation due to a) unmyelinated sheath b) myelinated sheath [10].

2.1.4.4. Axon regeneration. The peripheral nervous system axons are very sensitive, they can easily be injured or damaged. However, if a small part of the neurilemma remains, the axon can be regenerated.

The regeneration process depends on three factors: the severity of the trauma, the nerve growth factors, and the distance between the injured axon and the muscle/gland [9]. This regeneration cycle is called the Wallerian Degeneration process as shown in Figure 2.3.

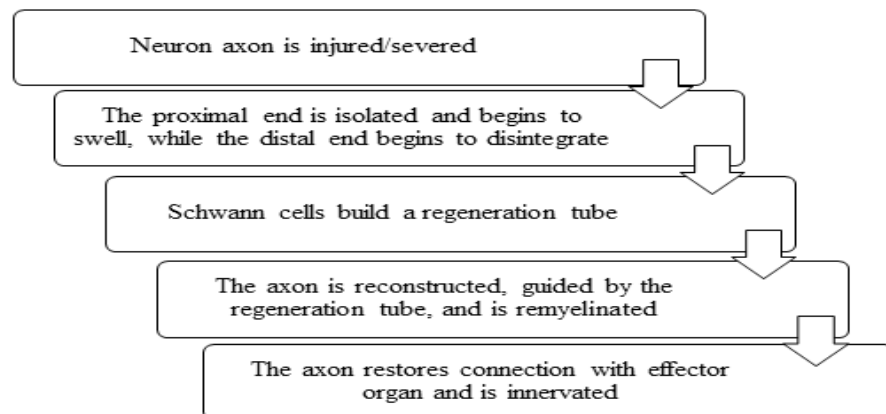


Figure 2.3: The axon regeneration process [9].

2.2. Neural Interfaces

A wide range of treatments with the help of neural electrodes for tissue-electrode interface have introduced for chronic conditions using stimulation to excite or inhibit the target organ and electrical recording providing tunability and selectivity of the electrical interfaces and then specificity to the individual's needs [11, 12]. These treatments demonstrate compelling alternatives to pharmaceutical options without side effects for the same conditions along with added specificity of the delivery [13, 14]. Moreover, thanks to the swift evolution of implantable neural interface technologies, the same technology has been developed remarkably in prosthetic applications demonstrating significant sensory feedback by providing electrical interfaces with the nervous system immediately to the peripheral nervous system (PNS) [15, 16] and to the cortex [17].

This method had shown to be a convincing replacement for the indirect sensory feedback approaches for prosthetic such as vibrotactile stimulation, electro-tactile stimulation, and modality-matched feedback which do not noticeable stability, selectivity by myoelectric control [18-21]. The peripheral nerves are composed of nerve fibers which they are made of axons of motor or sensory neurons which are arranged in fascicle groups in a sheath that keeps them in bundles and then fascicle layer surrounds the entire nerve. This intricated system needs to be considered when designing any device that has interaction of electrodes with the nerve's structures. Signals go through peripheral nerves which have bidirectional pathways for both sensation and motor commands from and to periphery and spinal cord.

However, they can be blocked or lost in sever peripheral injuries which causes loss of functionality [22]. However, with the help of surgical techniques and using bioengineered neuroelectronic interfaces and specified prostheses recently it is possible to overcome these deficits [23, 24]. At first neural electrodes application were limited to studying the properties of nerves and its relationship with spinal and cortical tissues [25, 26]. By increasing the understanding of peripheral nerves and the emergence of advanced technologies, neural electrodes step into development of clinically applicable neuroelectronic interfaces [27-29].

A selective approach is needed to provide an interface for the loss of motor and sensory pathways to reanimate the stimulating and recording potentials. For instance,

regarding nerve dysfunction, an appropriate electrical stimulation can be used to target a specific muscular response, such as implementing functional electrical stimulation bladder control in paraplegia [30-32], or in foot drop [33, 34], and epilepsy treatment with the help of vagal nerve stimulation [35, 36]. Moreover, in the case of amputees, prosthetic control would be possible by recording motor action potentials of nerves [37, 38].

However, with advances in electromyogram (EMG) decomposition approaches, this method may get a promising alternative [39-42]. A recent study by Gesslbauer and co-workers [43] on brachial plexus and its derivative nerves in human limbs demonstrates that the ration of sensory axons to motor axons is 9:1. Thus, regarding the fact that developing direct interfaces on the peripheral nerves may be a useful approach, however, being able to replace these sensory inputs through direct electrical stimulation could be a game changer in prostheses design. Recent studies have shown that transdermal cuff in upper limb amputees can coarsely stimulate the sense of touch when coupled with a prosthetic limb [35, 44-46].

However, yet there are some challenges remaining about permanent use of percutaneous systems for the risk of wound breakdown, infections, and material failure [47]. Wireless systems could be boon to these approaches if the technical challenges of biocompatibility and power delivery can be overcome.

Implementing cochlear implants to overcome hearing loss is a convincing instance of transcutaneous interfacing with the nervous system. As a well-developed technology with convincing clinical results, it demonstrates that sensory deficits can be treated with appropriate neuroelectronic interfacing [48, 49].

2.3. Bioelectrodes

Bio electrodes are sensors that are used to transfer information into or out of the body. They are used to connect the body with electronics. In this thesis, these bio electrodes were investigated for their ability to transmit any signal from the instrumentation system to the target tissue nerve/muscle [2, 50].

2.3.1. Types of bioelectrodes. PNS electrodes can be placed next to, around, or within the peripheral nerve trunks/spinal roots [9]. The bioelectrodes can be classified into several groups based on their selectivity and invasiveness, as shown in Figure 2.4.

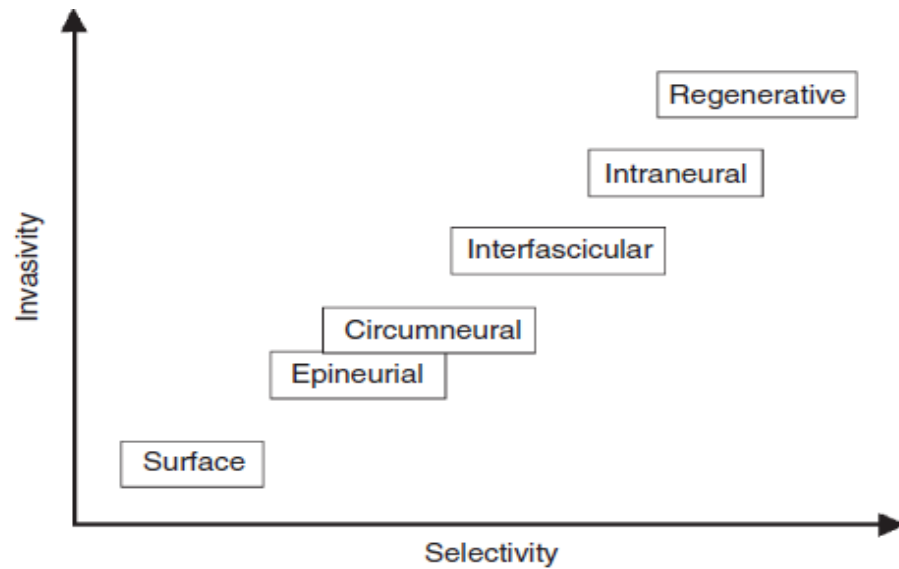


Figure 2.4: Types of bioelectrodes interfacing with PNS [51].

2.3.1.1. Body surface electrodes. Also called transcutaneous electrodes, these electrodes are minimally invasive and are placed on the body surface. They can be used to record body signals such as electromyogram (EMG), electrocardiogram (ECG), and electroencephalograph (EEG) [2, 50]. This type of electrodes cannot be used in neural sensing.

2.3.1.2. Neural electrodes. These electrodes work as an interface between neurons and the brain-machine interface. The neural electrodes can be classified as intra-neural and extra-neural based on the insertion site.

These electrodes are manufactured from silicone which is a flexible material that helps in insulation and protection. These electrodes are placed in contact with the nerve. Several materials are also used, such as graphene and conductive polymers such as PEDOT [51-53].

2.3.1.2.1. Intra-neural electrodes. This type of electrodes is inserted within the cell. They are located within the epineurium sheath of the peripheral nerve. These electrodes have active contact with the bundles of the fascicles.

These electrodes are generally developed to improve the selectivity and signal to noise ratio of the recording. One type of intra-neural electrodes is the intrafascicular electrodes. It is called intrafascicular because the electrode was attached to small fascicles in the nerve bundle, as shown in Figure 2.5 [2], [54].

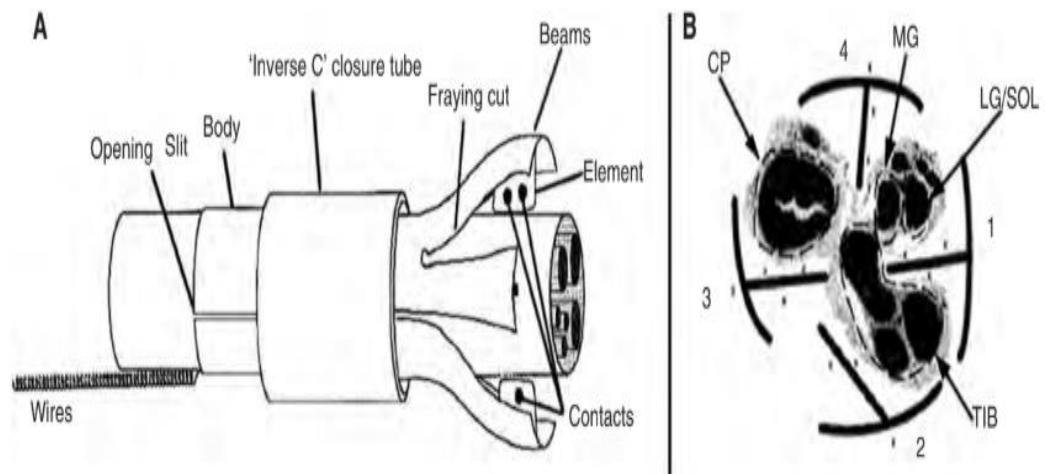


Figure 2.5: (A) Schematic representation of a slowly penetrating interfascicular nerve electrode. (B) Cross-section of an implanted nerve electrode [50].

2.3.1.2.2 *Extra-neural electrodes.* This type of electrodes is not implanted in a single cell. It is attached to the extracellular fluid near to the cell. Types of extraneural electrodes are circumneural, epineurial, and helicoidal. The epineurial and helicoidal are inserted along with the nerve.

The cuff electrode is one type of circumneural electrode. It is an open tube shape that is placed around the peripheral nerve. The electrodes are placed inside the cuff to get in touch with the nerve, as shown in Figure 2.6 [2, 55].

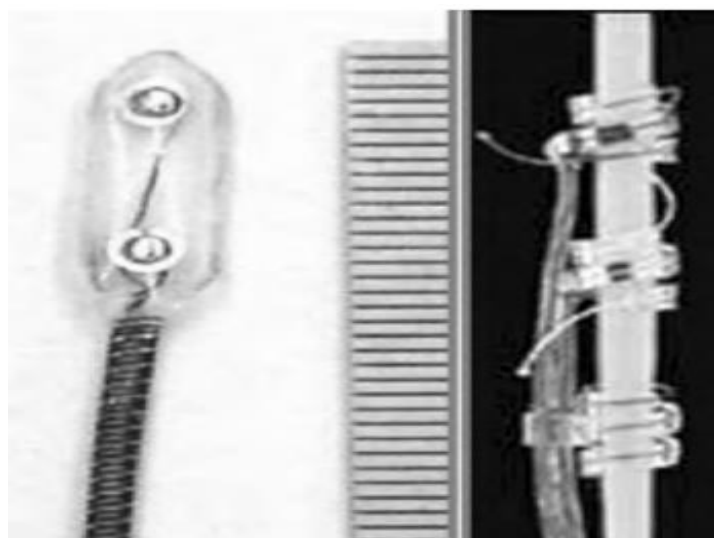


Figure 2.6: Examples of epineural electrode [50].

2.3.1.3. Muscle electrode. This type of electrode is attached to the epimysium, which is a mask for the entire skeletal muscle, but can capture good quality EMG signals. It is used to transmit the electrical stimulation from the muscle to the instrument. One type of muscular electrodes is an intramuscular electrode, which has two fine wires inserted into the selected muscle within a hypodermic needle (one as active wire and the other one will work as a reference) [56]. Muscle electrodes have been widely used in the medical field, such as Rheumatic, Rehabilitation, implantable neuromuscular stimulation system, neuroprosthesis control, and hybrid bionic systems [50-58].

2.3.1.4. Recording electrodes. When the detected signal distinguishes a single neuron firing, the neuron activity can be recorded as an action potential or as an extracellular potential. If the microelectrode is implanted near to the target neuron for single-unit recording, its geometric surface area should not be larger than 2000–4000 μm^2 , and is usually much smaller. Such neural recordings, especially from large sets of neurons, are the basis for prostheses that could provide the mental control of existing prosthetic devices to help patients with paralysis [59, 60]. Specific uses of multielectrode neural recordings, wherein the recorded neural signals assess the output of implanted stimulation electrodes, it is also used for adaptive deep brain stimulation and functional stimulation for epilepsy [61, 62].

2.3.1.5. Stimulation electrodes. The purpose of stimulation is to provide enough charge to activate an action potential at a particular location. Muscle, peripheral nerve, and the cortical surface layer require to charge up to 0.2 to 5 mC per stimulation, a pulse is needed, and the intracortical region needs only 8 to 64 nC per stimulation pulse [63, 64]. As the electrode area goes down, the amount of charge density increases, contributing to electrode failure.

Optimizing the Charge Store Capacity (CSC) parameter offers more charge per electrode area, thereby preventing electrode failure from extending its usable life. This parameter can be obtained via the Cyclic Voltammetry (CV) wave, where the cathodic area (negative current) is correlated with the sum of electrons that the electrode provide at a specified voltage range. Stimulation protocols are usually performed in the form of voltage or current pulses, where the latter is more common. Several combinations can

be used, but charge-balanced biphasic protocols are usually standard since the net charge is zero [1].

2.3.1.6. Penetrating microelectrodes. Microneurography has been widely used as a low invasive technique for humans. Measurement of multi-unit peripheral nerve activity has become an essential tool for the study of somatosensory, motor, and autonomic physiology and pathophysiology. A Tungsten microelectrode is usually implanted percutaneously into limb fascicles and peripheral facial nerves of conscious human subjects to detect afferent or efferent nerve fiber activity, as shown in Figure 2.7 [65].

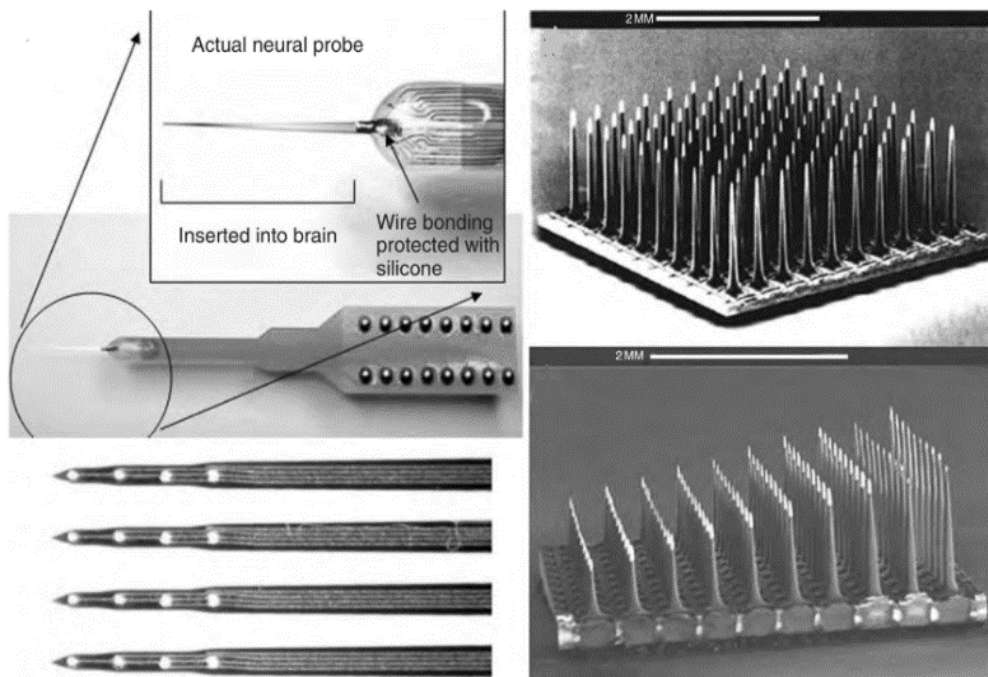


Figure 2.7: Penetrating microelectrodes types [65].

2.3.2. Implantable electrodes materials. Several materials are used in the manufacture of implantable electrodes, and this section addresses some materials such as Carbon, Silver, Gold, Platinum (Metals), Polyaniline, PEDOT, Polypyrrole, and PMMA (conductive polymers) [65].

2.3.2.1. Criteria for choosing materials. Four main factors must be well-thought-out for choosing the materials for implantable electrodes; these factors are: 1) Allergic response 2) Tissue response 3) Electrode-Tissue impedance and radiographic visibility [66].

2.3.2.2. Metals. To date, many electrodes have depended primarily on metallic materials such as gold (Au), silver (Ag), titanium (Ti), stainless steel, and platinum (Pt) in addition to some metal alloys [6]. Platinum is the most commonly used metal in neural prosthesis [67-69] and widely used in medical applications.

Platinum was used in conjunction with polyimide (as a microelectrode) for chronic in vivo neurophysiology [70]. Some metals cause foreign body response and lead to unevenness in the collected signal, so researchers have found that they can coat the metals with another material that is usually conductive polymer to avoid foreign body response (FBR) [71].

2.3.2.3 Conductive polymers. Also known as intrinsically conductive polymers (ICP). This type of polymers have high conductivity and improved mechanical properties. Moreover, conductive polymers have high processability, their physical and chemical properties can be adjusted according to the function [72-90].

2.3.2.3.1. Polyaniline (PANI). Previously called aniline black, it was the first conductive polymer produced in 1862. There are different forms of polyaniline based on the degree of oxidation in sulfuric acid so that each form has its conductivity [72-74]. The major issues with the use of PANI are its rigidity, and it can lose its conductivity in a high pH environment. It is one of the most used conductive polymers in implanted electrodes. It has several advantages including the low cost, stability and it does not show any abnormalities signs in the body. Also, it is biocompatible and non-biodegradable material and widely used in biomedical applications, particularly for long-term implants [3, 63, 75]. Due to the low cost and many advantages associated with it, PANI is the choice of study in this thesis.

2.3.2.3.2. Polypyrrole (PPy). It is a heterocyclic polymer and the most studied polymer in bioelectrodes. Polypyrrole has high electrical conductivity and stability under high temperatures (around 200C). It is a rigid material, but at the same time, it is brittle [77]. The conductivity of polypyrrole may be increased by ten times by using perchlorate instead of the oxalate. It is used widely in drug delivery and tissue engineering [78-80].

2.3.2.3.3. Polythiophene (PTh). It becomes conductive when it is oxidized. It has the same structure as polypyrrole, but in the aromatic ring, it has sulfur instead of

nitrogen [81]. It has many derivatives such as poly 3, 4-ethylene dioxythiophene polystyrene sulfonate (PEDOT: PSS) and poly 3, 4-ethylene dioxythiophene (PEDOT). PEDOT: PSS is one of the best conductive polymers due to its high conductivity and stability and has therefore been widely used in medical applications such as biosensors [82, 83], nerve growth [84, 85]. Unfortunately, PEDOT: PSS is a ductile material. Some issues are identified when used in long-term implants [85]. Such as low conductivity and the internal mechanisms are ambiguous.

2.3.2.3.4. Poly (3, 4- ethylene dioxythiophene) (PEDOT). It is the most popular polythiophene derivative due to its properties, High conductivity, and secure polymer processing. Researches have shown that it can be used to improve long-term neural implants, biosensors [65, 87 - 86].

2.3.2.3.5. Polyimide (PI, Kapton). Polyimide is a rigid material, but it is a brittle material at the same time. It has a high-performance polymer. It is made up of a chain imide monomers. Polyimide has excellent mechanical properties with high conductivity and an active insulation polymer [87]. Nevertheless, it has been widely used in biomedical engineering, especially in long term implants [88], [89].

To sum up, conductive polymers generally have high conductivity, stability, and biocompatibility. Nevertheless, their rigidity and brittleness prevent the use of them in implantable applications.

2.4. Electrical Stimulation

Neuromodulation (NM) and functional electrical stimulation (FES) are widely used in medical applications, implantable bioelectrodes played a huge role in acquiring and sending electrical signal from/to the human body.

2.4.1. Neuromodulation (NM). In the field of medicine, neuromodulation grow rapidly in many different areas affecting millions of patients with several disorders across the globe. “It is a procedure of electrical or chemical prevention, relaxation, regulation, or therapeutic alteration of an action in the nervous systems.” [91]. The most extensive and rapidly expanding field of neuromodulation is the peripheral nervous stimulation (PNS). This growth has become feasible due to technological and medical developments in pain management [92]. The theory is also applied to autonomic dysfunction conditions such as Parkinson's disease [69]. Furthermore,

Neuromodulation is established in percutaneous activation of the posterior tibial nerve at regular intervals [93], Cardiac and Visceral Pain [94], and augmentation of sexual function [95]. Additionally, such stimulation is accomplished by combining peripheral and spinal cord nerves [96].

2.4.2. Functional electrical stimulation (FES). FES is an application which uses the electrical current to stimulate the tissue to either supplement or restore the function which is missing in the neurologically affected person. FES purpose is to enable the function by substituting or assisting the voluntary ability of a patient. FES can restore both sensory and motor functionality. Neuroprostheses is referred to the instruments or structures which can be used as a replacement for impaired neurological function. Some examples for the FES are auditory and visual neuroprosthesis which are used to restore the functions of the sensory system. This approach focuses on attenuating muscular atrophy while at the same time promoting the reconstruction of neuronal connections. Even though, the stimulation electrodes are placed on the targeted muscle, the trigger action is almost certainly to stimulate the nerve instead of the muscle fiber; because the nerve has a lower threshold than the muscle fibers. Normally the FES systems are designed to be worn by the patients, because a stimulus from these systems is needed to achieve the required function. “FES systems have been established to restore the function in the lower extremity, upper extremity, bowel, bladder and respiratory system” [97]. The block diagram of the FES system is shown in Figure 2.8.

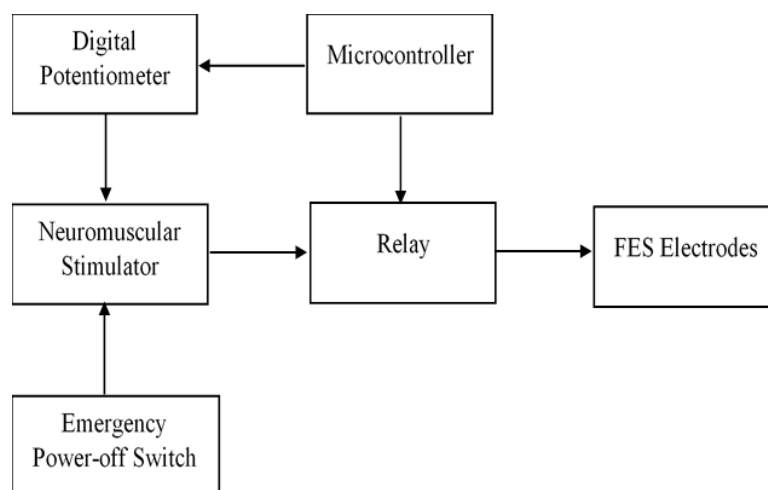


Figure 2.8: Block diagram of the FES system [2].

The electrical stimulation has achieved great results in both preventing the muscle atrophy and peripheral axonal regeneration. But the peripheral axonal regeneration depends hugely on the presence of Schwann cells in the damaged sites. It was proven that both the stimulation of neurons and schwann cells advances the neurite outgrowth. [98 - 100].

Numerous studies about FES in the upper and lower limbs were conducted. An example is the freehand implanted system, consisting of a transmitting/receiving coil, stimulator/telemeter, EMG recording/stimulation electrodes, and an external control unit placed within the chest inserted at the trigger points of the forearm and hand muscles as shown in Figure 2.9.

The external components consist of a transmitting/receiving coil based on radio frequency, an additional programmable control unit, and a transducer which is used for the monitoring of contralateral shoulder motions.

The shoulder movement controls the degree of the flexing and extending of the hand muscle. Patients with C5 or C6 tetraplegia used the free hand method to achieve lateral and palmar grasp [97]. The Freehand device was approved by the FDA and has been implanted in hundreds of individuals worldwide [97, 101, 102].

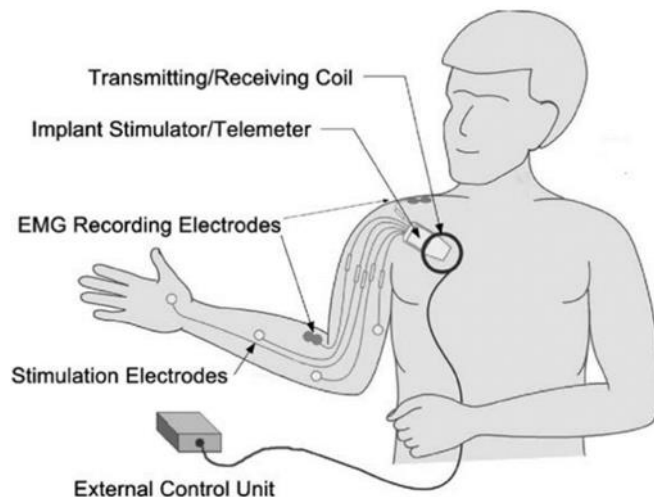


Figure 2.9: The freehand is an implanted system [97].

2.5. Material for Neural Interface Design

In the last 30 years, all carbon-based polymers were particularly known as insulators, for this purpose they are commonly used by the electronics industry, they were used as insulating materials. These properties have changed after mixing the

conductive polymers with other polymers (conventional polymers); this combination provides a new polymeric material with special properties. By mixing the conventional polymers with conductive polymers such as polyaniline, polypyrrole, PDMS, etc.... the mechanical properties improved, and the main drawbacks of conductive polymers such as brittleness and lack of processability can be eliminated. In this section several studies about blends of conductive polymers were described, then they were summarized in Table 2.1.

Table 2.1: Blends of conductive polymers.

Blends(materials)	Properties	Applications
PEDOT in the (Au nanorod) (Au-nr) [2]	Improve adhesion and stability.	Recording and stimulating neural activity, neural regeneration, and therapeutic drug delivery.
PEDOT was electrochemically coated on (Mg microwires) [3]	A biocompatible, biodegradable and conductive electrode, reduce the degradation risk, and enhance the biocompatibility of electrodes for future neural electrode applications.	Neural recording and stimulation applications.
PEDOT: PSS [8]	Low impedance.	Biosensors, tissue engineering, and neuronal cell stimulation or pan-bioelectronics
PEDOT-TFB [9]	Reduce signal to noise ratio, reduce the insulation.	Recording brain areas, electrophysiology applications.
PEDOT: PSS and platinum black (Pt-black) on the wrinkled microelectrode [65]	Good adhesion, excellent biocompatibility and stability.	In vivo ECoG recordings, microelectrode biosensors,
A novel graphene composite functionalized polyaniline [75]	Promising electrical,	Electrical stimulation.

	mechanical and biocompatible properties	
Hydroxyethyl cellulose (HEC)/soy protein (SPI)/Polyaniline (PANI) sponges (HSPS), were prepared by lyophilization of HEC / SPI solution [76]	Strong biocompatibility, flexibility, and reliability.	Nerve repair, nerve tissue engineering.
Two different CPs, PPy and PEDOT [77].	Stretchable, good adhesion.	Cellular engineering, and tissue engineering,
Single walled carbon nanotube (SWNT)/Polypyrrole (PPy) composite [78]	Good electrical and mechanical properties, small size, and biocompatible.	Neural interface, and it is used in biomedical studies.
PEDOT/PSS - based film [79]	Reduce signal to noise ratio, improve adherence.	—
Glassy carbon coated PEDOT: PSS [81]	Reduced gaps between the implants material and the host tissue, and good signal to noise ratios.	Main clinical applications, and chronic applications.
polypyrrole containing the anionic dopant dodecylbenzenesulfonate (DBS) [82]	Biocompatibility, higher conductivity.	Tissue engineering.
Doped polypyrrole and PEDOT with sulphate (SO ₄) or para-toluene sulfonate [83]	Improve the charge density while decreasing the impedance at a frequency of 1 kHz	Neural recording.
Composite of polypyrrole and carbon nanotubes [84]	Enhance the signal-to-noise ratio.	Neural recording.
Titanium and gold were deposited onto polyimide films [84]	Hard, patterned, conductive, thin-film metals	Neuroprosthetic applications, transplants.
PEDOT: PSS [101]	—	Brain-computer-interface (BCI) applications, electrocorticography (ECoG)

Polypyrrole and PEDOT nanotubes [102]	Enhance the long-term efficiency of neural microelectrodes low impedance, and high load storage capacity	Neural protheses.
PEDOT/MWCNT neural E\electrode coating [102]	—	Neural interface applications.
PEDOT: PSS [103]	Small size, supplying low impedance for high-quality in vivo neural activity recordings	Optical imaging,
Carbon fibers (CFs) and polyimide (PI) [103]	Improve mechanical properties	—
AuNPs-PEDOT deposited tetodes [104]	Reduce impedance, good load storage capacity, increase the surface area, improve recording efficiency	In vivo recording in the posterior medial ventral (VPM) nucleus of the thalamus (Brain).
Polypyrrole/chitosan (PPy/CHI) composite coated Ti [106]	Enhanced microhardness and adhesion strength.	Drug delivery, tissue engineering, bio actuators and biosensors.
Graphene oxide and poly (3, 4-ethylene dioxythiophene) - poly (styrene sulfonate) coated knitted textile fabrics [107]	—	ECG monitoring.
Hyaluronic acid doped-poly(3,4-ethylenedioxythiophene)/chitosan/gelat in (PEDOT-HA/Cs/Gel) [108]	Increase mechanical and electrical properties while decreasing the porosity and water	Nerve tissue regeneration.

	absorption.	
PEDOT/taurine bio composite on screen printed electrode [109].	Improve the charge transport properties	Biomedical device (biosensors) and drug delivery system.
Black-platinum coatings on flexible, polymer micro ECoG Arrays [110]	Enhance signal to noise ratio, minor increase in electrical impedance, stable interface between tissue and device.	Brain applications (EEG).
Polyimide-insulated microelectrodes with a bioactive peptide KHIFSDDSSE [111]	Improve the biocompatibility, small and flexible electrode.	Neural recording and brain-machine interfaces

To summarize this chapter, bioelectrodes are type of sensors which are used to transmit a signal from the body to the instrument (they work as an interface between the body and the instrument). Different materials were used to fabricate these bioelectrodes such as gold, platinum, and conductive polymers. Flexible electrode is a type of electrodes which is widely used in the field of bioelectrodes, this type of electrode works as a bridge between the injured nerve and the proximal end of the muscle. The human body has several signals that can be transmitted such as ECG, EMG, EOG, and EEG (which is an important signal used in nervous system diagnostic). There are many types of bioelectrodes used in biomedical applications such as Body surface electrodes, Neural electrodes, and implantable electrodes. Finally, A wide range of these materials were used in the medical field such as Optical imaging, Neural protheses, Biosensors, tissue engineering, neuronal cell stimulation, recording and stimulating neural activity, neural regeneration, and therapeutic drug delivery.

Chapter 3. Methodology

In this chapter, sample preparation and characterization methods are discussed in addition to the characterization methods used, such as (EIS, CV, and mechanical testing).

3.1. PANI Preparation Materials

In this section, materials used for preparing PANI to use it in this experimental work were described.

Table 3.1: PANI preparation materials [112].

Material	Percentage	Supplied by	Used	Country
Aniline monomers	99.9% (Weight/Weight)	Sigma	--	Spain, Germany, United Kingdom
Sodium Dodecyl Sulfate	99% (Weight/Volume)	Sigma	To form micelles in solution.	Spain, Germany, United Kingdom
Nonylphenol Ethoxylate 9	--	Ilchil Chemical Co	To form micelles in solution.	Korea
APS	98% (Weight/Weight)	Kanto Chemical Co.	To initiate the polymerization	Japan
Methanol	99.9% (Weight/Volume)	Mallinckrodt	To wash the PANI particles after the reaction	USA
Acetone	96% (Weight/Volume)	Kanto Chemical Co.	To wash the PANI particles after the reaction	Japan
HCl	35% (Weight/Volume)	Matsunoen	As a doping agent.	---

3.2. Samples Preparation

To prepare nine bioelectrode samples, mixtures of different variation of Poly-aniline (PANI), silicone, glycerol, and PMMA as shown in Table 3.2 were added and mixed well (manually in a small plastic plate) for several minutes until they became a paste. The paste mixture was then applied in a Teflon mold and allowed to dry for 24

hours in the fume hood (at room temperature). Figure 3.1 illustrates a sample of the prepared electrodes.



Figure 3.1: The electrode sample [This work].

Table 3.2: Comparison between different prepared electrode mass compositions.

Sample	PANI (%)	Silicone (%)	Glycerol (%)	PMMA (%)
Sample 1	0.9 g (30 %)	1.5 g (50 %)	0.6 g (20 %)	--
Sample 2	0.6 g (20 %)	1.5 g (50 %)	0.9 g (30 %)	--
Sample 3	0.3 g (10 %)	1.8 g (60 %)	0.9 g (30 %)	--
Sample 4	0.9 g (27%)	1.5 g (45%)	0.6 g (19%)	0.3 g (9%)
Sample 5	0.6 g (18%)	1.5 g (45%)	0.9 g (28%)	0.3 g (9%)
Sample 6	0.3 g (9%)	1.8 g (55%)	0.9 g (27%)	0.3 g (9%)
Sample 7	0.4 g (15 %)	2.2 g (70 %)	0.4 g (15 %)	--
Sample 8	0.6 g (20 %)	1.5 g (50 %)	0.9 g (30 %)	--
Sample 9	0.2 g (6 %)	2.9 g (72 %)	0.9 g (22 %)	--

3.3. Samples Characterization using EIS

Electrochemical impedance spectroscopy was used to determine the electrochemical properties (bulk impedance, impedance at 1 kHz, and conductivity) of the dried electrode samples.

To get the results in EIS, the four-probe method and a custom-made stainless-steel cell electrode were used. The results were displayed as a Nyquist plot.

3.3.1. Electrochemical impedance spectroscopy. EIS is a technique which is used to measure the impedance of a device using a sinusoidal signal. An impedance scale is observed by varying frequencies (100 Hz-7MHz) over the desired range. An alternating current was applied, and the output was observed as a function of frequency. The EIS calculations were carried out with the aid of a Potentiostat (Biologic, model SP-200 with EC lab software v11.02), as shown in Figure 3.2. The EIS data is provided as a Nyquist plot, which was analyzed to determine the sample's bulk impedance. At a standard frequency of 1 kHz, the sample impedance was also measured. The equation below was used to determine the conductivity of the fabricated samples (σ):

$$\sigma = t/R * A \quad (1)$$

Where t and R represents the thickness of the sample and the sample's electrical resistance respectively and A represents the cell's cross-sectional area. The bulk impedance is the intercept of the curve with the x-axis which can be determined by the Nyquist plot. The impedance can be shown as a sum of real and imaginary impedance ($R_u + R_p$), the metal electrode which is used in our work composed of a resistor in series with a parallel combination of a resistor and a capacitor as shown in Figure 3.3.

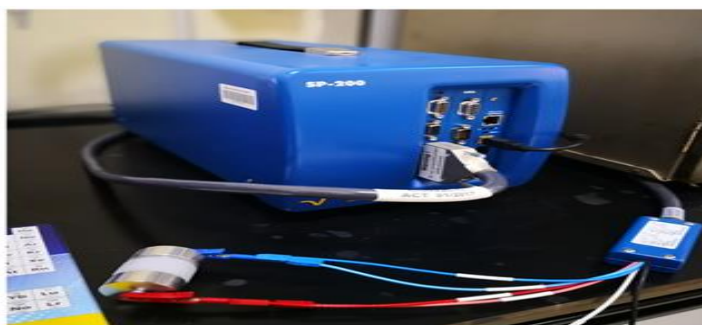


Figure 3.2: Experimental setup used to measure the characterization of my sample.

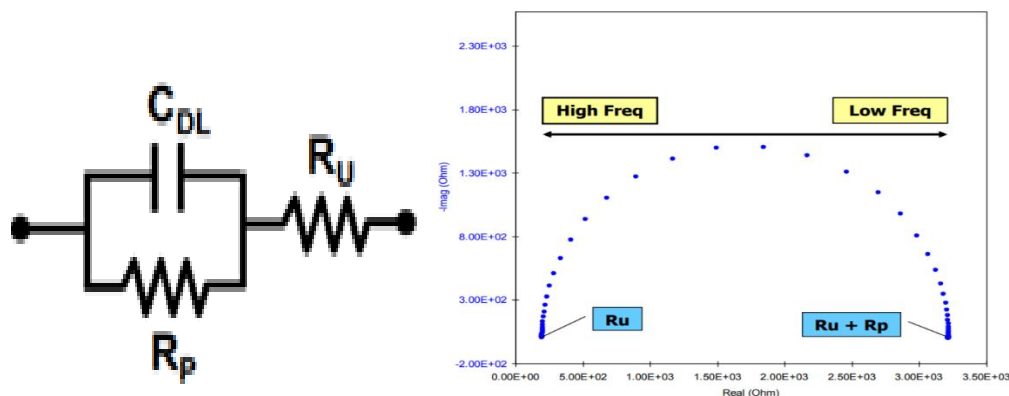


Figure 3.3: Equivalent circuit and its corresponding Nyquist plot.

3.3.2. Cyclic voltammetry (CV). Cyclic voltammetry (CV) is an electrochemical test that enables the investigation of the samples stability (oxidation/reduction reactions) and possible oxidation/reduction process. After applying an alternating voltage to the tested sample, oxidation and reduction reactions may take place, as well as determining the stability of the reaction products or intermediate possibilities. It was performed by applying a cyclic potential at the electrode and measuring the generated current within the electrode, then plotting the data in a voltammogram, as shown in Figure 3.4. Both the height and the location of the peaks were measured and were used in the characterization phase. Potentiostat (SP-200, Biologic + metallic cell) were also used to perform the CV test, with a frequency range of (100 Hz-7MHz) and a voltage range of (-2V- 2V). Moreover, the data was recorded and analyzed using EC lab software v11.02. The data was also used to calculate the charge density, According to Dong-Wook Park et. Al, the charge density can be calculated by integrating the cathodal current density enclosed by CV and dividing it by the sweep rate of 10mV/sec [113].

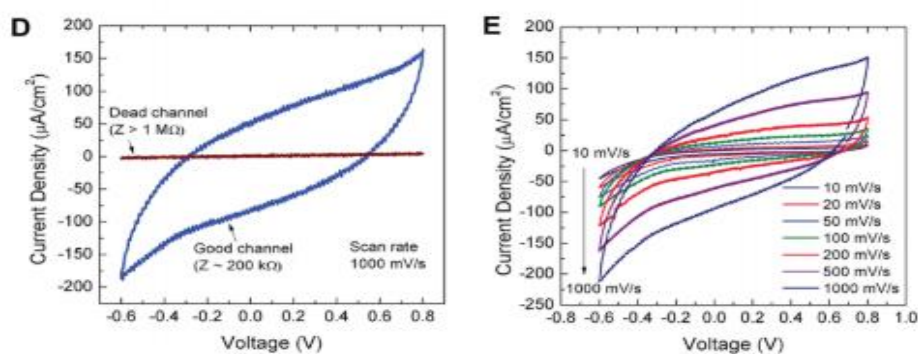


Figure 3.4: Cyclic voltammetry output [113].

3.3.3. Mechanical testing. The chosen method was Instron 5582 Universal Testing Machine (as shown in Figure 3.5) (using Instron Bluehill software), this test is used to measure the relationship between the stress of the material and the strain of a bioelectrode sample as shown in Figure 3.6. It shows that stress and strain are somehow related, the output seems to be linear until it hits the fraction point (break). To find the slope (stress/strain) a straight line was drawn, the slope was used to calculate the young modulus using equation (2) and it was equal to 0.1468 MPa [114].

$$E \text{ (Young modulus)} = \text{Stress } (\sigma) / \text{Strain } (\epsilon) \quad (2)$$

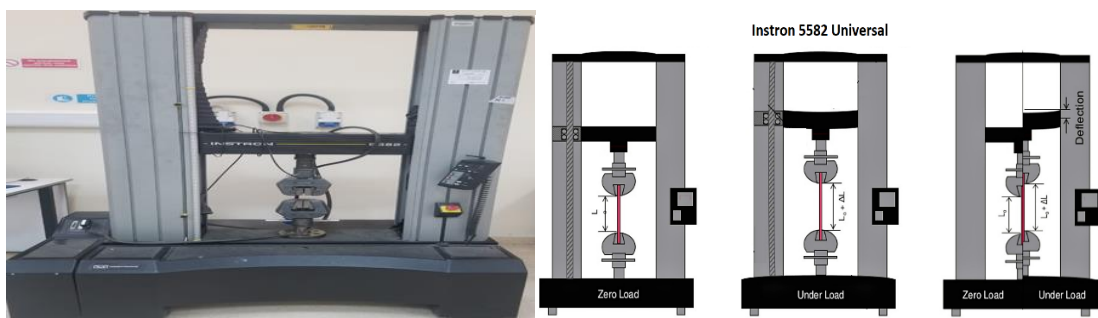


Figure 3.5: Mechanical tests performed for our sample [114].

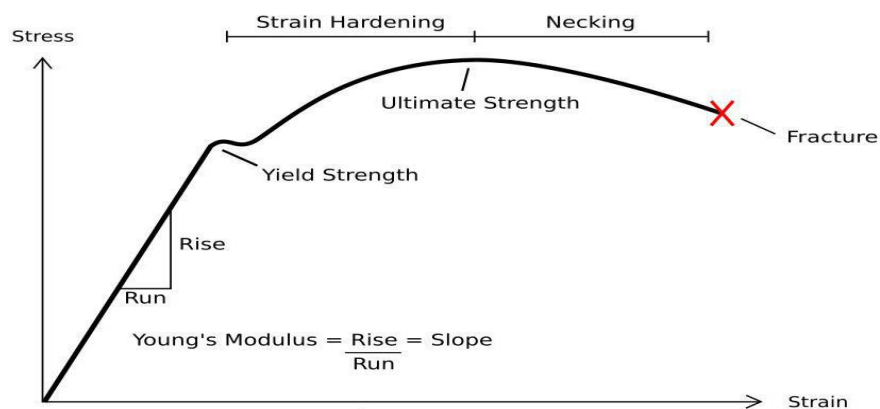


Figure 3.6: Stress-strain relationship [114].

3.4. Impedance with Time Test

This test was performed to investigate what is the effect of long-term implantation of the bioelectrode material properties. The samples were immersed in a phosphate buffer solution (PBS), the PBS pH is similar to that of the body (pH around 7.4), the samples stayed in the PBS for eight weeks with three-four days testing intervals

(EIS and CV). The EIS and CV tests were performed to measure the change of the impedance with time. This test helped to understand how long the bioelectrode can stay within the body.

3.5. ECG Test

Following approval of the AUS-IRB, human electrocardiograph (ECG) was recorded. The purpose of this test was to conduct a simultaneous recording of electrocardiograph (ECG) using standard Ag-AgCl electrodes and our fabricated electrodes. Electrode samples were prepared at the Biomedical Engineering Laboratory. The conductive side of the electrodes was placed on the participant's body surface to record ECG lead I. The electrodes were then connected to a differential amplifier. The output of the amplifier is then digitized and sampled using the Power Lab system and the "Lab Chart software". The recorded ECG signals is then stored for display or further processing.

Chapter 4. Results and Discussion

In this chapter, the experimental results for electrochemical and mechanical testing of silicone-PANI composite samples are presented. The confidence interval and the ECG tests were performed to make sure that the results were in the expected range and to test the conductivity of the samples.

4.1. PANI-Silicone Electrodes Samples

In order to understand the effect of each component in the composite on the electrochemical and mechanical properties of the electrodes, a batch of three samples of varying ratios of PANI, silicone, glycerol were first prepared (Table 4.1). In samples 1 and 2, the silicone composition was kept constant at 50% while the composition of PANI and glycerol alternated between 20 and 30%. Sample 3 was then prepared such that glycerol composition was similar to that of sample 2 while the ratios of PANI and silicone were modified.

Table 4.1: Comparison between different prepared electrode mass compositions.

Sample	PANI (%)	Silicone (%)	Glycerol (%)	Bulk Impedance (k Ω)	Impedance at 1kHz + References	Conductivity (S/cm)
Sample 1	30 %	50 %	20 %	4 k Ω	28.4 k Ω	8.33×10^{-8} S/cm
Sample 2	20 %	50 %	30 %	5.3 k Ω	8.74 k Ω	6.28×10^{-8} S/cm
Sample 3	10 %	60 %	30 %	$5.01 \times 10^4 \Omega$	$9.71 \times 10^5 \Omega$	6.65×10^{-9} S/cm
Poly-aniline-coated foam electrodes	--	--	--	7 k Ω	1.45M Ω [3]	--
PEDOT : PSS	--	--	--	2.23 k Ω	2.54k Ω [4]	0.2 S/cm [115]

In order to evaluate the electrochemical properties of the electrodes, impedances and CV results were compared to previously reported electrodes [116-121] such as PANI and PEDOT electrodes as shown in Table 4.1.

4.1.1 EIS results. The results for the composite PANI-silicone samples are shown in (Figure 4.1 – Figure 4.3) as a Nyquist plot. From the Nyquist plot, the bulk impedance, the impedance at 1 kHz, and the conductivity were measured using equation (1).

By comparing the three prepared samples, in terms of impedance sample 1 had the best result for the bulk impedance and conductivity, and they were equal to (4 kΩ and 8.33×10^{-8} S/cm) respectively. At 1kHz, sample 2 had the lowest impedance which is equal to 8.74 kΩ.

In terms of composition, adding more amount of PANI to the sample resulted in an increase in conductivity, increase in impedance at 1 kHz, and a decrease in the bulk impedance. On the other hand, decreasing the amount of PANI of the sample resulted in the opposite effect.

Furthermore, the addition of glycerol and silicone compensated for some of the electrochemical properties. Compared to PANI-coated foam electrode, the electrochemical results showed that the bulk impedance of sample 1 (4kΩ) is lower than that of PANI-coated foam electrode (7 kΩ) [3]. The impedance at 1kHz of the prepared sample was equal to 28.4 kΩ which is much lower than that of PANI-coated foam electrode (1.45 MΩ) [3].

$$\sigma = t/R * A \quad (1)$$

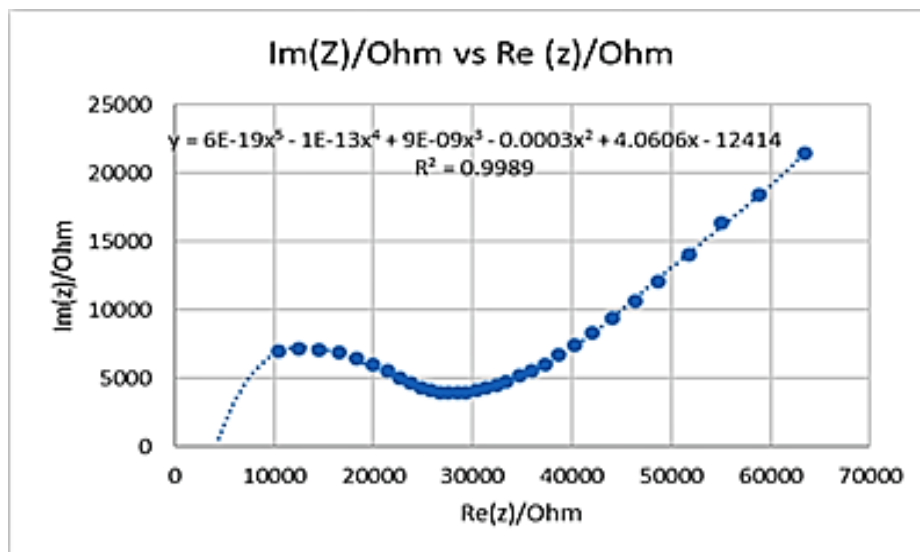


Figure 4.1: Nyquist plot for the sample 1.

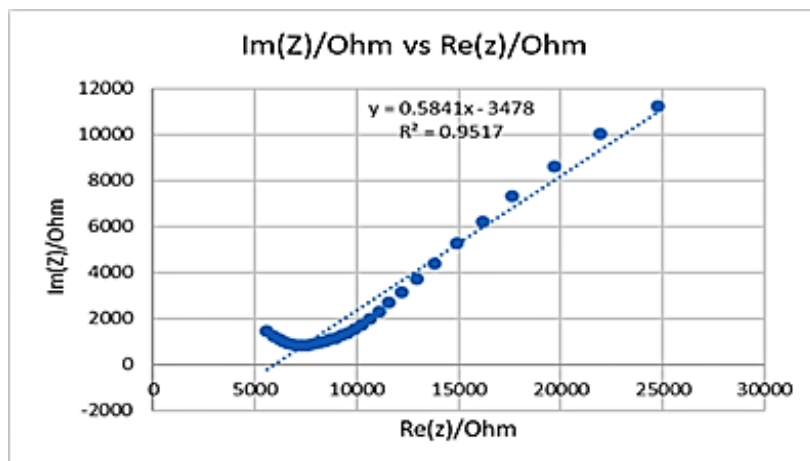


Figure 4.2: Nyquist plot for sample 2.

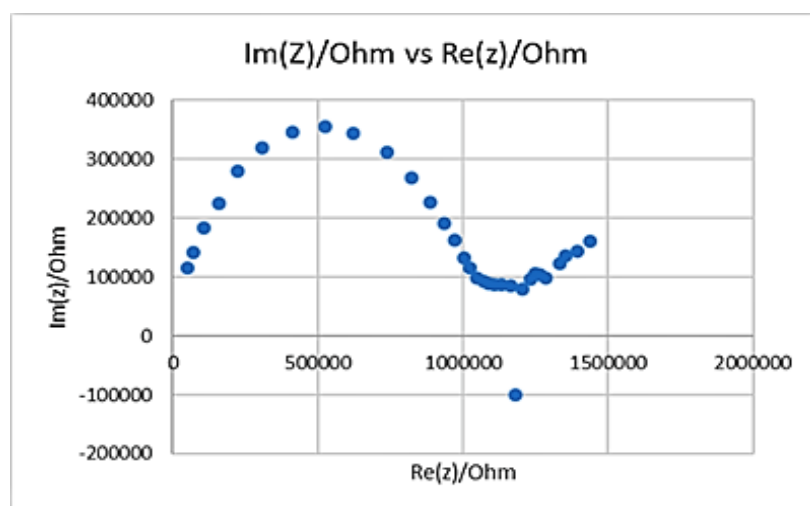


Figure 4.3: Nyquist plot for the sample 3.

4.1.2. CV results. The CV test was performed to enable the investigation of the samples stability (oxidation/reduction reactions) and possible oxidation/reduction process. As shown in the Figures (4.4- 4.7) the samples did not have any peaks in the plots.

This means that there are no oxidation/reduction reactions taking place within the samples while applying the alternative voltage, so the samples considered stable at these conditions. The charge storage capacity was calculated by integrating the cathodal portion of the graph (which is the negative current density enclosed within the Cyclic Voltammetry) as shown in Figure. 4.5, and then dividing it by the scanning rate (10 mV/sec). Table 4.2 shows a comparison between this work and literature charge density.

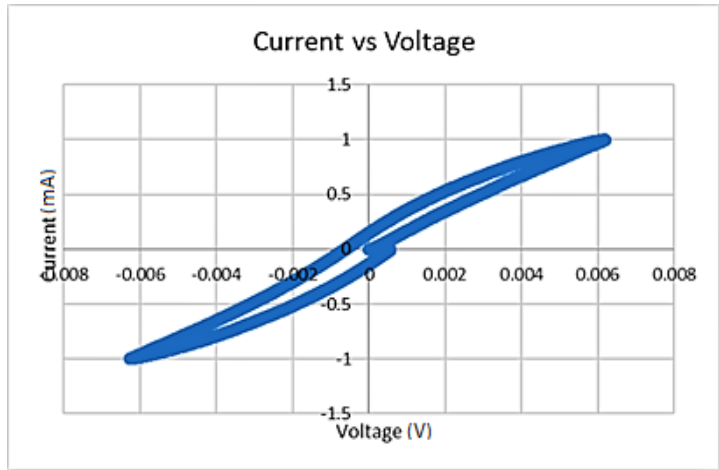


Figure 4.4: Cyclic voltammetry test for the sample 1.

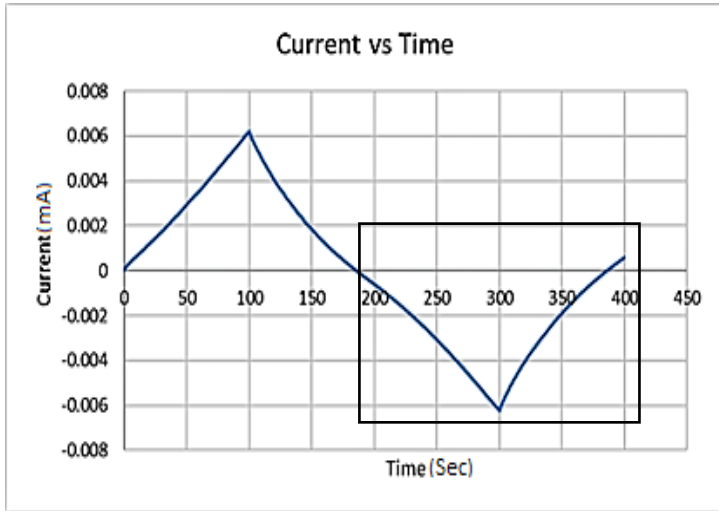


Figure 4.5: The relationship between time and current.

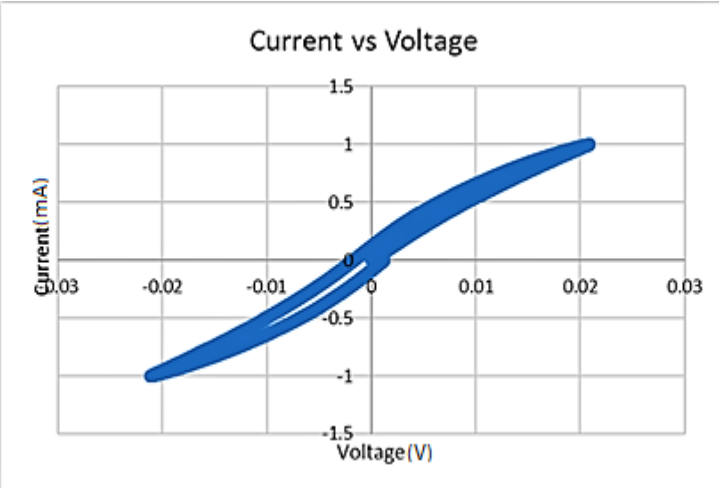


Figure 4.6: Cyclic voltammetry test for sample 2.

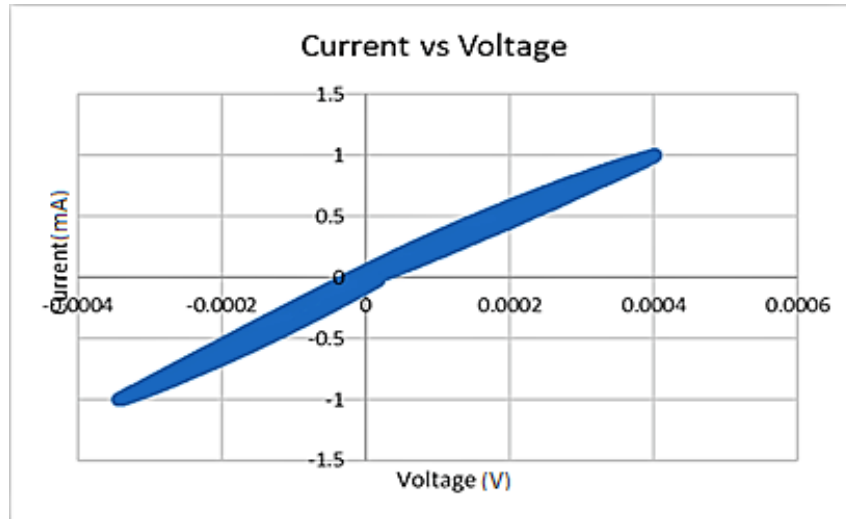


Figure 4.7: Cyclic voltammetry test for sample 3.

Table 4.2: A comparison table for charge density for the first batch of the prepared samples.

Composite	PANI (%)	Silicone (%)	Glycerol (%)	Charge density	Reference
Sample 1	30 %	50%	20 %	4.3124 C/ Cm ²	--
Sample 2	20 %	50%	30 %	14.4945 C/ Cm ²	--
Sample 3	10 %	60 %	30 %	0.2575 C/ Cm ²	--
Graphene	--	--	--	1.42 × 10 ⁻⁹ C/Cm ²	[9]
Poly-aniline	--	--	--	0.02 C/ Cm ²	[9]

By comparing the results of the prepared samples, sample 2 had the highest charge density compared to the other prepared samples; which is considered to be the best result, while sample 3 had the lowest charge density; having more charge density is necessary for acquiring a large number of charges from the target neurons. The result of sample 2 was compared with PANI [9], the result showed that the CSC of the

prepared sample was much higher than that of PANI [9] from the literature, this indicates that it can store higher charge density within the sample in one cycle.

4.1.3. Mechanical testing results. This test was used to measure the relationship between the stress and the strain of the prepared bioelectrode sample (sample 1) as shown in Figure 4.8. It shows that stress and strain are somehow related, the output seems to be linear until it hits the fraction point (break).

To find the young modulus, a straight line was drawn and by the aid of equation (2) the young modulus was calculated and it was equal to 0.1468 MPa. A comparison between the mechanical properties of the fabricated electrode samples to those presented in the literature is shown in Table. 4.3.

$$E \text{ (Young modulus)} = \text{Stress } (\sigma) / \text{Strain } (\epsilon) \quad (2)$$

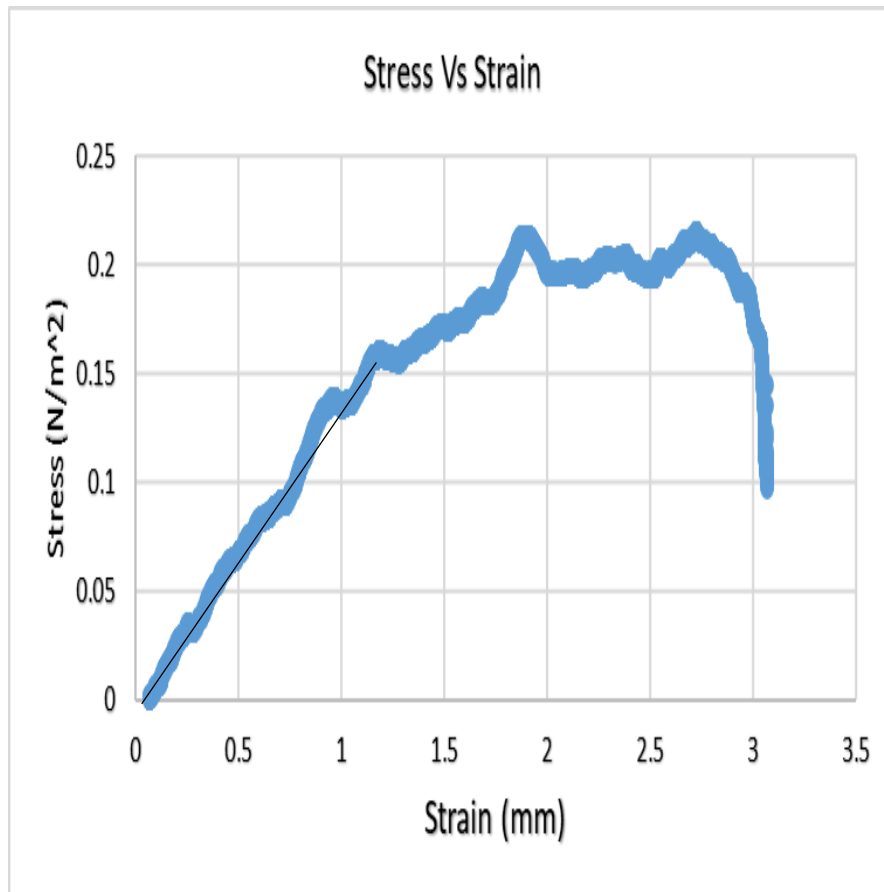


Figure 4.8: Stress of the material VS strain for the sample 1.

Table 4.3: Literature values for mechanical properties of conductive polymers.

Material	Sample 1	Skin tissue	PEDOT : PSS	Polyimide	Gold	Platinum	Polyaniline
Young Modulus (MPa)	0.1468	83.33 ± 4.9 [122]	1800±200	6000	69100	1400	N/A (Brittle material).
Elongation	306.9 %	---	4.3± 2.3%	<10%	---	35%	---

A comparison between the tested prepared sample of PANI-silicone-glycerol and the skin tissue from the literature showed that the young modulus of this sample was not satisfying; the young modulus of sample 1 was equal to 0.1468 MPa which was much lower than that of the skin tissue 83.33 ± 4.9 MPa [122]; which means that the fabricated electrode was more brittle compared to the skin tissue.

To further more improve the young modulus and the flexibility of the sample, a new batch consists of three samples were prepared (an amount of 0.3 g of PMMA was added to the samples). PMMA is a thermoplastic polymer which can be used to improve the flexibility of the material, but at the same time it may affect the electrochemical properties; PMMA has many advantages such as high melting point (160 C), high tensile strength, transparency, and stability. By applying physical/chemical changes, some of the material disadvantages such as brittleness and low resistance can be eliminated [123].

4.2. PANI-Silicone-PMMA Electrodes Samples

In order to improve the mechanical properties of the fabricated electrodes, in this section, 0.3 g of PMMA was added to a batch of three samples of varying ratios of PANI, silicone, glycerol, were prepared (Table 4.4). In samples 4 and 5, the silicone composition was kept constant at 45% while the composition of PANI and glycerol alternated between 20-30%. Sample 6 was then prepared such that glycerol composition was similar to that of sample 5 while the ratios of PANI and silicone were modified.

Table 4.4: Comparison of prepared samples with different mass ratios.

	PA NI (%)	Silico ne (%)	Glyce rol (%)	PM MA (%)	Bulk Impeda nce (kΩ)	Impeda nce at 1kHz + Referen ces	Conducti vity (S/cm)
Sampl e 4	27 %	45 %	19%	9%	4 k Ω	31.1 k Ω	8.33x10 ⁻⁸ S/cm
Sampl e 5	18 %	45%	28%	9%	5.3 k Ω	576k Ω	6.28x10 ⁻⁸ S/cm
Sampl e 6	9%	54%	28%	9%	5.3 k Ω	5.76x10 ⁵ Ω	6.28x10 ⁻⁸ S/cm
Poly- aniline -coated foam electro des	--	--	--	--	7 k Ω	1.45M Ω [3]	--
PEDO T: PSS	--	--	--	--	2.23 k Ω	2.54k Ω [4]	0.2 S/cm [115]

4.2.1. EIS results. The results for the composite silicone-PANI sample after adding PMMA are shown in (Figures 4.9-4.11) as a Nyquist plot. The EIS test showed that the electrochemical properties have improved for sample 4 only. In terms of impedance sample 4 had the best outcome for the bulk impedance, impedance at 1 kHz, and conductivity, and they were equal to (4 k Ω , 31.1 k Ω and 8.33x10⁻⁸ S/cm) respectively. Compared to the previously prepared samples the addition of PMMA into the samples resulted in an increase of the electrochemical properties for sample 4 and sample 5, but they decreased for sample 6. The impedance at 1kHz of the sample 4 was equal to 4 k Ω which is much lower than that of PANI-coated foam electrode (1.45 M Ω) [3], at the same time it was higher than that of PEDOT: PSS [115], as shown in Table 4.4.

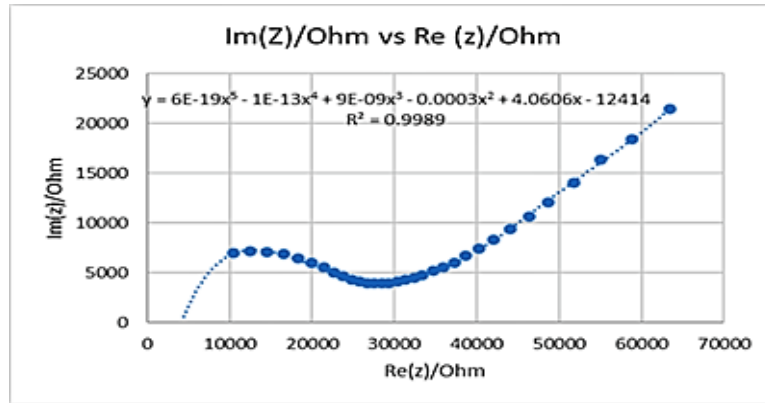


Figure 4.9: Nyquist plot for sample 4.

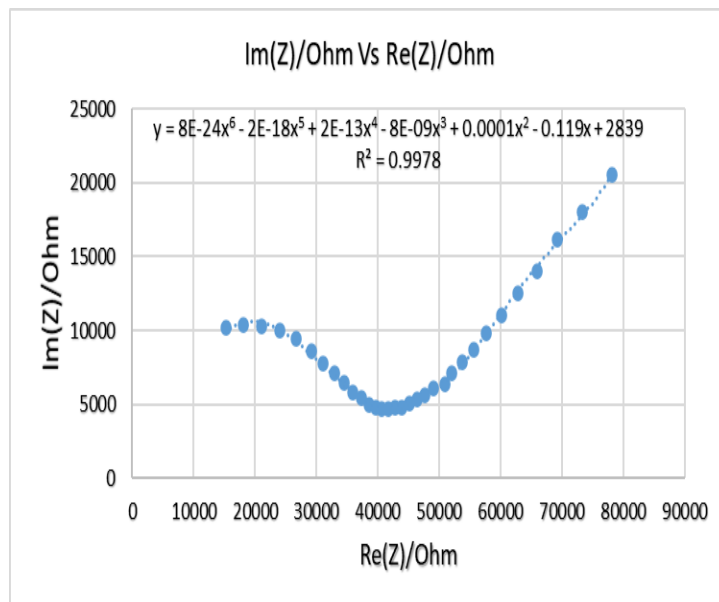


Figure 4.10: Nyquist plot for sample 5.

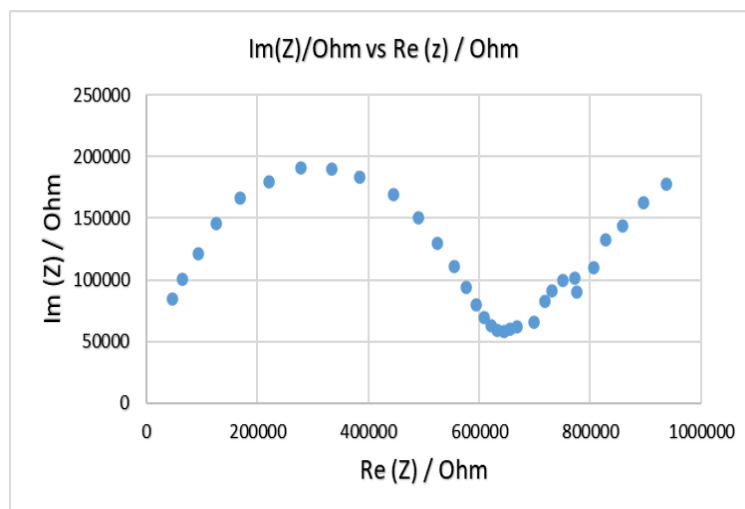


Figure 4.11: Nyquist plot for sample 6.

4.2.2. CV results. The CV test was performed to enable the investigation of the samples stability (oxidation/reduction reactions) and possible oxidation/reduction process, as shown in (Figures 4.16 - 4.18), the samples do not have any peak in the plots. This means that there are no oxidation/reduction reactions taking place within the samples while applying the alternative voltage, so the samples are considered as stable. The charge storage capacity was calculated by integrating the cathodal portion of the graph (which is the negative current density enclosed within the Cyclic Voltammetry) as shown in Figure 4.18, and then dividing it by the scanning rate (10 mV/sec), as shown in Table 4.5.

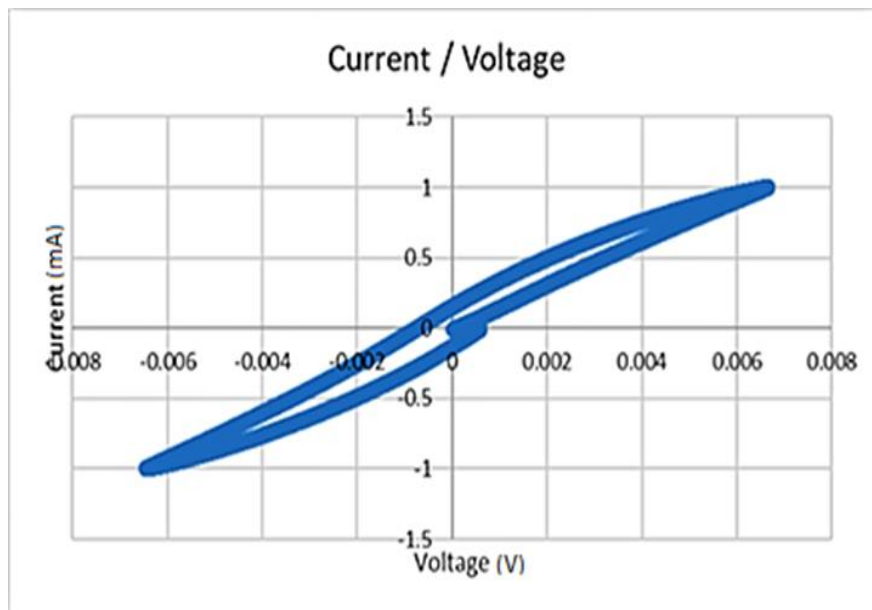


Figure 4.11: Cyclic voltammetry test for sample 4.

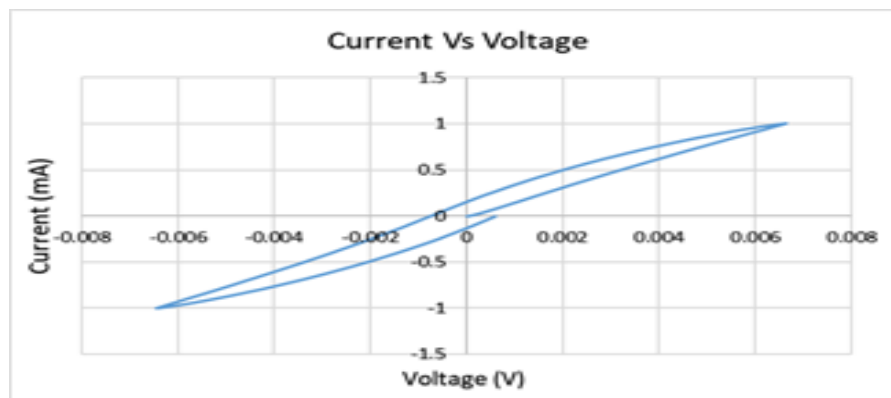


Figure 4.12: Cyclic voltammetry test for sample 5.

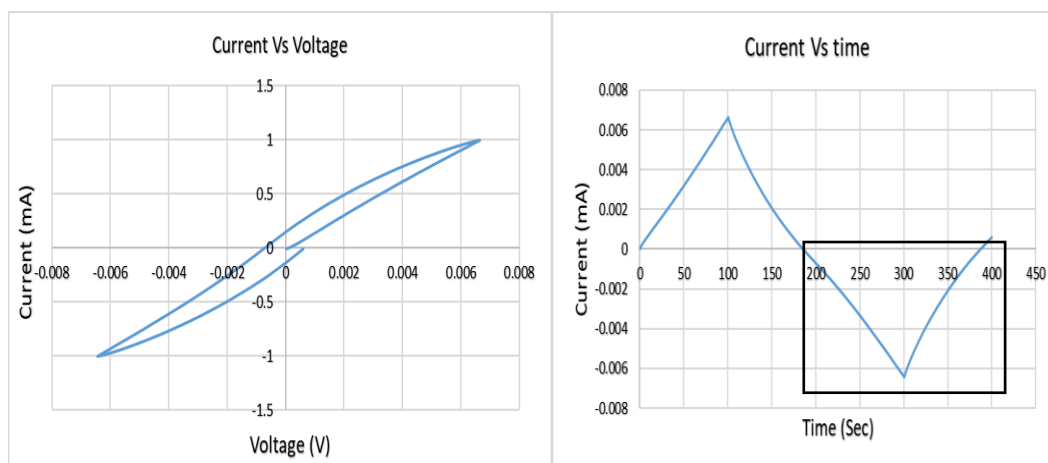


Figure 4.13: Cyclic voltammetry test for sample 6.

Table 4.5: A comparison table for charge density.

Composite	PANI (%)	Silicone (%)	Glycerol (%)	PMMA (%)	Charge density + reference
Sample 4	27 %	45 %	19%	9%	4.3124 C/ Cm ²
Sample 5	18%	45%	28%	9%	4.5927 C/ Cm ²
Sample 6	9%	54%	28%	9%	4.5927 C/ Cm ²
Graphene	--	--	--	--	1.42×10^{-9} C/Cm ² [9]
Poly-aniline	--	--	--	--	0.02 C/ Cm ² [9]

By comparing the results of the prepared samples after the addition of PMMA, sample 5 and sample 6 had higher charge density compared to sample 4. The results of sample 5 and sample 6 was compared with PANI [9], the result showed that the CSC of the fabricated sample was higher than that of PANI [9] from the literature, this indicates that it can store higher charge density within the sample in one cycle. Compared to the previously prepared sample (1,2, and 3), the addition of PMMA did not improve the CSC for the sample. Unfortunately, the addition of PMMA does not improve the mechanical properties (the samples became more brittle), therefore a preparation of a new batch of samples was decided. In this batch, three more samples with a systematic decrease of PANI concentration were prepared and tested.

4.3. PANI-Silicone Electrodes Samples (Last batch)

In order to improve the mechanical and the electrochemical properties of the fabricated electrodes, a batch of three samples with a varying ratio of PANI, silicone, glycerol, were prepared (Table 4.6). The composition of PANI alternated between 6% and 20%. The composition of PANI was replaced with silicone and glycerol to compensate some of the electrochemical properties; the expected results are predicted to reduce the bulk impedance and the impedance at 1 kHz, increase of the conductivity, increase the charge storage capacity, and increase the flexibility of the samples. The silicon percentage alternated between 50 and 72%, while the glycerol percentage alternated between 15 and 30%. This new batch was expected to have better electrochemical and mechanical properties.

Table 4.6: Comparison between different prepared electrode samples.

Sample	PANI (%)	Silicone (%)	Glycerol (%)	PMMA (%)	Bulk Impedance (kΩ)	Impedance at 1kHz + References	Conductivity (S/cm)
Sample 7	15 %	70 %	15 %	--	25Ω	79.1396 Ω	1.33×10^{-5} S/cm
Sample 8	20 %	50 %	30 %	--	22Ω	56.5978 Ω	1.51×10^{-5} S/cm
Sample 9	6 %	72 %	22 %	--	600Ω	1.6 kΩ	5.55×10^{-7} S/cm
Poly-aniline-coated foam electrodes	--	--	--	--	7 kΩ	1.45MΩ [3]	--

4.3.1. EIS results. The results for the composite silicone-PANI samples are shown in Figures (4.14 - 4.16) as a Nyquist plot. In terms of impedance, sample 8 had the best results for the bulk impedance and conductivity which are equal to (22Ω and 1.51×10^{-5} S/cm) respectively, but the sample was brittle compared to sample 9, which had higher impedance and conductivity (600Ω and 5.55×10^{-7} S/cm) but it has better flexibility. The EIS test showed that the electrochemical properties for sample 9 have improved compared to the previously prepared samples; as expected, the bulk impedance has been reduced from 4 kΩ to 600 Ω, the impedance at 1 kHz has been

reduced from 28.4 k Ω to 1.6 k Ω , which is much lower than that of PANI-coated foam electrode (1.45 M Ω) [3], at the same time it was higher than that of PEDOT: PSS [115] as shown in Table 4.6, the conductivity has increased from 8.33x10⁻⁸ S/cm to 5.55x10⁻⁷ S/cm because of the change in dimension, decreasing of PANI concentration, and increasing of the silicone and glycerol concentration. In terms of composition, the decrease of the PANI concentrations within the samples improved the electrochemical and mechanical properties for sample 7, 8 and sample 9.

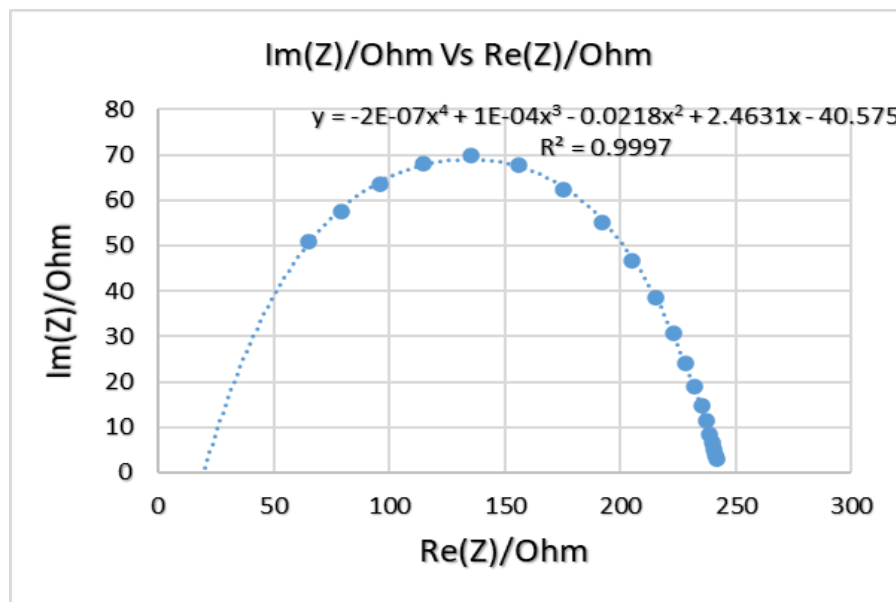


Figure 4.14: Nyquist plot for sample 7.

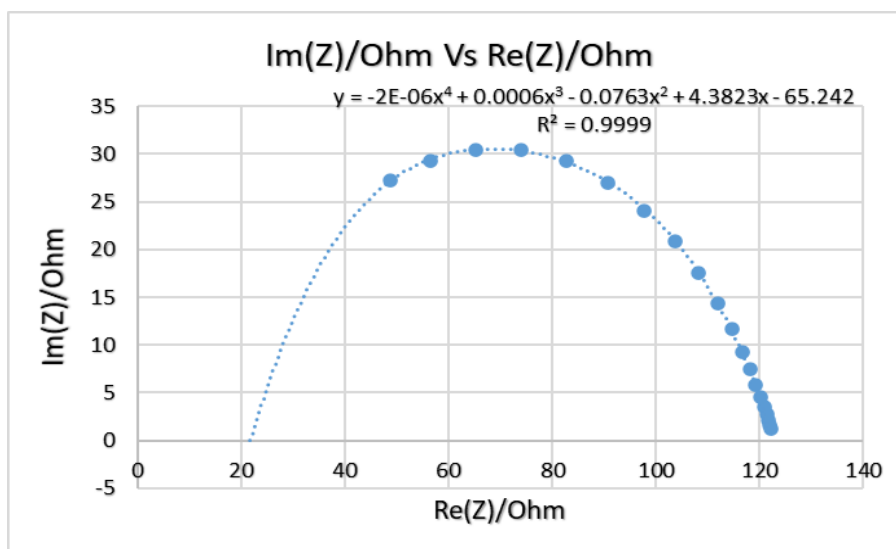


Figure 4.15: Nyquist plot for sample 8.

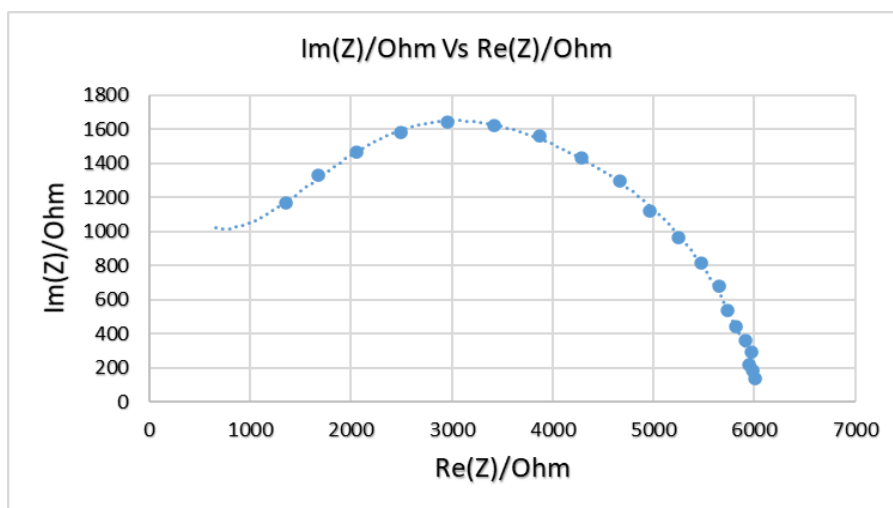


Figure 4.16: Nyquist plot for sample 9.

4.3.2. CV results. The CV test was performed to enable the investigation of the samples stability (oxidation/reduction reactions) and possible oxidation/reduction process, as shown in Figures (4.17 - 4.19), the samples do not have any peak in the plots. This means that there are no oxidation/reduction reactions taking place within the samples while applying the alternative voltage, so the samples are considered as stable samples. The charge storage capacity was calculated by integrating the cathodal portion of the graph (which is the negative current density enclosed within the Cyclic Voltammetry) as shown in Figure 4.17, and then dividing it by the scanning rate (10 mV/sec), the charge storage capacity was calculated and it is equal to (0.0730 C/cm²).

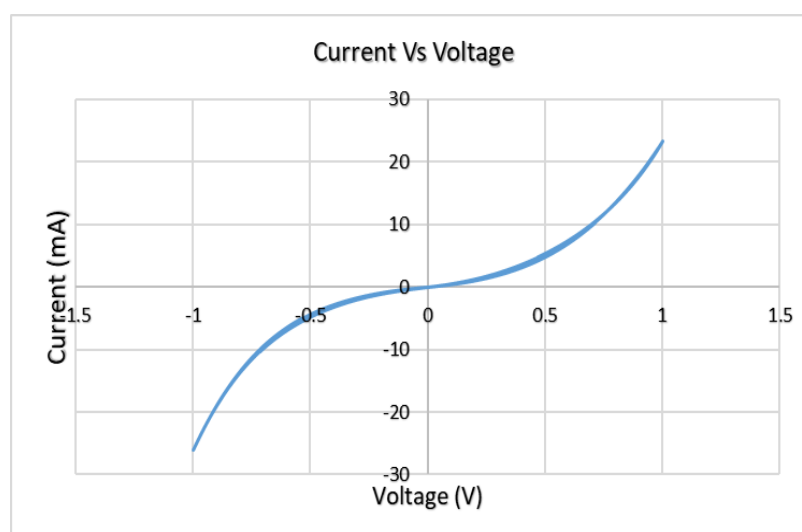


Figure 4.17: Cyclic Voltammetry for sample 7.

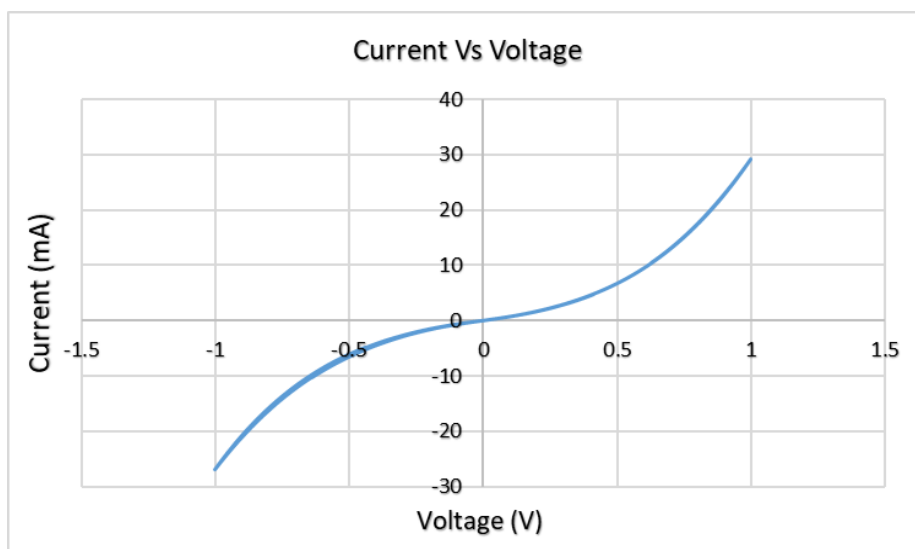


Figure 4.18: Cyclic Voltammetry for sample 8.

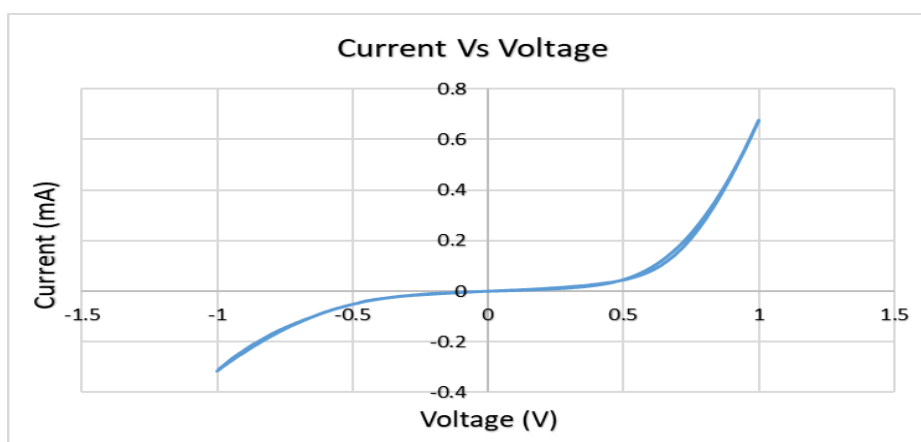


Figure 4.19: Cyclic Voltammetry for sample 9.

Table 4.7: A comparison table for charge density.

Composite	PANI (%)	Silicone (%)	Glycerol (%)	PMMA (%)	Charge density + reference
Sample 7	15 %	70 %	15 %	--	$9.9113 \times 10^3 \text{ C/ Cm}^2$
Sample 8	20 %	50 %	30 %	--	$1.3607 \times 10^4 \text{ C/ Cm}^2$
Sample 9	6 %	72 %	22 %	--	138.14 C/ Cm^2
Graphene	--	--	--	--	$1.42 \times 10^{-9} \text{ C/ Cm}^2$ [9]
Polyaniline	--	--	--	--	0.02 C/ Cm^2 [9]

By comparing the results of the prepared samples, sample 9 had highest charge density compared to the other prepared samples. As assumed, the result of sample 9 was compared with PANI [9], the result showed that the CSC of the sample 9 was much higher than that of PANI [9] from the literature, which indicates that it can store higher amount of current within the sample in one cycle.

4.3.3. Mechanical testing results. This test was used to measure the relationship between the stress and the strain of the prepared bioelectrode sample (sample 9) as shown in Figure 4.20. It shows that stress and strain are somehow related, the output seems to be linear until it hits the fraction point (break).

To find the young modulus, a straight line was drawn and by the aid of equation (2) the young modulus was calculated and it was equal to 75.312 MPa. A comparison between the mechanical properties of the fabricated electrode samples to those presented in the literature is shown in Table. 4.8.

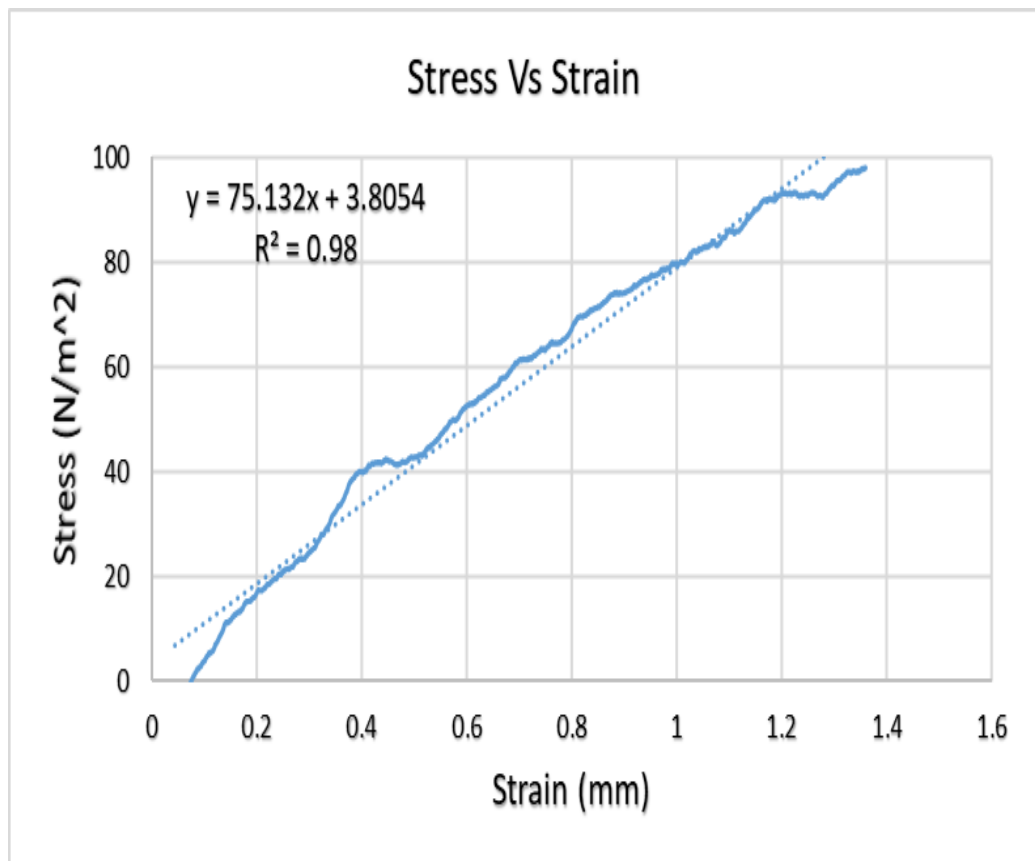


Figure 4.20: Stress of the material VS strain for the sample 9.

Table 4.8: Literature values for mechanical properties of conductive polymers.

Material	Sample 9	Skin tissue	PEDOT: PSS	Polyimide	Gold	Platinum	Polyaniline
Young Modulus (MPa)	75.312	83.33 ± 4.9 [122]	1800 ± 200	6000	69100	1400	N/A (Brittle material).
Elongation	---	---	$4.3 \pm 2.3\%$	<10%	---	35%	---

By comparing sample 9 with the previously prepared sample (sample 1); as predicted, the young modulus for sample 9 (75.312 MPa) was much higher than that of sample 1 (0.1468 MPa). A comparison between the tested prepared sample of PANI-silicone-glycerol and the skin tissue from the literature showed that the young modulus of the prepared sample (sample 9) was equal to 75.312 MPa and it was lower than that of the skin tissue 83.33 ± 4.9 MPa [122].

4.3.4. Long term impedance test results. This test was performed to investigate the effect of long-term implantation of the bioelectrode material properties; this test helped to understand how long the bioelectrode can stay within the body.

In order to assess the values on impedance, two samples were prepared. The samples composition was (0.25g PANI, 2.9g Silicone, and 0.9g Glycerol). Each sample was cut into four small pieces, then they were immersed in eight different tubes; each tube consists of 10.5mL of 10% PBS solution with three to four days test intervals. Before each test, the sample was separated from the tube and the weight of the sample was measured then left to dry for 15 minutes in the fume hood.

The EIS-CV-EIS test has been performed. The Weight changes are shown in Figure 4.21. The findings of the EIS-CV-EIS pre-CV and post-CV test are shown in Figures 4.22, 4.23 and 4.24.

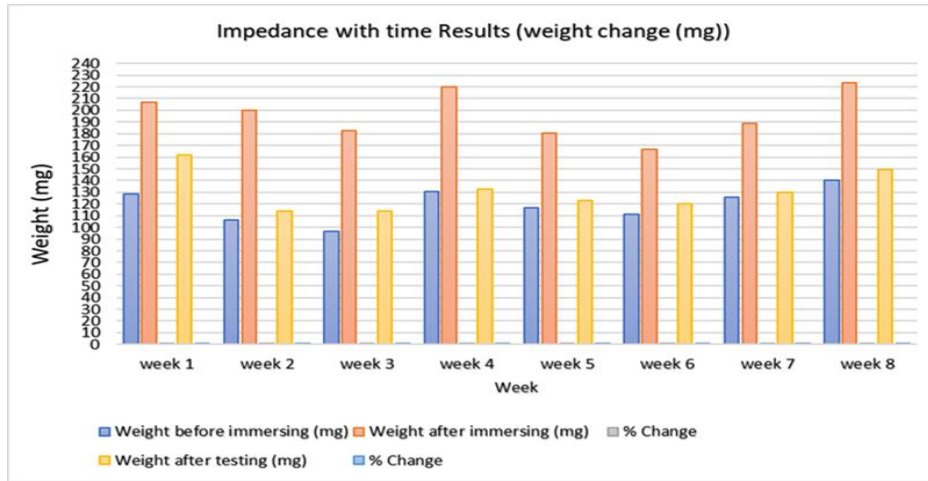


Figure 4.21: Change of samples weight over testing period.

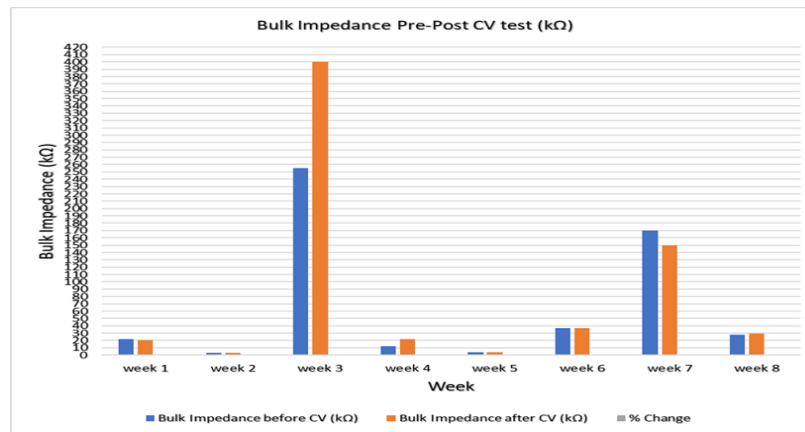


Figure 4.22: Change of bulk impedance in long-term samples pre/post CV test.

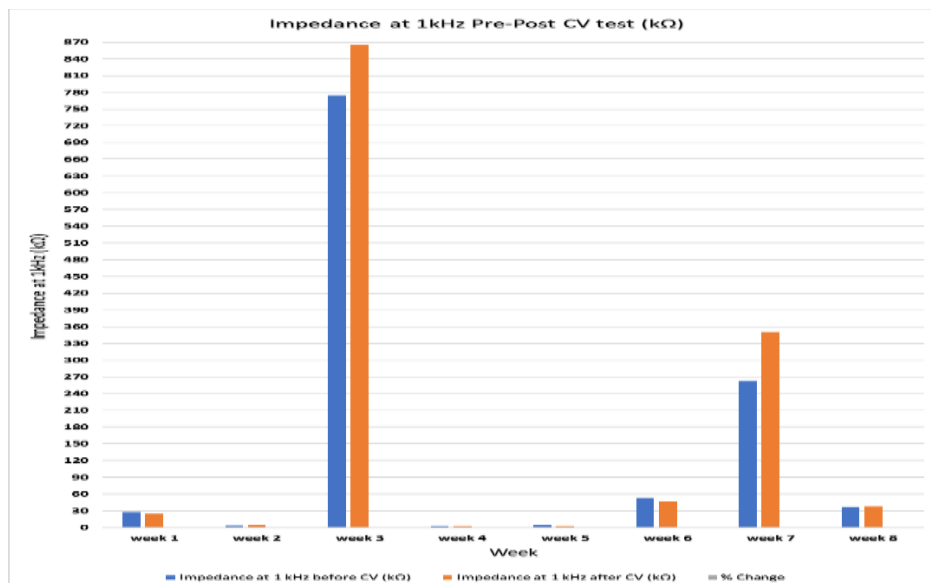


Figure 4.23: Change of impedance at 1 kHz in long-term samples pre/post CV test.

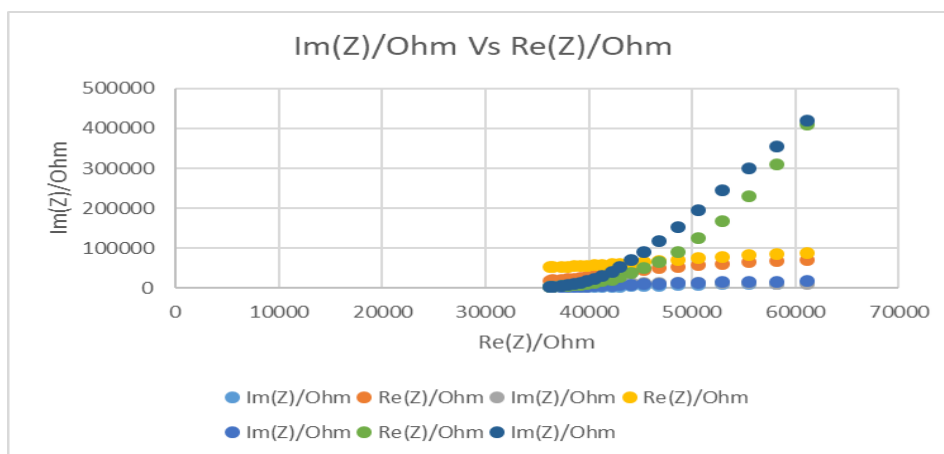


Figure 4.24: Displays resulting voltammograms from performing cyclic voltammetry on prepared samples after immersion in PBS.

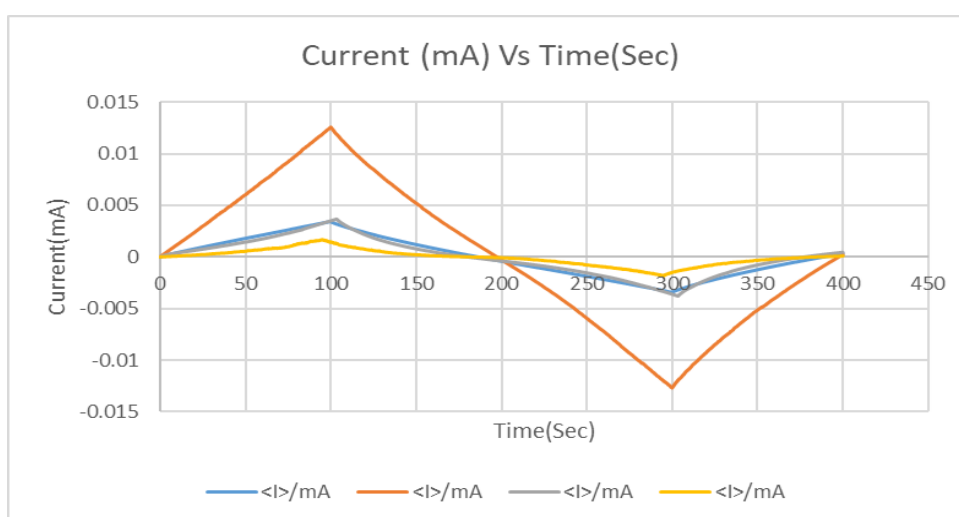


Figure 4.25: Displays the change of current density during the cyclic voltammetry test over 4 weeks of immersion.

The readings from Figure 4.25 are used to calculate the change of charge storage capacity over the immersion period, as shown in Table 4.9.

Table 4.9: Change of charge storage capacity in long-term PANI based samples.

Week	Charge storage capacity (C/cm^2)
1	0.6696 C/cm^2
2	2.9222 C/cm^2
3	0.0968 C/cm^2
4	9.1325 C/cm^2
5	0.9969 C/cm^2
6	2.2490 C/cm^2
7	0.9234 C/cm^2
8	2.5546 C/cm^2

As for the long-term testing of sample 9, the shape of the samples did not change during the immersion phase. The weight of the samples before and after immersion was measured, the weight after immersion increased in all samples due to the soaking of the PBS solution.

In terms of impedance, the bulk impedance has variation results over the immersion phase, which can be due to the soaking of the PBS solution, so the dimensions of the sample may change slightly (micro spaces); this change affected the electrochemical properties of the immersed sample (decreased the impedance). However, the impedance at 1 kHz and the CSC slightly varied during the immersion phase, yet there is no behaviour observed. This shows that the fabricated electrode sample can maintain resistant to alteration of electrochemical properties when subjected to body fluids.

4.4. Confidence Interval and ECG Test

In order to make sure that the given values of the fabricated electrodes were precise and accurate, a confidence interval test was performed with a composition similar to sample 9. Furthermore, to test the samples conductivity; the ECG test was performed. The results are shown in Figures (4. 27 - 4.29).

4.4.1. Confidence intervals. The 95% confidence is the value that can be 95% true to the fabricated samples that were prepared in this thesis. Before calculating the 95% confidence, the mean and the standard deviation should be found using equation (3 and 4), and their values were used in equation (5) to find the value of the 95% confidence.

The samples were prepared with a composition of (6 % PANI, 22 % Glycerol, and 72 % Silicone) using a circular mold as shown in Figure 4.26. The disk's dimensions are (radius= 9.415 mm, thickness= 2.87 mm). The EIS test was used to test and evaluate the electrochemical properties of the samples. The relationship between the impedance and frequency at 1kHz is shown in Figure 4.27.

$$\bar{x} \text{ (Mean)} = \frac{\sum Xi}{\text{The number of } x \text{ values } (n)} \quad (3)$$

$$S \text{ (Standard Deviation)} = \frac{\sqrt{(Xi-X)^2}}{n-1} \quad (4)$$

$$\mu \text{ (95\% confidence)} = \bar{x} - \frac{1.96\sigma}{\sqrt{n}} \leq \mu \leq \bar{x} + \frac{1.96\sigma}{\sqrt{n}} \quad (5)$$

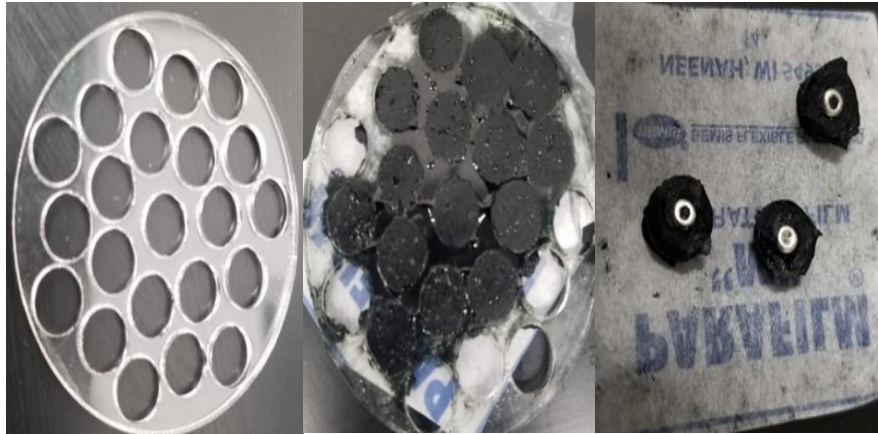


Figure 4.26: Bioelectrode sample consists of (6 % PANI, 22 % Glycerol, and 72 % Silicone).

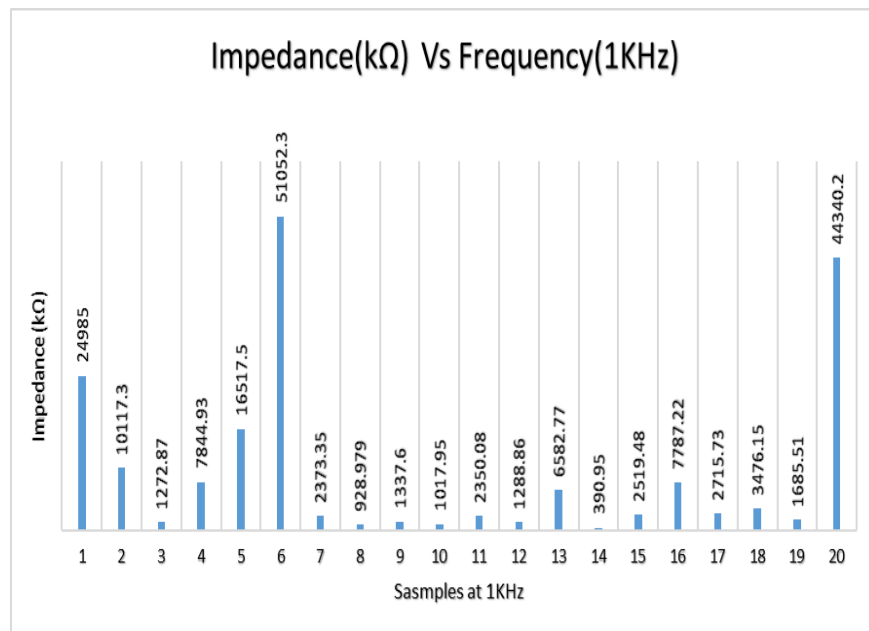


Figure 4.27: The relationship between the impedance and frequency at 1kHz for 20 Bioelectrode samples consists of (6% PANI, 22 % Glycerol, and 72% Silicone).

4.4.2. ECG test results. The purpose of this test was to conduct a simultaneous recording of electrocardiograph (ECG) using standard Ag-AgCl electrodes and the fabricated electrodes. To perform this test, three samples were taken from the mold (as shown in Figure 4.22). A metal conductive tip was placed within the electrode samples and the tip was connected to the ECG probes. Those three electrodes were placed on the participant limbs (two hands, right leg) and the other end was connected to the “PowerLab 26T”. The results were compared to the standard Ag-Agcl electrodes as shown in Figures 4.25, and Figure 4.26.

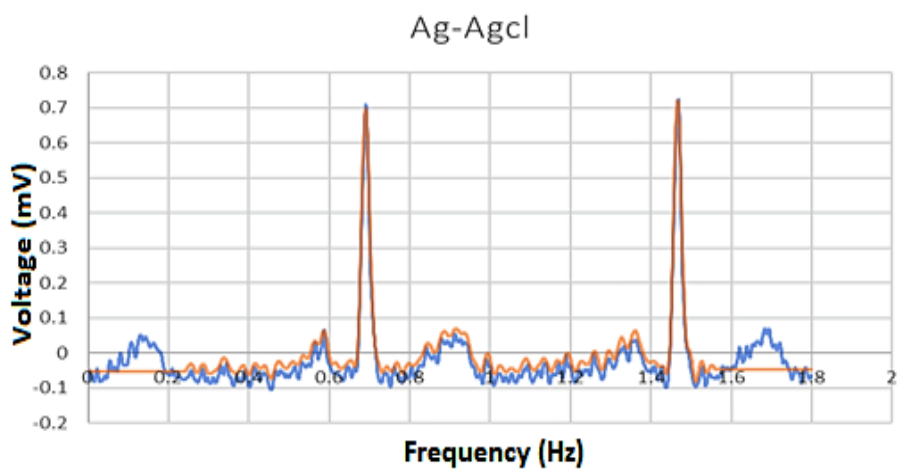


Figure 4.28: ECG result using the standard Ag-AgCl Electrodes (The blue graph is without filtering and the orange is after the filtering).

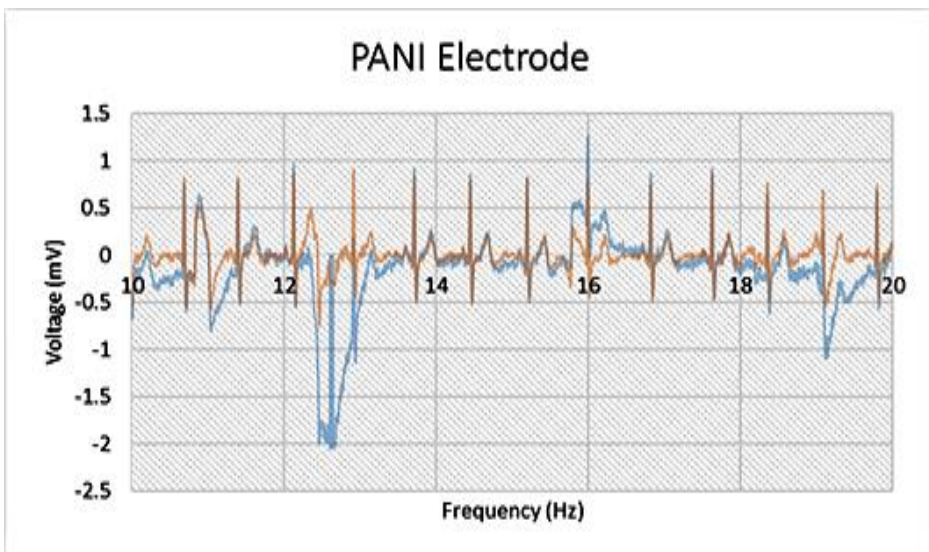


Figure 4.29: ECG result using the fabricated Electrodes (The blue graph is without filtering and the orange is after the filtering).

Regarding the confidence test and ECG test, several samples with same composition (sample 9) were prepared and tested for their electrochemical properties. The confidence interval result was $9529.23645 \pm 6333.7015 \Omega$. An ECG comparison between the fabricated PANI electrodes and the standard Ag-AgCl electrodes was done as shown in Figure 4.25 and Figure 4.26. The ECG result using the fabricated electrodes was promising, but the signal to noise ratio is a bit higher than the standard Ag-AgCl electrodes; the reason could be due to the motion artifact or the 50 Hz noise within the room.

Throughout this section, the EIS test showed that the electrochemical properties for sample 9 have been improved compared to other samples. The bulk impedance has been reduced from 4 k Ω to 600 Ω , the impedance at 1 kHz has been reduced from 28.4 k Ω to 1.6 k Ω , and the conductivity increased from 8.33x10⁻⁸ S/cm to 5.55x10⁻⁷ S/cm because of the change in dimension, decreasing of PANI concentration, and increasing of the glycerol. In terms of charge storage capacity, the CSC has been increased from 4.3124 C/ Cm² to 138.14 C/ Cm². The mechanical properties have been increased from 0.1468 MPa to 75.312 MPa, compared to the skin tissue young modulus 83.33 \pm 4.9 MPa [122]; the mechanical properties of sample 9 was promising, so it has been selected as the best sample.

Throughout the thesis, the experimental findings from the fabricated PANI, Silicone, Glycerol samples, and their combination with PMMA demonstrated improved electrochemical properties compared to the literature. The bulk impedance of the prepared samples was equivalent to that of graphene and Poly-aniline-coated foam electrodes. In terms of impedance at 1 kHz, the experimental results of the fabricated materials were comparable to the conductive polymers such as Poly-aniline-coated foam electrodes.

Chapter 5. Conclusions and Future Work

In conclusion, the purpose of this thesis was to fabricate a flexible implantable electrode based on conductive polymer (PANI) and silicone. Two types of electrode materials were prepared: PANI, PMMA, and Glycerol in addition to a mixture of PANI, Glycerol, and PMMA all supported on silicone.

To find the best combination of these materials, eleven samples with different compositions were prepared and tested, such as sample 1 and sample 9. The EIS was used to test and evaluate the electrochemical properties of the bioelectrodes, the results were $4\text{ k}\Omega$ and $600\ \Omega$ respectively. The results were compared to the literature for some materials such as PEDOT: PSS, metals, and Polyaniline-coated foam electrodes. The Cyclic Voltammetry test were used to test the stability of the sample and to calculate the charge density, the results were 4.3124 C/ Cm^2 and 138.14 C/ Cm^2 respectively. Moreover, the mechanical test was performed to calculate the Young Modulus of the samples; the mechanical properties for sample 1 and sample 9 were the most distinguished properties, with higher elasticity and ductility, and the results were 0.1468 MPa and 75 MPa respectively. Compared to conductive polymers and metals, the elasticity modulus was $1.8 \pm 0.2\text{ GPa}$, while the fabricated samples were 0.1468 MPa and 75.312 MPa respectively. The comparison also showed that the fabricated electrodes were promising compared to the body skin tissue which is equal to $83.33 \pm 4.9\text{ MPa}$. More research was conducted to improve the electrochemical properties of the fabricated electrode samples, prepare more samples, analyze them, and enhance their mechanical properties. The long-term stability of the implantable electrodes was studied and evaluated. The obtainable results showed promising electrochemical impedance. The ECG Test for the fabricated electrodes was performed and the results are as capable as the Ag-AgCl electrodes.

For future work, it is recommended to focus on further optimization of the Sample's composition and their electrochemical properties. More work is recommended to improve the mechanical properties of the prepared samples ECG testing to get results without signal to noise ratios either by using these fabricated electrodes or new fabricated materials. It is also recommended to study more materials (thermoplastic polymer (PPMA) bind with stainless-steel, PMMA, and PANI bind with stainless-steel,

PMMA + PANI + Silicon bind with stainless-steel. Moreover, the fabricated sample can be studied after implanting in animals for further testing.

References

- [1] S. F. Cogan, "Neural stimulation and recording electrodes," *Annual Review of Biomedical Engineering*, vol. 10, pp. 275-309, 2008, doi: 10.1146/annurev.bioeng.10.061807.160518.
- [2] B. D. Ratner, A. S. Hoffman, M. J. Yaszemski, J. E. Lemons, and F. J. Schoen, *Biomaterials Science: An Introduction to Materials in Medicine*. San Diego, United States: Elsevier Science & Technology, 2012, pp. 957-991.
- [3] N. Muthukumar, G. Thilagavathi, and T. Kannaian, "Polyaniline-coated foam electrodes for electroencephalography (EEG) measurement," *Journal of The Textile Institute*, vol. 107, no. 3, pp. 283-290, 2016, doi: 10.1080/00405000.2015.1028248.
- [4] Z. Wang, J. Xu, Y. Yao, L. Zhang, Y. Wen, H. Song, D. Zhu, "Facile preparation of highly water-stable and flexible PEDOT: PSS organic/inorganic composite materials and their application in electrochemical sensors," *Sensors and Actuators B: Chemical*, vol. 196, pp. 357-369, 2014, doi: 10.1016/j.snb.2014.02.035.
- [5] A. Al-Othman, A. Y. Tremblay, W. Pell, S. Letaief, Y. Liu, B. A. Peppley, M. Ternan, "A modified silicic acid (Si) and sulphuric acid (S)-ZrP/PTFE/glycerol composite membrane for high temperature direct hydrocarbon fuel cells," *Journal of Power Sources*, vol. 224, pp. 158-167, 2013, doi: 10.1016/j.jpowsour.2012.09.067.
- [6] K. C. Cheung, P. Renaud, H. Tanila, and K. Djupsund, "Flexible polyimide microelectrode array for in vivo recordings and current source density analysis," *Biosens Bioelectron*, vol. 22, no. 8, pp. 1783-1790, 2007, doi: 10.1016/j.bios.2006.08.035.
- [7] A. Al-Othman, A. Alatoon, A. Farooq, M. Al-Sayah and H. Al-Nashash, "Novel flexible implantable electrodes based on conductive polymers and Titanium dioxide," *2018 IEEE 4th Middle East Conference on Biomedical Engineering (MECBME), Tunis, Tunisia*, 2018, pp. 30-33, doi: 10.1109/MECBME.2018.8402401.
- [8] E. N. Marieb, *Essentials of human anatomy & physiology*. Harlow: Pearson Education, 2015, pp. 225-238.
- [9] M. P. McKinley and V. D. O'Loughlin, *Human anatomy*. New York: McGraw-Hill, 2012, pp. 412-426.
- [10] M. R. Taylor, E. J. Simon, J. Dickey, K. A. Hogan, J. B. Reece, and N. A. Campbell, *Campbell biology: concepts & connections*. New York, NY, PEARSON EDUCATION Limited, 2018, pp. 130-140.
- [11] K. Scholten, E. Meng, G. Knaack, and D. Song, "Interfacing with the Peripheral Nervous System," *Journal of Neuroscience Methods*, vol. 340, no. 108745, pp. 1-2, 2020, doi: 10.1016/j.jneumeth.2020.108745.

- [12] P. Li, H. P. Anwar Ali, W. Cheng, J. Yang, and B. C. K. Tee, “Bioinspired Prosthetic Interfaces,” *Advanced Materials Technologies*, vol. 5, no. 3, pp. 1-32, 2020, doi: 10.1002/admt.201900856.
- [13] S. Mishra, “Electroceuticals in medicine – The brave new future,” *Indian Heart Journal*, vol. 69, no. 5, pp. 685-686, 2017, doi: 10.1016/j.ihj.2017.10.001.
- [14] B. J. Seicol, S. Bejarano, N. Behnke, and L. Guo, “Neuromodulation of metabolic functions: From pharmaceuticals to bioelectronics to biocircuits,” *Journal of Biological Engineering*, vol. 13, no. 67, pp. 1-12, 2019, doi: 10.1186/s13036-019-0194-z.
- [15] C. Günter, J. Delbeke, and M. Ortiz-Catalan, “Correction to: Safety of long-term electrical peripheral nerve stimulation: review of the state of the art,” *Journal of NeuroEngineering and Rehabilitation*, vol. 17, no. 1, pp. 1-16, 2020, doi: 10.1186/s12984-020-00695-1.
- [16] A. M. Dingle, J. P. Ness, J. Novello, J. S. Israel, R. Sanchez, A. X.t. Millevolte, S. Brodnick, L. Krugner-Higby, B. Nemke, Y. Lu, A. J. Suminski, M. D. Markel, J. C. Williams, S. O. Poore, “Methodology for creating a chronic osseointegrated neural interface for prosthetic control in rabbits,” *Journal of Neuroscience Methods*, vol. 331, no. 108504, pp. 1-9, 2020, doi: 10.1016/j.jneumeth.2019.108504.
- [17] S. Niketeghad and N. Pouratian, “Brain Machine Interfaces for Vision Restoration: The Current State of Cortical Visual Prosthetics,” *Journal of Neurotherapeutics*, vol. 16, no. 1, pp. 134-143, 2019, doi: 10.1007/s13311-018-0660-1.
- [18] U. Ghafoor, S. Kim, and K. S. Hong, “Selectivity and longevity of peripheral-nerve and machine interfaces: A review,” *Frontiers in Neurorobotics*, vol. 11, no. 59, pp. 1-21, 2017, doi: 10.3389/fnbot.2017.00059.
- [19] K. Z. Zhuang, N. Sommer, V. Mendez, S. Aryan, E. Formento, E. D’Anna, F. Artoni, F. Petrini, G. Granata, G. Cannaviello, W. Raffoul, A. Billard, and S. Micera, “Shared human–robot proportional control of a dexterous myoelectric prosthesis,” *Nature Machine Intelligence*, vol. 1, no. 9, pp. 400-411, 2019, doi: 10.1038/s42256-019-0093-5.
- [20] A. Krasoulis, S. Vijayakumar, and K. Nazarpour, “Effect of User Practice on Prosthetic Finger Control With an Intuitive Myoelectric Decoder,” *Frontiers in Neuroscience*, vol. 13, no. 891, pp. 1-16, 2019, doi: 10.3389/fnins.2019.00891.
- [21] C. Igual, L. A. Pardo, J. M. Hahne, and J. Igual, “Myoelectric control for upper limb prostheses,” *Electronics*, vol. 8, no. 11, pp. 1-21, 2019, doi: 10.3390/electronics8111244.
- [22] S. Ramachandran and R. Midha, “Recent advances in nerve repair,” *Neurology India*, vol. 67, no. 7, pp. 106, 2019, doi: 10.4103/0028-3886.250702.
- [23] A. D. Roche, B. Lakey, I. Mendez, I. Vujaklija, D. Farina, and O. C. Aszmann, “Clinical Perspectives in Upper Limb Prostheses: An Update,” *Current Surgery Reports*, vol. 7, no. 5, pp. 1-10, 2019, doi: 10.1007/s40137-019-0227-z.

- [24] T. J. Bates, J. R. Fergason, and S. N. Pierrie, "Technological Advances in Prosthesis Design and Rehabilitation Following Upper Extremity Limb Loss," *Current Reviews in Musculoskeletal Medicine*, vol. 13, no. 4, pp. 485-493, 2020, doi: 10.1007/s12178-020-09656-6.
- [25] S. Raspopovic, A. Cimolato, A. Panarese, F. Vallone, J. D. Valle, S. Micera, and X. Navarro, "Neural signal recording and processing in somatic neuroprosthetic applications. A review," *Journal of Neuroscience Methods*, vol. 337, no. 108653, pp. 1-13, 2020, doi: 10.1016/j.jneumeth.2020.108653.
- [26] W. Li and Z. Yang, "An Animal Spinal Cord Neural Signal Regeneration Circuit," *Journal of Physics: Conference Series*, vol. 1237, no. 3, no. 032076, pp. 1-6, 2019, doi: 10.1088/1742-6596/1237/3/032076.
- [27] Q. Zhang, H. Yu, M. Barbiero, B. Wang, and M. Gu, "Artificial neural networks enabled by nanophotonics," *Light: Science and Applications*, vol. 8, no. 42, pp. 1-14, 2019, doi: 10.1038/s41377-019-0151-0.
- [28] L. H. Madkour, "Interfacing Biology Systems with Nanoelectronics for Nanodevices," *Advanced Structured Materials*, vol. 116, pp. 701-759, 2019.
- [29] G. H. Kim, K. Kim, E. Lee, T. An, W. Choi, G. Lim, and J. Shin, "Recent progress on microelectrodes in neural interfaces," *Materials*, vol. 11, no. 10, pp. 1995, 2018, doi: 10.3390/ma11101995.
- [30] A. Stampas, R. Korupolu, L. Zhu, C. P. Smith, and K. Gustafson, "Safety, Feasibility, and Efficacy of Transcutaneous Tibial Nerve Stimulation in Acute Spinal Cord Injury Neurogenic Bladder: A Randomized Control Pilot Trial," *Neuromodulation*, vol. 22, no. 6, pp. 716-722, 2019, doi: 10.1111/ner.12855.
- [31] Y. Zhong, B. Qian, Y. Zhu, Z. Ren, J. Deng, J. Liu, Q. Bai, and X. Zhang, "Development of an Implantable Wireless and Batteryless Bladder Pressure Monitor System for Lower Urinary Tract Dysfunction," *IEEE Journal of Translational Engineering in Health and Medicine*, vol. 8, pp. 1-7, 2020, doi: 10.1109/JTEHM.2019.2943170.
- [32] S. Hajebrahimi, C. R. Chapple, F. Pashazadeh, and S. Pourmehr, "Management of neurogenic bladder in patients with parkinson's disease: A systematic review," *Neurol Urodynamics*, vol. 38, pp. 31-62, 2019.
- [33] J. Gil-Castillo, F. Alnajjar, A. Koutsou, D. Torricelli, and J. C. Moreno, "Advances in neuroprosthetic management of foot drop: A review," *Journal of NeuroEngineering and Rehabilitation*, vol. 17, no. 46, pp. 1-19, 2020, doi: 10.1186/s12984-020-00668-4.
- [34] L. Meng, U. Martinez-Hernandez, C. Childs, A. A. Dehghani-Sani, and A. Buis, "A Practical Gait Feedback Method Based on Wearable Inertial Sensors for a Drop Foot Assistance Device," *IEEE Sensors Journal*, vol. 19, no. 24, pp. 12235-12243, 2019, doi: 10.1109/JSEN.2019.2938764.
- [35] J. Yang and J. H. Phi, "The present and future of vagus nerve stimulation," *Journal of Korean Neurosurgical Society*, vol. 62, no. 3, pp. 344-352, 2019, doi: 10.3340/jkns.2019.0037.

- [36] A. Broncel, R. Bocian, P. Kłos-Wojtczak, K. Kulbat-Warycha, and J. Konopacki, "Vagal nerve stimulation as a promising tool in the improvement of cognitive disorders," *Brain Research Bulletin*, vol. 155, pp. 37-47, 2020, doi: 10.1016/j.brainresbull.2019.11.011.
- [37] J. Zhu, T. Zhang, Y. Yang, and R. Huang, "A comprehensive review on emerging artificial neuromorphic devices," *Applied Physics Reviews*, vol. 7, no. 1, pp. 011312, 2020, doi: 10.1063/1.5118217.
- [38] H. Lim, H. S. Kim, R. Qazi, Y. Kwon, J. Jeong, and W. Yeo, "Wearable Flexible Hybrid Electronics: Advanced Soft Materials, Sensor Integrations, and Applications of Wearable Flexible Hybrid Electronics in Healthcare, Energy, and Environment (Adv. Mater. 15/2020)," *Advanced Materials*, vol. 32, no. 15, pp. 2070116, 2020, doi: 10.1002/adma.202070116.
- [39] A. S. Dhawan, B. Mukherjee, S. Patwardhan, N. Akhlaghi, G. Diao, G. Levay, R. Holley, W. M. Joiner, M. Harris-Love, and S. Sikdar, "Proprioceptive Sonomyographic Control: A novel method for intuitive and proportional control of multiple degrees-of-freedom for individuals with upper extremity limb loss," *Scientific Reports*, vol. 9, no. 9499, pp. 1-15, 2019, doi: 10.1038/s41598-019-45459-7.
- [40] T. Kapelner, M. Sartori, F. Negro, and D. Farina, "Neuro-Musculoskeletal Mapping for Man-Machine Interfacing," *Scientific Reports*, vol. 10, no. 5834, pp. 1-10, 2020, doi: 10.1038/s41598-020-62773-7.
- [41] M. Stachaczyk, S. F. Atashzar, S. Dupan, I. Vujaklija, and D. Farina, "Toward Universal Neural Interfaces for Daily Use: Decoding the Neural Drive to Muscles Generalises Highly Accurate Finger Task Identification across Humans," *IEEE Access*, vol. 8, pp. 149025- 149035, 2020, doi: 10.1109/ACCESS.2020.3015761.
- [42] A. Ameri, M. A. Akhaee, E. Scheme, and K. Englehart, "Regression convolutional neural network for improved simultaneous EMG control," *Journal of Neural Engineering*, vol. 16, no. 3, pp. 036015, 2019, doi: 10.1088/1741-2552/ab0e2e.
- [43] B. Gesslbauer, L. A. Hruby, A. D. Roche, D. Farina, R. Blumer, and O. C. Aszmann, "Axonal components of nerves innervating the human arm," *Annals of Neurology*, vol. 82, no. 3, pp. 396-408, 2017, doi: 10.1002/ana.25018.
- [44] J. A. George, D. T. Kluger, T. S. Davis, S. M. Wendelken, E. V. Okorokova, Q. He, C. C. Duncan, D. T. Hutchinson, Z. C. Thumser, D. T. Beckler, P. D. Marasco, S. J. Bensmaia, G. A. Clark, "Biomimetic sensory feedback through peripheral nerve stimulation improves dexterous use of a bionic hand," *Science Robotics*, vol. 4, no. 32, pp. 1-12, 2019, doi: 10.1126/scirobotics. aax2352.
- [45] F. Clemente, G. Valle, M. Controzzi, I. Strauss, F. Iberite, T. Stieglitz, G. Granata, P. Rossini, F. Petrini, S. Micera, and C. Cipriani "Intraneural sensory feedback restores grip force control and motor coordination while using a prosthetic hand," *Journal of Neural Engineering*, vol. 16, no. 2, pp. 026034, 2019, doi: 10.1088/1741-2552/ab059b.

- [46] H. Kim, A. Dingle, J. Ness, D. Baek, J. Bong, I. Lee, N. O. Shulzhenko, W. Zeng, J. S. Israel, J. A. Pisaniello, A. X.t. Millevolte, D. Park, A. J. Suminski, J. C. Williams, S. O. Poore, and Z. Ma “Cuff and sieve electrode (CASE): The combination of neural electrodes for bi-directional peripheral nerve interfacing,” *Journal of Neuroscience Methods*, vol. 336, pp. 108602, 2020, doi: 10.1016/j.jneumeth.2020.108602.
- [47] K. Noblett and N. T. Sudol, "Peripheral nerve evaluation," in *Adult and Pediatric Neuromodulation*, Springer International Publishing 2018, pp. 63-73.
- [48] S. Park, G. Loke, Y. Fink, and P. Anikeeva, “Flexible fiber-based optoelectronics for neural interfaces,” *Chemical Society Reviews*, vol. 48, no. 6. pp. 1826- 1852, 2019, doi: 10.1039/c8cs00710a.
- [49] C. Russell, A. D. Roche, and S. Chakrabarty, “Peripheral nerve bionic interface: a review of electrodes,” *International Journal of Intelligent Robotics and Applications*, vol. 3, no. 1, pp. 11-18, 2019, doi: 10.1007/s41315-019-00086-3.
- [50] N. Cram, "Medical Instrumentation, Application & Design," 3rd ed. Reading, by John G. Webster, *Annals of Biomedical Engineering*, vol. 28, no. 2, pp. 218, 2000.
- [51] X. Navarro, T. B. Krueger, N. Lago, S. Micera, T. Stieglitz, and P. Dario, “A critical review of interfaces with the peripheral nervous system for the control of neuroprostheses and hybrid bionic systems,” *Journal of the Peripheral Nervous System*, vol. 10, no. 3, pp. 229-258, 2005, doi: 10.1111/j.1085-9489.2005.10303. x.
- [52] S. Zhao, X. Liu, Z. Xu, H. Ren, B. Deng, M. Tang, L. Lu, X. Fu, H. Peng, Z. Liu, and X. Duan, “Graphene Encapsulated Copper Microwires as Highly MRI Compatible Neural Electrodes,” *Nano Letters*, vol. 16, no. 12, pp. 7731–7738, 2016, doi: 10.1021/acs.nanolett.6b03829.
- [53] K. A. Ludwig, N. B. Langhals, M. D. Joseph, S. M. Richardson-Burns, J. L. Hendricks, and D. R. Kipke, “Poly(3,4-ethylenedioxythiophene) (PEDOT) polymer coatings facilitate smaller neural recording electrodes,” *Journal of Neural Engineering*, vol. 8, no. 014001, pp. 1-14, 2011, doi: 10.1088/1741-2560/8/1/014001.
- [54] M. Frankel, “Peripheral Nerve Interface, Intraneural Electrode,” *Encyclopedia of Computational Neuroscience*, pp. 1-3, 2014.
- [55] K. P. Hoffmann, K. P. Koch, T. Doerge, and S. Micera, “New technologies in manufacturing of different implantable microelectrodes as an interface to the peripheral nervous system,” *Proceedings of the First IEEE/RAS-EMBS International Conference on Biomedical Robotics and Biomechatronics*, 2006, pp. 414-419, doi: 10.1109/BIOROB.2006.1639123.
- [56] T. A. Park and G. F. Harris, “Guided” intramuscular fine wire electrode placement: A new technique,” *American Journal of Physical Medicine & Rehabilitation*, vol. 75, no. 3, pp. 232-234, 1996, doi: 10.1097/00002060-199605000-00018.
- [57] W. D. Memberg, P. H. Peckham, and M. W. Keith, “A Surgically-Implanted Intramuscular Electrode for an Implantable Neuromuscular Stimulation

- System,” *IEEE Transactions on Rehabilitation Engineering*, vol. 2, no. 2, pp. 80-91, 1994, doi: 10.1109/86.313149.
- [58] A. Prusinowska, A. Komorowski, and P. Syrówka, “The use of surface electromyography in rehabilitating rheumatic patients after knee arthroplasty (pilot study),” *Reumatologia/Rheumatology*, vol. 57, no. 4, pp. 199-206, 2019, doi: 10.5114/reum.2019.87613.
- [59] M. A. Lebedev and M. A. L. Nicolelis, “Brain-machine interfaces: past, present and future,” *Trends in Neurosciences*, vol. 29, no. 9, pp. 536-546, 2006, doi: 10.1016/j.tins.2006.07.004.
- [60] J. P. Donoghue, A. Nurmikko, M. Black, and L. R. Hochberg, “Assistive technology and robotic control using motor cortex ensemble-based neural interface systems in humans with tetraplegia,” *Journal of Physiology*, vol. 579, no. 3, pp. 603-611, 2007, doi: 10.1113/jphysiol.2006.127209.
- [61] D. McCreery, A. Lossinsky, V. Pikov, and X. Liu, “Microelectrode array for chronic deep-brain microstimulation and recording,” *IEEE Transactions on Biomedical Engineering*, vol. 53, no. 4, pp. 726- 737, 2006, doi: 10.1109/TBME.2006.870215.
- [62] B. J. Gluckman, H. Nguyen, S. L. Weinstein, and S. J. Schiff, “Adaptive electric field control of epileptic seizures,” *Acta Neurologica Scandinavica*, vol. 21, no. 2, pp. 5-52, 2001, doi: 10.1523/jneurosci.21-02-00590.2001.
- [63] R. D. Meyer, S. F. Cogan, T. H. Nguyen, and R. D. Rauh, “Electrodeposited iridium oxide for neural stimulation and recording electrodes,” *IEEE Transactions on Neural Systems and Rehabilitation Engineering*, vol. 9, no. 1, pp. 2-11, 2001, doi: 10.1109/7333.918271.
- [64] J. D. Weiland and D. J. Anderson, “Chronic neural stimulation with thin-film, iridium oxide electrodes,” *IEEE Transactions on Biomedical Engineering*, vol. 47, no. 7, pp. 911-918, 2000, doi: 10.1109/10.846685.
- [65] L. Ghasemi-Mobarakeh, M. P. Prabhakaran, M. Morshed, M. H. Nasr-Esfahani, H. Baharvand, S. Kiani, S. S. Al-Deyab, and S. Ramakrishna, “Application of conductive polymers, scaffolds and electrical stimulation for nerve tissue engineering,” *Journal of Tissue Engineering and Regenerative Medicine*, vol. 5, no. 4, pp. 17-35, 2011, doi: 10.1002/term.383.
- [66] L. A. Geddes and R. Roeder, “Criteria for the selection of materials for implanted electrodes,” *Annals of Biomedical Engineering*, vol. 31, no. 7, pp. 879-890, 2003, doi: 10.1114/1.1581292.
- [67] R. W. Griffith and D. R. Humphrey, “Long-term gliosis around chronically implanted platinum electrodes in the Rhesus macaque motor cortex,” *Neuroscience Letters*, vol. 406, no. 1-2, pp. 81-86, 2006, doi: 10.1016/j.neulet.2006.07.018.
- [68] E. M. Hudak, D. W. Kumsa, H. B. Martin, and J. T. Mortimer, “Electron transfer processes occurring on platinum neural stimulating electrodes: Calculated charge-storage capacities are inaccessible during applied stimulation,” *Journal of Neural Engineering*, vol. 14, no. 046012, pp. 1-16, 2017, doi: 10.1088/1741-2552/aa6945.

- [69] C. Im and J. M. Seo, "A review of electrodes for the electrical brain signal recording," *Biomedical Engineering Letters*, vol. 6, no. 3, pp. 104-112, 2016, doi: 10.1007/s13534-016-0235-1.
- [70] G. Márton, G. Orbán, M. Kiss, R. Fiáth, A. Pongrácz, and I. Ulbert, "A multimodal, SU-8 - Platinum - Polyimide microelectrode array for chronic in vivo neurophysiology," *Plos One*, vol. 10, no. 12, pp. 1-16, 2015, doi: 10.1371/journal.pone.0145307.
- [71] F. Lotti, F. Ranieri, G. Vadalà, L. Zollo, and G. Di Pino, "Invasive intraneural interfaces: Foreign body reaction issues," *Frontiers in Neuroscience*, vol. 11, pp. 1-14, 2017, doi: 10.3389/fnins.2017.00497.
- [72] N. Yi and M. R. Abidian, "Conducting polymers and their biomedical applications," in *Biosynthetic Polymers for Medical Applications*, Elsevier Inc., Elsevier Inc., 2016, pp. 243-276.
- [73] A. de Leon and R. C. Advincula, "Conducting Polymers with Superhydrophobic Effects as Anticorrosion Coating," in *Intelligent Coatings for Corrosion Control*, Elsevier Inc., 2015, pp. 409-430.
- [74] H. Liu, J. Ge, E. Ma, and L. Yang, "Advanced biomaterials for biosensor and theranostics," in *Biomaterials in Translational Medicine: A Biomaterials Approach*, Elsevier, 2018, pp.213-255.
- [75] A. Borriello, V. Guarino, L. Schiavo, M. A. Alvarez-Perez, and L. Ambrosio, "Optimizing PANi doped electroactive substrates as patches for the regeneration of cardiac muscle," *Journal of Materials Science: Materials in Medicine*, vol. 22, no. 4, pp. 1053-1062, 2011, doi: 10.1007/s10856-011-4259-x.
- [76] N. Yusoff, "Graphene-polymer modified electrochemical sensors," in *Graphene-Based Electrochemical Sensors for Biomolecules: A Volume in Micro and Nano Technologies*, Elsevier, 2018, pp. 155-186.
- [77] P. K. Prabhakar, S. Raj, P. R. Anuradha, S. N. Sawant, and M. Doble, "Biocompatibility studies on polyaniline and polyaniline-silver nanoparticle coated polyurethane composite," *Colloids and Surfaces B: Biointerfaces*, vol. 86, no. 1, pp. 146-153, 2011, doi: 10.1016/j.colsurfb.2011.03.033.
- [78] X. Feng, G. Yang, Q. Xu, W. Hou, and J. J. Zhu, "Self-assembly of polyaniline/Au composites: From nanotubes to nanofibers," *Macromolecular Rapid Communications*, vol. 27, no. 1, pp. 31-36, 2006, doi: 10.1002/marc.200500642.
- [79] K. Arshak and O. Korostynska, "Investigation of Thick-Film Polyaniline-Based Conductimetric pH Sensors for Medical Applications," *IEEE Sensors Journal*, vol. 9, no. 5, pp. 555-562, 2009, doi: 10.1109/JSEN.2009.2016608.
- [80] A. Ramanavičius, A. Ramanavičiene, and A. Malinauskas, "Electrochemical sensors based on conducting polymer-polypyrrole," *Electrochimica Acta*, vol. 51, no. 27, pp. 6025-6037, 2006, doi: 10.1016/j.electacta.2005.11.052.

- [81] J. Ge, E. Neofytou, T. J. Cahill, R. E. Beygui, and R. N. Zare, "Drug release from electric-field-responsive nanoparticles," *ACS Nano*, vol. 6, no. 1, pp. 227-233, 2012, doi: 10.1021/nn203430m.
- [82] N. Gomez and C. E. Schmidt, "Nerve growth factor-immobilized polypyrrole: Bioactive electrically conducting polymer for enhanced neurite extension," *Journal of Biomedical Materials Research Part A*, vol. 81, no. 1, pp. 135-149, 2007, doi: 10.1002/jbm.a.31047.
- [83] D. Kai, M. P. Prabhakaran, G. Jin, and S. Ramakrishna, "Polypyrrole-contained electrospun conductive nanofibrous membranes for cardiac tissue engineering," *Journal of Biomedical Materials Research Part A*, vol. 99 A, no. 3, pp. 376-385, 2011, doi: 10.1002/jbm.a.33200.
- [84] R. Balint, N. J. Cassidy, and S. H. Cartmell, "Conductive polymers: Towards a smart biomaterial for tissue engineering," *Acta Biomaterialia*, vol. 10, no. 6, pp. 2341-2353, 2014, doi: 10.1016/j.actbio.2014.02.015.
- [85] W. F. Quirós-Solano, N. Gaio, C. Silvestri, G. Pandraud, and P. M. Sarro, "PEDOT: PSS: A Conductive and Flexible Polymer for Sensor Integration in Organ-on-Chip Platforms," *Procedia Engineering*, vol. 168, pp. 1184-1187, 2016, doi: 10.1016/j.proeng.2016.11.401.
- [86] U. Lang, N. Naujoks, and J. Dual, "Mechanical characterization of PEDOT: PSS thin films," *Synthetic Metals*, vol. 159, no. 5-6, pp. 473-479, 2009, doi: 10.1016/j.synthmet.2008.11.005.
- [87] D. Mantione, I. del Agua, A. Sanchez-Sanchez, and D. Mecerreyes, "Poly(3,4-ethylenedioxythiophene) (PEDOT) derivatives: Innovative conductive polymers for bioelectronics," *Polymers*, vol. 9, no. 8, pp. 354, 2017, doi: 10.3390/polym9080354.
- [88] N. Rozlosnik, "New directions in medical biosensors employing poly(3,4-ethylenedioxy thiophene) derivative-based electrodes," *Analytical and Bioanalytical Chemistry*, vol. 395, no. 3, pp. 637-645, 2009, doi: 10.1007/s00216-009-2981-8.
- [89] X. T. Cui and D. D. Zhou, "Poly (3,4-ethylenedioxythiophene) for chronic neural stimulation," *IEEE Transactions on Neural Systems and Rehabilitation*, vol. 15, no. 4, pp. 502-508, 2007, doi: 10.1109/TNSRE.2007.909811.
- [90] C. Qu, J. Hu, X. Liu, Z. Li, and Y. Ding, "Morphology and mechanical properties of polyimide films: The effects of UV irradiation on microscale surface," *Materials*, vol. 10, no. 11, pp. 1329, 2017, doi: 10.3390/ma10111329.
- [91] S. H. Ahn, J. Jeong, and S. J. Kim, "Emerging encapsulation technologies for long-term reliability of microfabricated implantable devices," *Micromachines*, vol. 10, no. 8, pp. 508, 2019, doi: 10.3390/mi10080508.
- [92] Y. Sun, S. Lacour, R. Brooks, N. Rushton, J. Fawcett and R. Cameron, "Assessment of the biocompatibility of photosensitive polyimide for implantable medical device use," *Journal of Biomedical Materials Research Part A*, vol. 90, no. 3, pp. 648-655, 2009.

- [93] E. S. Krames, P. Hunter Peckham, A. R. Rezai, and F. Aboelsaad, "What Is Neuromodulation?," in *Neuromodulation*, vol.1, Elsevier, 2009, pp. 3-8.
- [94] T. Goroszeniuk and D. Pang, "Peripheral neuromodulation: A review," *Neuromodulation: Technology at the Neural Interface*, vol. 18, no. 5, pp.486, 2014, doi: 10.1007/s11916-014-0412-9.
- [95] H. Fodstad and M. Hariz, "Electricity in the treatment of nervous system disease," *Operative Neuromodulation Acta Neurochirurgica Supplements*, vol. 97 PART 1, pp. 11-19, 2007, doi: 10.1007/978-3-211-33079-1_2.
- [96] J. M. A. E. Biemans and M. R. Van Balken, "Efficacy and effectiveness of percutaneous tibial nerve stimulation in the treatment of pelvic organ disorders: A systematic review," *Neuromodulation: Technology at the Neural Interface*, vol. 16, no. 1, pp. 25-34, 2013, doi: 10.1111/j.1525-1403.2012.00504. x.
- [97] O. Ekre, T. Eliasson, H. Norrsell, P. Währborg, and C. Mannheimer, "Long-term effects of spinal cord stimulation and coronary artery bypass grafting on quality of life and survival in the ESBY study," *European Heart Journal*, vol. 23, no. 24, pp. 1938- 1945, 2002, doi: 10.1053/euhj.2002.3286.
- [98] T. S. Meloy and J. P. Southern, "Neurally augmented sexual function in human females: A preliminary investigation," *Neuromodulation: Technology at the Neural Interface*, vol. 9, no. 1, pp. 34-40, 2006, doi: 10.1111/j.1525-1403.2006.00040. x.
- [99] Y. E. Mironer, J. K. Hutcheson, J. R. Satterthwaite, and P. C. LaTourette, "Prospective, two-part study of the interaction between spinal cord stimulation and peripheral nerve field stimulation in patients with low back pain: Development of a new spinal-peripheral neurostimulation method," *Neuromodulation: Technology at the Neural Interface*, vol. 14, no. 2, pp. 151-155, 2011, doi: 10.1111/j.1525-1403.2010.00316. x.
- [100] P. H. Peckham and J. S. Knutson, "Functional electrical stimulation for neuromuscular applications," *Annual Review of Biomedical Engineering*, vol. 7, pp. 327-360, 2005, doi: 10.1146/annurev.bioeng.6.040803.140103.
- [101] G. Kaur, R. Adhikari, P. Cass, M. Bown, and P. Gunatillake, "Electrically conductive polymers and composites for biomedical applications," *RSC Advances*, vol. 5, no. 47, pp. 37553- 37567, 2015, doi: 10.1039/c5ra01851j.
- [102] A. Ramanavičius, A. Ramanavičiene, and A. Malinauskas, "Electrochemical sensors based on conducting polymer-polypyrrole," *Electrochimica Acta*, vol. 51, no. 27, pp. 6025- 6037, 2006, doi: 10.1016/j.electacta.2005.11.052.
- [103] M. Gerard, A. Chaubey, and B. D. Malhotra, "Application of conducting polymers to biosensors," *Biosensors and Bioelectronics*, vol. 17, no. 5, pp. 345-359, 2002, doi: 10.1016/S0956-5663(01)00312-8.
- [104] R. Ravichandran, S. Sundarajan, J. R. Venugopal, S. Mukherjee, and S. Ramakrishna, "Applications of conducting polymers and their issues in biomedical engineering," *Journal of the Royal Society Interface*, vol. 7, no. SUPPL. 5, pp. 59-79, 2010, doi: 10.1098/rsif.2010.0120.focus.

- [105] D. D. Ateh, H. A. Navsaria, and P. Vadgama, "Polypyrrole-based conducting polymers and interactions with biological tissues," *Journal of the Royal Society Interface*, vol. 3, no. 11, pp. 741-752, 2006, doi: 10.1098/rsif.2006.0141.
- [106] A. Gelmi, M. J. Higgins, and G. G. Wallace, "Physical surface and electromechanical properties of doped polypyrrole biomaterials," *Biomaterials*, vol. 31, no. 8, pp. 1974-1983, 2010, doi: 10.1016/j.biomaterials.2009.11.040.
- [107] X. Cui, J. Wiler, M. Dzaman, R. A. Altschuler and D. C. Martin, "In Vivo Studies of Polypyrrole/Peptide Coated Neural Probes," *Biomaterials*, vol. 24, no. 5, pp. 777-787, 2003.
- [108] A. N. Koppes, A. L. Nordberg, G. M. Paolillo, N. M. Goodsell, H. A. Darwish, L. Zhang, and D. M. Thompson, "Electrical stimulation of schwann cells promotes sustained increases in neurite outgrowth," *Tissue Engineering Part A*, vol. 20, no. 3-4, pp. 1-13, 2014, doi: 10.1089/ten.tea.2013.0012.
- [109] X. Liu, Z. Yue, M. J. Higgins, and G. G. Wallace, "Conducting polymers with immobilised fibrillar collagen for enhanced neural interfacing," *Biomaterials*, vol. 32, no. 30, pp. 7309-7317, 2011, doi: 10.1016/j.biomaterials.2011.06.047.
- [110] R. L. Williams and P. J. Doherty, "A preliminary assessment of poly(pyrrole) in nerve guide studies," *Journal of Materials Science: Materials in Medicine*, vol. 5, no. 6-7, pp. 429-433, 1994, doi: 10.1007/BF00058978.
- [111] A. H. Do, P. T. Wang, C. E. King, A. Abiri, and Z. Nenadic, "Brain-computer interface controlled functional electrical stimulation system for ankle movement," *Journal of NeuroEngineering and Rehabilitation*, vol. 8, no. 1, pp. 49, 2011, doi: 10.1186/1743-0003-8-49.
- [112] B. J. Kim, S. G. Oh, M. G. Han, and S. S. Im, "Preparation of polyaniline nanoparticles in micellar solutions as polymerization medium," *Langmuir*, vol. 16, no. 14, pp. 5841-5845, 2000, doi: 10.1021/la9915320. (Personal communication with Dr. Mohammad Al-Sayah, AUS, 30, Oct, 2019).
- [113] D. W. Park, J. P. Ness, S. K. Brodnick, C. Esquibel, J. Novello, F. Atry, D.-H. Baek, H. Kim, J. Bong, K. I. Swanson, A. J. Suminski, K. J. Otto, R. Pashaie, J. C. Williams, and Z. Ma, "Electrical Neural Stimulation and Simultaneous in Vivo Monitoring with Transparent Graphene Electrode Arrays Implanted in GCaMP6f Mice," *ACS Nano*, vol. 12, no. 1, pp. 148-157, 2018, doi: 10.1021/acsnano.7b04321.
- [114] H. Lim and S. W. Hoag, "Plasticizer effects on physical-mechanical properties of solvent cast Soluplus® films," *AAPS PharmSciTech*, vol. 14, no. 3, pp. 903-910, 2013, doi: 10.1208/s12249-013-9971-z.
- [115] Z. Yu, Y. Xia, D. Du, and J. Ouyang, "PEDOT: PSS Films with Metallic Conductivity through a Treatment with Common Organic Solutions of Organic Salts and Their Application as a Transparent Electrode of Polymer Solar Cells," *ACS Applied Materials & Interfaces*, vol. 8, no. 18, pp. 11629-11638, 2016, doi: 10.1021/acsami.6b00317.
- [116] E. T. McAdams, J. Jossinet, R. Subramanian, and R. G. E. McCauley, "Characterization of gold electrodes in phosphate buffered saline solution by impedance and noise measurements for biological applications," *International*

Conference of the IEEE Engineering in Medicine and Biology Society, New York, NY, USA, 2006, pp. 4594-4597, doi: 10.1109/IEMBS.2006.260406.

- [117] S. Bauerdick, C. Burkhardt, D. P. Kern, and W. Nisch, "Substrate-integrated microelectrodes with improved charge transfer capacity by 30-dimensional micro-fabrication," *Biomedical Microdevices*, vol. 5, no. 2, pp. 93-99, 2003, doi: 10.1023/A:1024526626016.
- [118] L. Etemadi, M. Mohammed, P. T. Thorbergsson, J. Ekstrand, A. Friberg, M. Granmo, L. M. E. Pettersson, and J. Schouenborg, "Embedded ultrathin cluster electrodes for long-term recordings in deep brain centers," *PLoS One*, vol. 11, no. 5, pp.1-18, 2016, doi: 10.1371/journal.pone.0155109.
- [119] Y. Lu, Y. Li, J. Pan, P. Wei, N. Liu, B. Wu, J. Cheng, C. Lu, and L. Wang, "Poly(3,4-ethylenedioxythiophene)/poly(styrenesulfonate)-poly (vinyl alcohol)/poly (acrylic acid) interpenetrating polymer networks for improving optrode-neural tissue interface in optogenetics," *Biomaterials*, vol. 33, no. 2, pp. 378-394, 2012, doi: 10.1016/j.biomaterials.2011.09.083.
- [120] A. M. Cruz and N. Casañ-Pastor, "Graded conducting titanium-iridium oxide coatings for bioelectrodes in neural systems," *Thin Solid Films*, vol. 534, pp. 316-324, 2013, doi: 10.1016/j.tsf.2013.02.031.
- [121] A. R. Harris, S. J. Morgan, J. Chen, R. M. I. Kapsa, G. G. Wallace, and A. G. Paolini, "Conducting polymer coated neural recording electrodes," *Journal of Neural Engineering*, vol. 10, no. 1, pp. 016004, 2013, doi: 10.1088/1741-2560/10/1/016004.
- [122] K. A and L. A, "Mechanical Behaviour of Skin: A Review," *Journal of Material Science & Engineering*, vol. 5, no. 4, pp. 1-7, 2016, doi: 10.4172/2169-0022.1000254.
- [123] A. Hashim, B. Abbas, "Recent Review on Poly-methyl methacrylate (PMMA)-Polystyrene (PS) Blend Doped with Nanoparticles for Modern Applications," *Research Journal of Agriculture and Biological Sciences*, vol 14, no. 3, pp. 6-12, 2019, doi: 10.22587/rjabs.2019.14.3.2.

Appendix A: Detailed Results

A.1. PANI Samples EIS Results

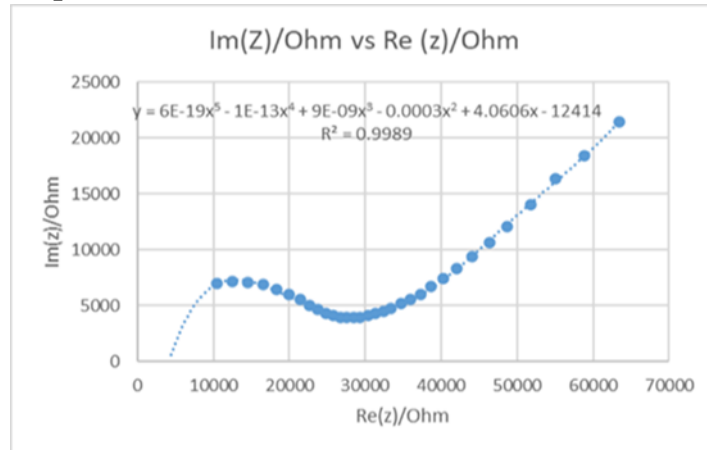


Figure A.1: EIS of a bioelectrode for sample 1 (intercept with the x-axis).

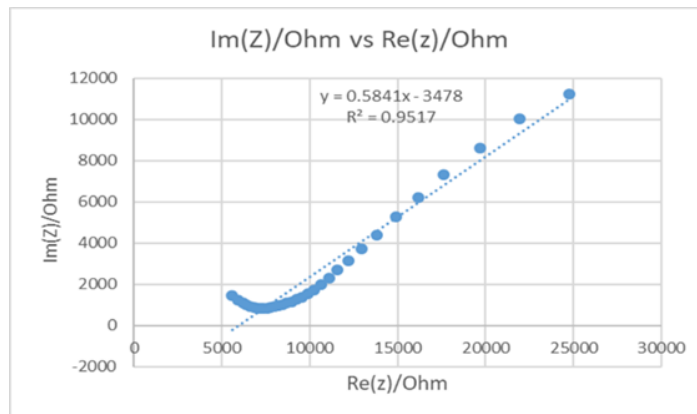


Figure A.2: Nyquist plot for sample 2.

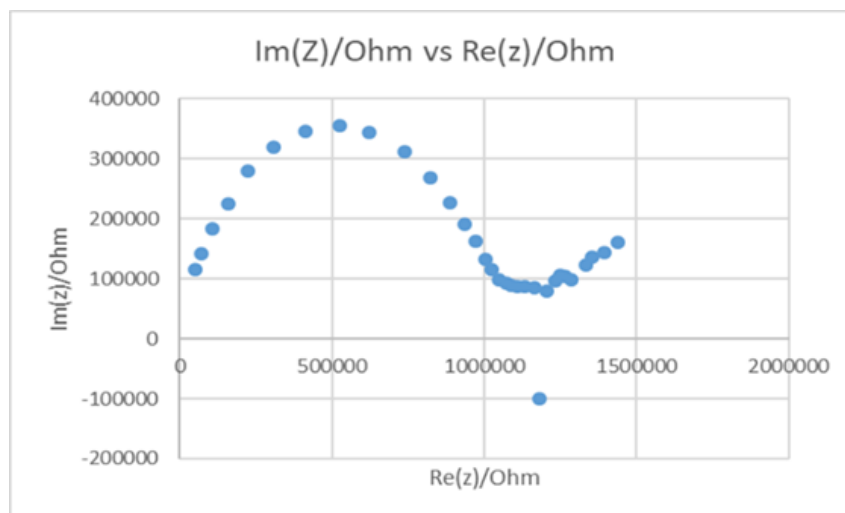


Figure A.3: Nyquist plot for sample 3.

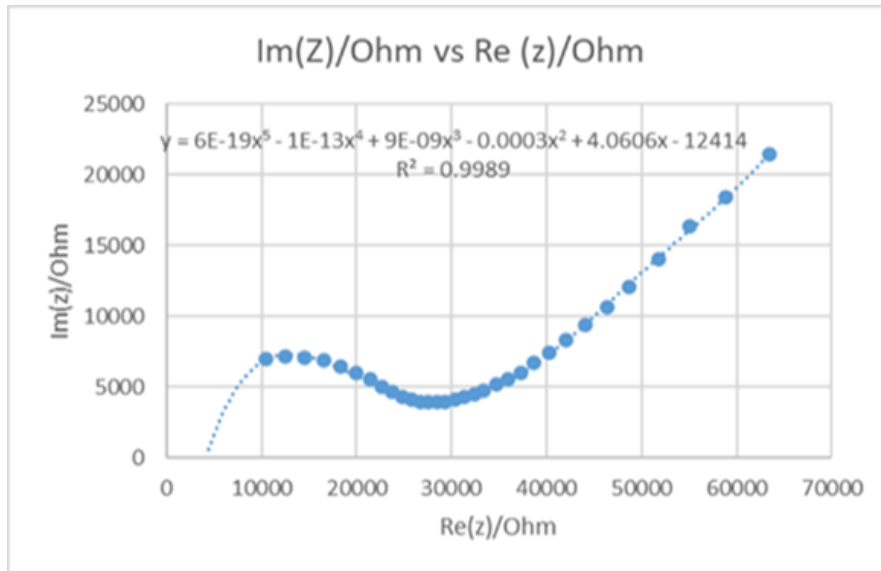


Figure A.4: Nyquist plot for sample 4.

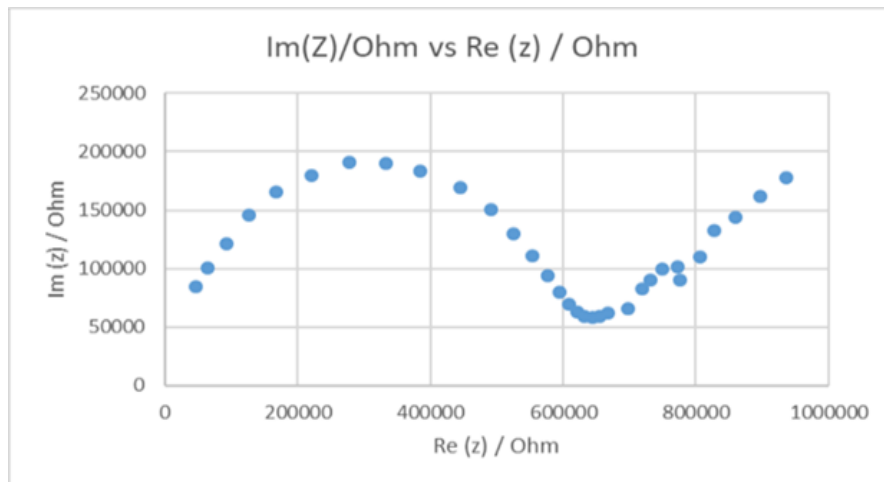


Figure A.5: Nyquist plot for sample 5.

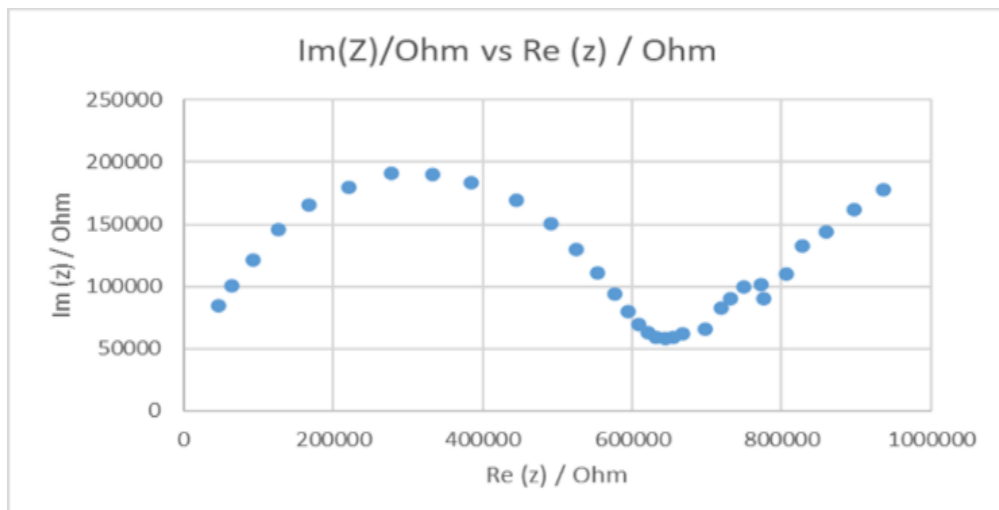


Figure A.6: Nyquist plot for sample 6.

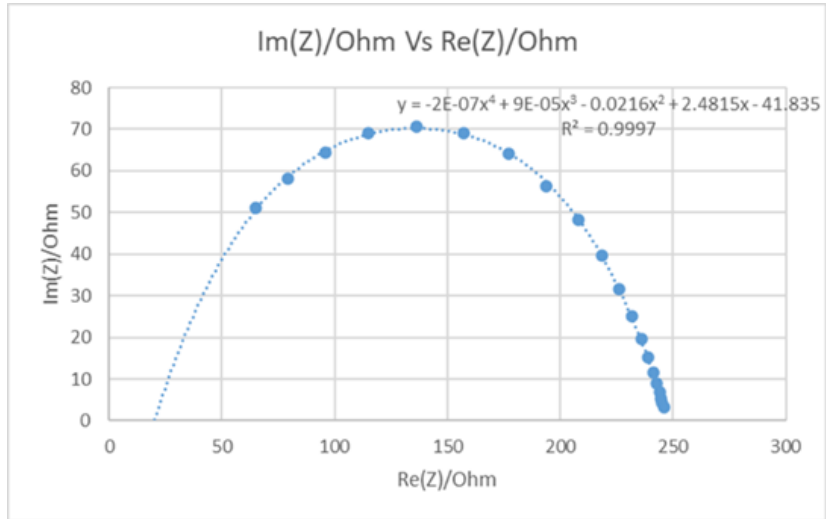


Figure A.7: Nyquist plot for sample 7.

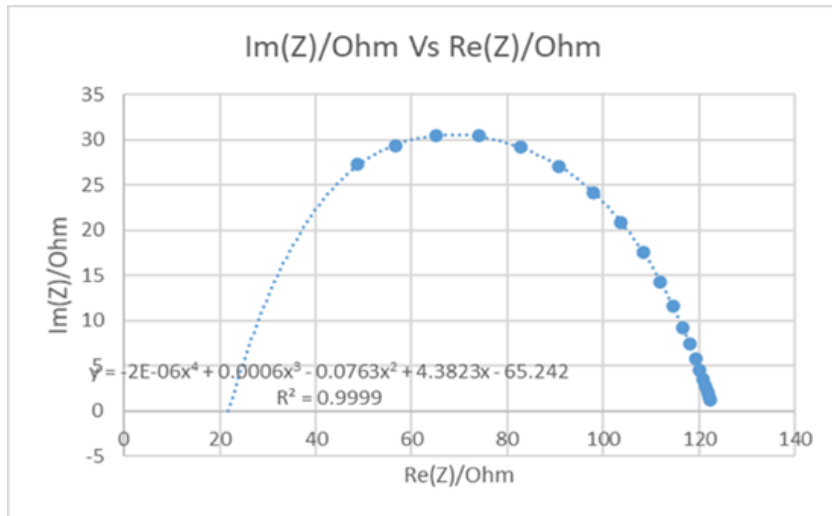


Figure A.8: Nyquist plot for sample 8.

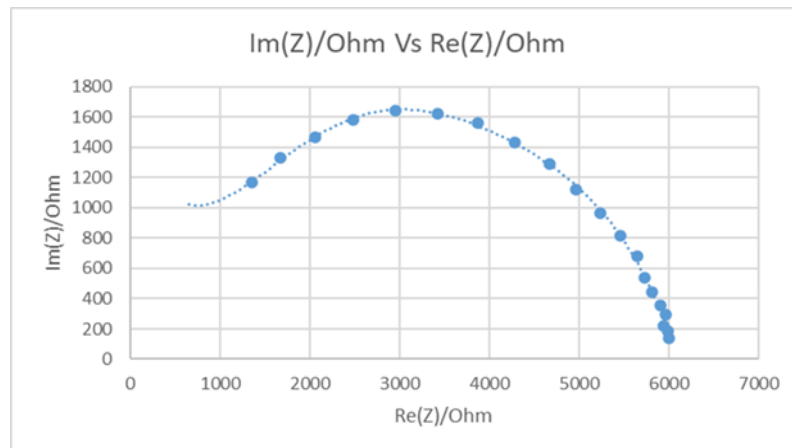


Figure A.9: Nyquist plot for sample. 9

Table A.1: Comparison between different prepared electrode samples.

Sample	PANI (%)	Silicone (%)	Glycerol (%)	PMMA (%)
Sample 1	30 %	50 %	20 %	--
Sample 2	20 %	50 %	30 %	--
Sample 3	10 %	60 %	30 %	--
Sample 4	27%	45%	18%	9%
Sample 5	18%	45%	27%	9%
Sample 6	9%	55%	27%	9%
Sample 7	15 %	70 %	15 %	--
Sample 8	20 %	50 %	30 %	--
Sample 9	6 %	72 %	22 %	--

Table A.2: Comparison of prepared samples with different ratios

Sample	PANI (%)	Silicone (%)	Glycerol (%)	PMMA (%)	Bulk Impedance (k Ω)	Impedance at 1kHz + References	Conductivity (S/cm)
Sample 1	30 %	50 %	20 %	--	4 k Ω	28.4 k Ω	8.33x10 ⁻⁸ S/cm
Sample 2	20 %	50 %	30 %	--	5.3 k Ω	8.74 k Ω	6.28x10 ⁻⁸ S/cm
Sample 3	10 %	60 %	30 %	--	5.01 x10 ⁻⁴ Ω	9.71 x10 ⁵ Ω	6.65x10 ⁻⁹ S/cm
Sample 4	27 %	45 %	19%	9%	4 k Ω	31.1 k Ω	8.33x10 ⁻⁸ S/cm
Sample 5	18 %	45%	28%	9%	5.3 k Ω	576 k Ω	6.28x10 ⁻⁸ S/cm
Sample 6	9%	54%	28%	9%	5.3 k Ω	5.76x10 ⁵ Ω	6.28x10 ⁻⁸ S/cm
Sample 7	15 %	70 %	15 %	--	25 Ω	79.1396 Ω	1.33x10 ⁻⁵ S/cm
Sample 8	20 %	50 %	30 %	--	22 Ω	56.5978 Ω	1.51x10 ⁻⁵ S/cm
Sample 9	6 %	72 %	22 %	--	600 Ω	1.6 k Ω	5.55x10 ⁻⁷ S/cm
Poly-aniline-coated foam electrodes	--	--	--	--	7 k Ω	1.45M Ω [3]	--

Table A.3: Change of bulk impedance in long-term samples pre/post CV test

Week	Bulk Impedance before CV (k Ω)	Bulk Impedance after CV (k Ω)	% Change
1	22 k Ω	20 k Ω	9.09%
2	3 k Ω	3 k Ω	0%
3	255 k Ω	400 k Ω	36.25%
4	12 k Ω	22 k Ω	45.45%
5	3.8 k Ω	3.9 k Ω	2.56%
6	37 k Ω	37 k Ω	0%
7	170 k Ω	150 k Ω	11.76%
8	28 k Ω	29 k Ω	3.44%

Table A.4: Change of impedance at 1 kHz in long-term samples pre/post CV test

Week	Impedance at 1 kHz before CV (k Ω)	Impedance at 1 kHz after CV (k Ω)	% Change
1	27.6 k Ω	24.8 k Ω	10.14%
2	3.6 k Ω	5 k Ω	28%
3	775 k Ω	864 k Ω	10.3%
4	3 k Ω	2 k Ω	33.33%
5	4.35 k Ω	3 k Ω	31.03%
6	52.9 k Ω	47.5 k Ω	10.2%
7	263 k Ω	350 k Ω	24.85%
8	36.4 k Ω	37.6 k Ω	3.19%

A.2. PANI Samples CV Results

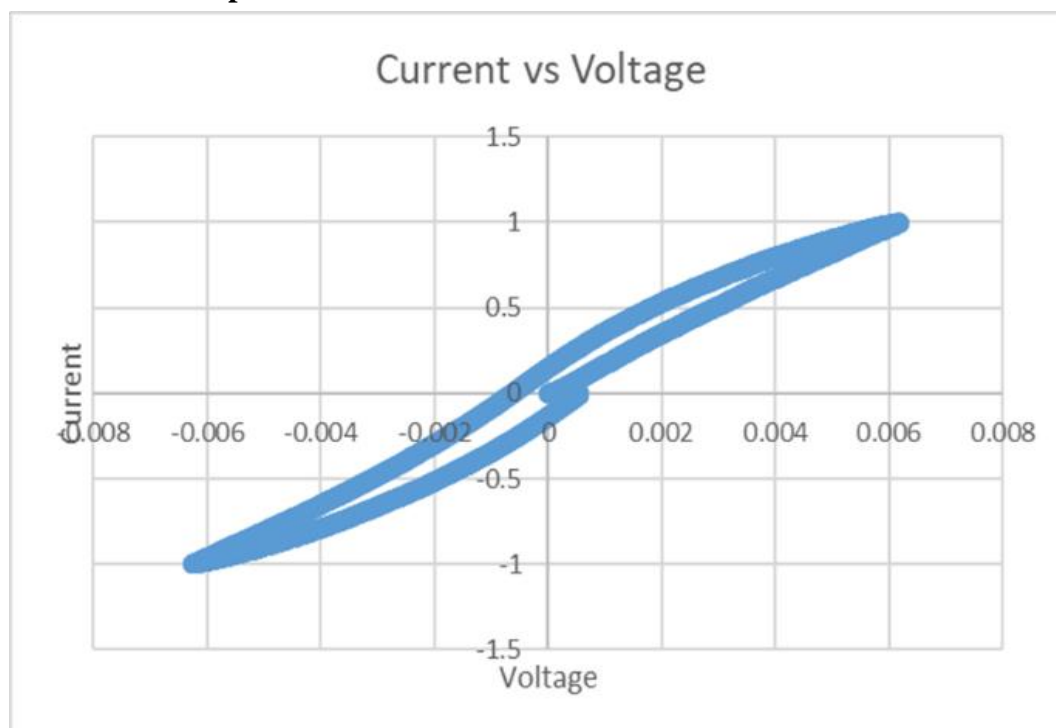


Figure A.10: Cyclic voltammetry test for the sample 1.

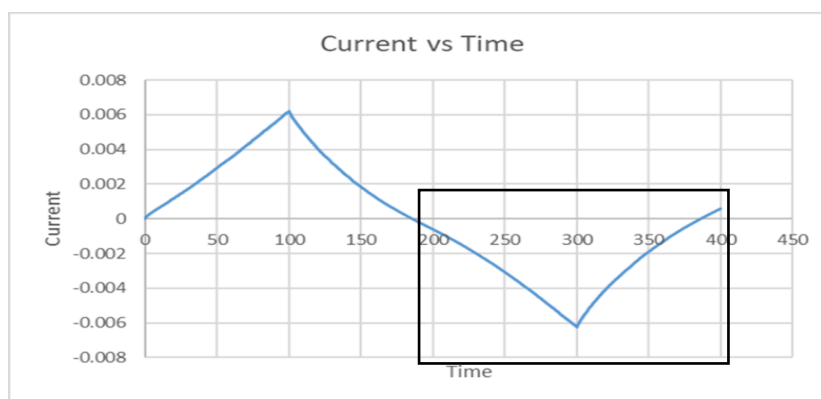


Figure A.11: The relationship between time and current.

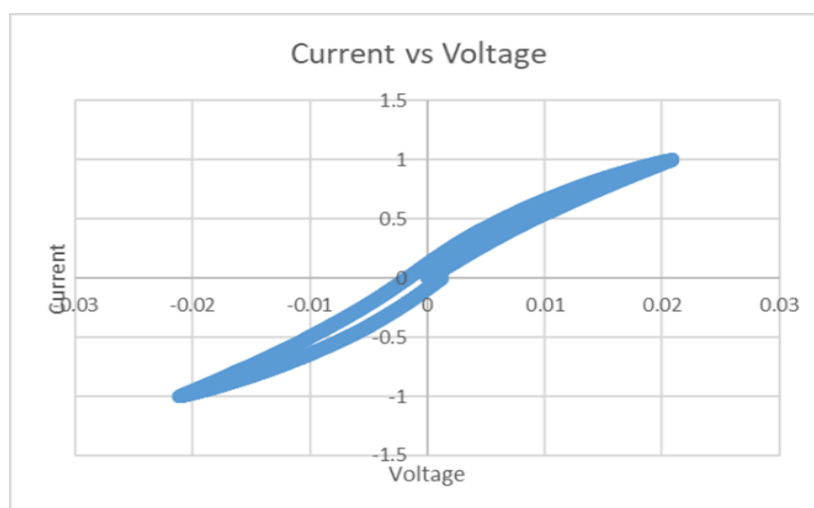


Figure A.12: Cyclic voltammetry test for the first sample 2.

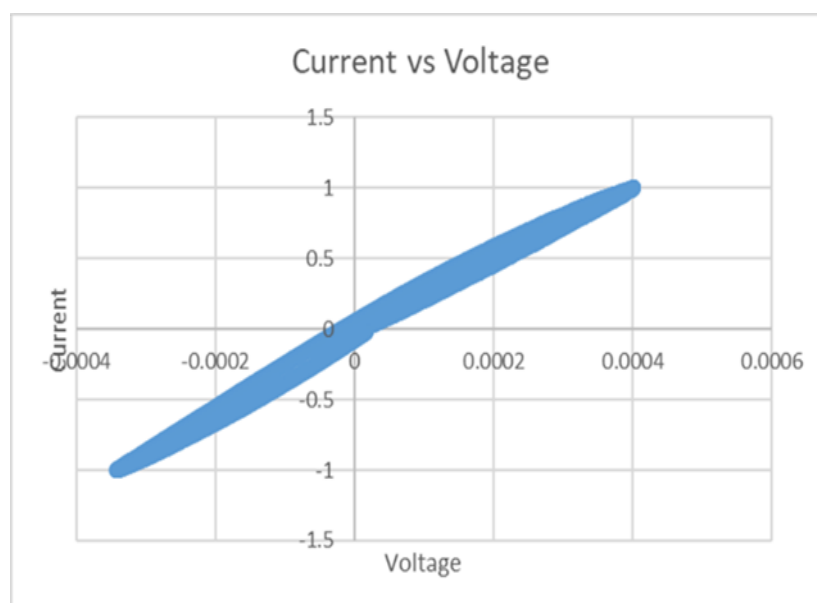


Figure A.13: Cyclic voltammetry test for the first sample 3.

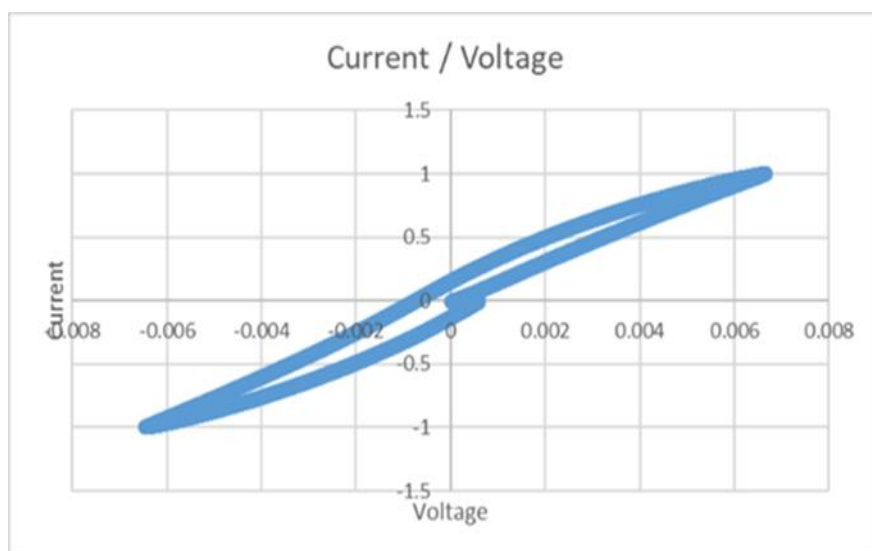


Figure A.14: Cyclic voltammetry test for sample 4.

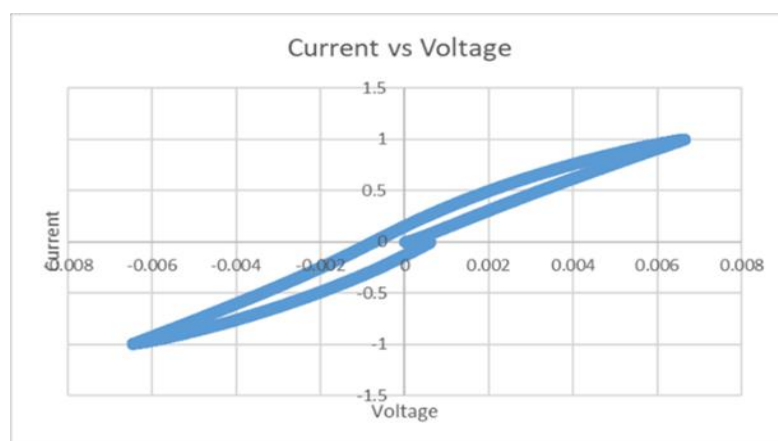


Figure A.15: Cyclic voltammetry test for sample 5.

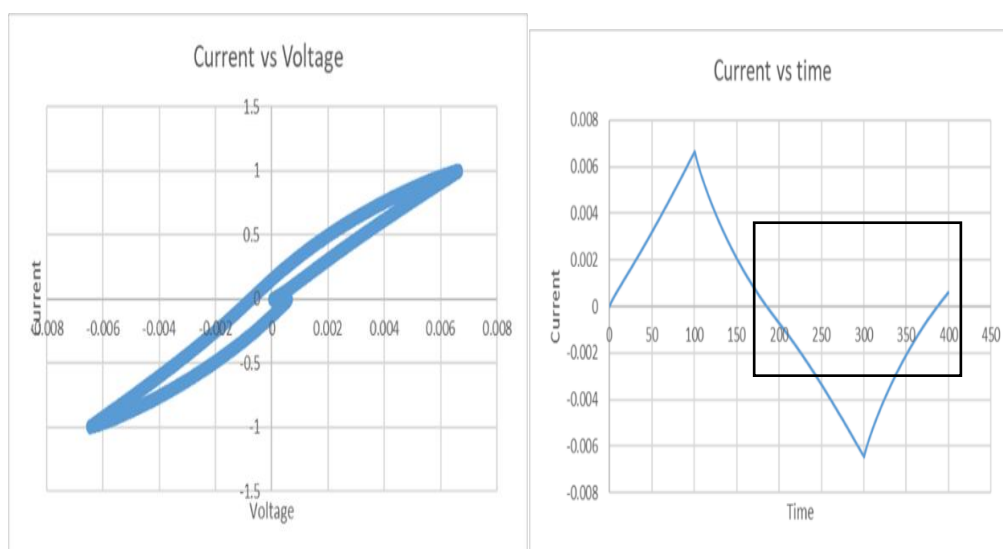


Figure A.16: Cyclic voltammetry test for sample 6.

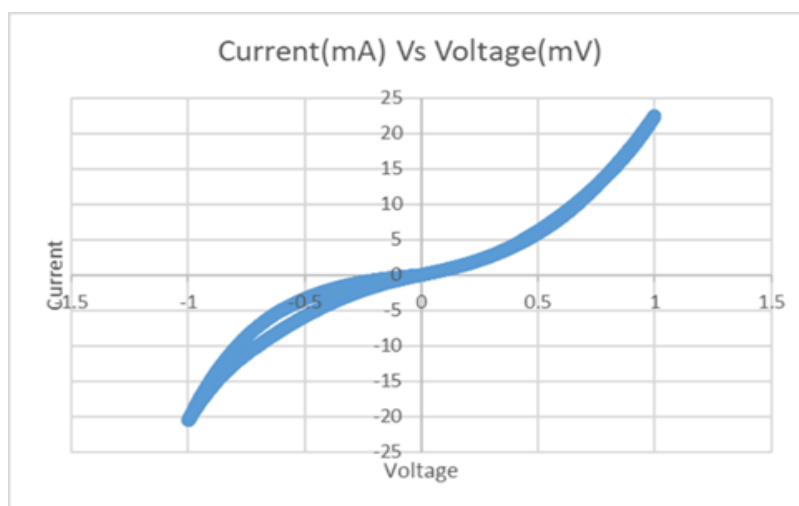


Figure A.17: Cyclic voltammetry test for sample 7.

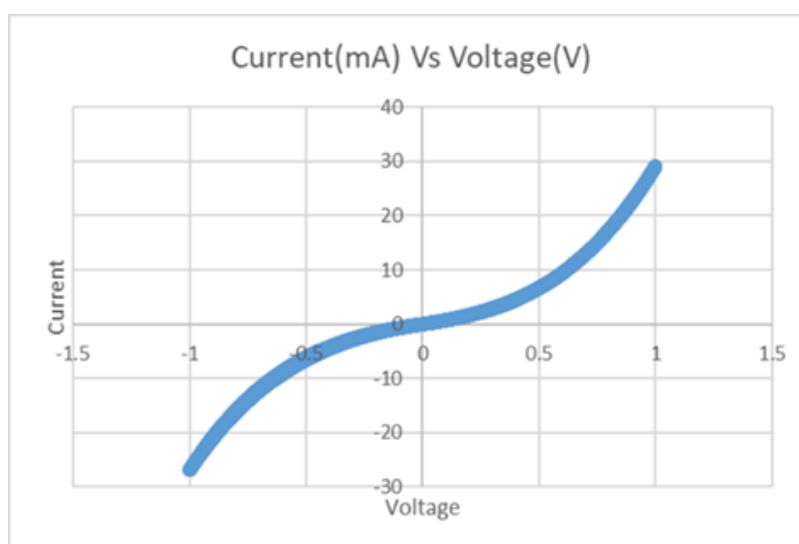


Figure A.18: Cyclic Voltammetry for sample 8.

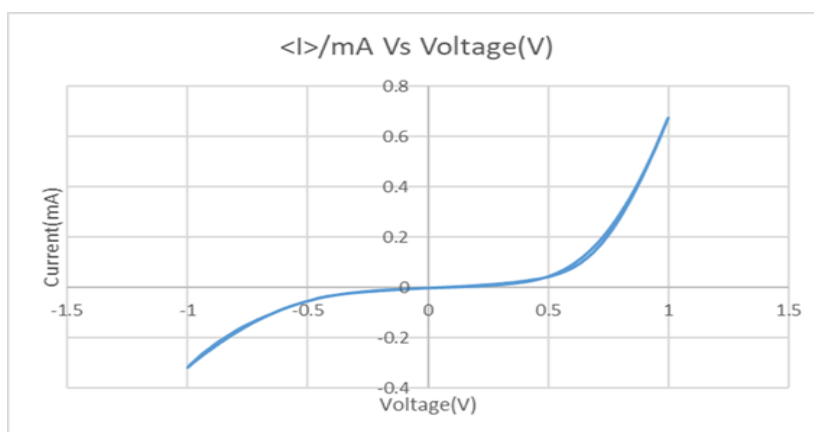


Figure A.19: Cyclic Voltammetry for sample 9.

Table A.5: A comparison table for charge density.

Composit e	PAN I (%)	Silicon e (%)	Glycero l (%)	PMM A (%)	Charge density	Referenc e
Sample 1	30 %	49.7 %	20 %	--	4.3124 C/ Cm2	--
Sample 2	20 %	49.6 %	30 %	--	14.4945 C/ Cm2	--
Sample 3	10 %	60 %	30 %	--	0.2575 C/ Cm2	--
Sample 4	27 %	45 %	19%	9%	4.3124 C/ Cm2	-
Sample 5	18%	45%	28%	9%	4.5927 C/ Cm2	-
Sample 6	9%	54%	28%	9%	4.5927 C/ Cm2	-
Sample 7	15 %	70 %	15 %	--	9.9113x10 3 C/ Cm2	-
Sample 8	20 %	50 %	30 %	--	1.3607x10 4 C/ Cm2	-
Sample 9	6 %	72 %	22 %	--	138.14 C/ Cm2	-
Graphene	--	--	--	--	1.42 × 10 ⁻⁹ C/Cm2	[9]
Poly- aniline	--	--	--	--	0.02 C/ Cm2	[10]

Table A.6: Change of charge storage capacity in long-term PANI based samples.

Week	Charge storage capacity (C/cm ²)
1	0.6696 C/cm ²
2	2.9222 C/cm ²
3	0.0968 C/cm ²
4	9.1325 C/cm ²
5	0.9969 C/cm ²
6	2.2490 C/cm ²
7	0.9234 C/cm ²
8	2.5546 C/cm ²

A.3. PANI Samples Mechanical Testing Results

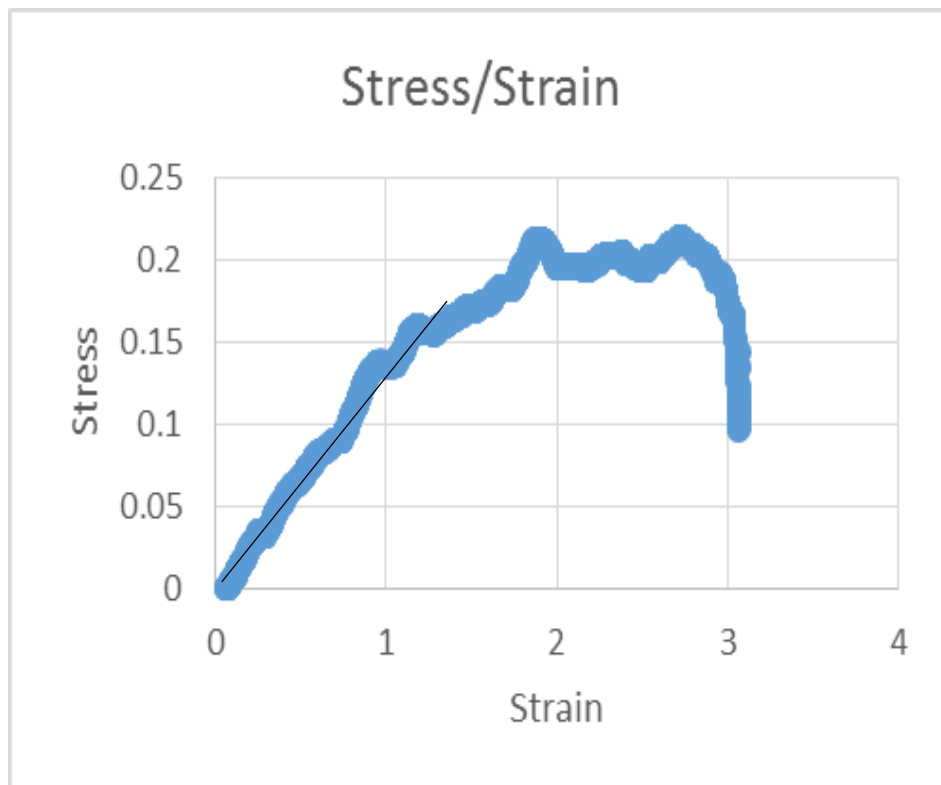


Figure A.20: Stress of the material VS strain of a bioelectrode sample 1.

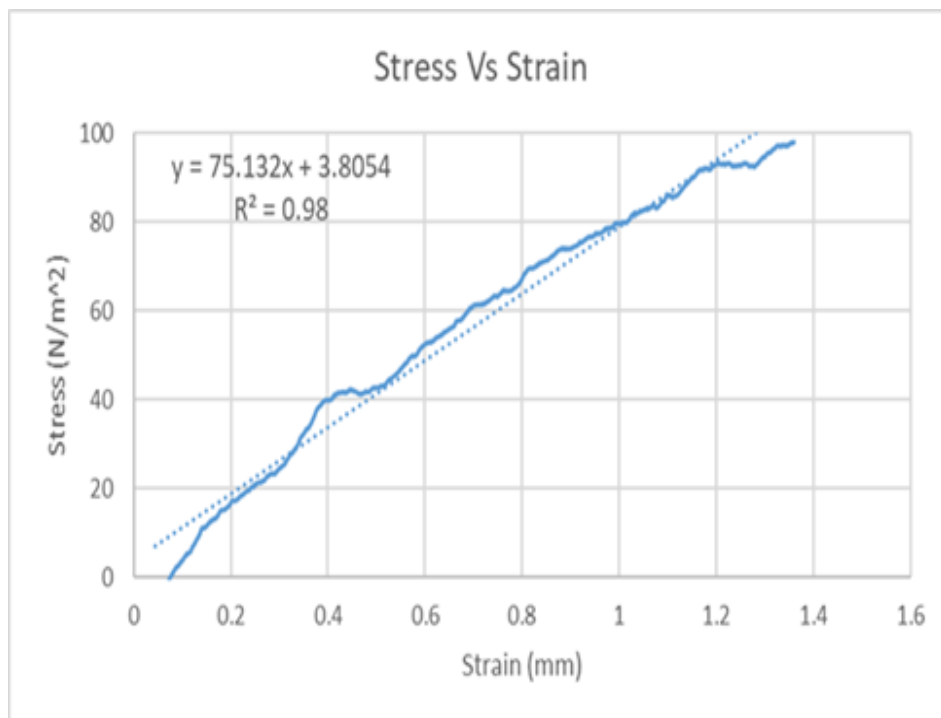


Figure A.21: Stress of the material VS strain of a bioelectrode sample contained for sample 9.

Table A.9: literature values for mechanical properties of conductive polymers.

Material	PANI (%)	Silicone (%)	Glycerol (%)	Young Modulus	Elongation
Sample 1	30 %	50 %	20 %	0.1468 MPa	306.9%
Sample 9	6 %	72 %	22 %	75.312 MPa	---
Skin tissue	--	--	--	83.33 ± 4.9 MPa [122]	--
PEDOT: PSS	--	--	--	1.8 ± 0.2 GPa	$4.3 \pm 2.3\%$
Polyimide	--	--	--	6000 MPa	<10%
Gold	--	--	--	69100 MPa	--
Platinum	--	--	--	1400 MPa	35%
Poly-aniline	--	--	--	N/A (Brittle material).	

A.4. Confidence interval test results

Sample Number	Impedance at 1kHz	Mean	Standard Deviation	95% Confidence
1	24985 Ω			
2	10117.3 Ω			
3	1272.87 Ω			
4	7844.93 Ω			
5	16517.5 Ω			
6	51052.3 Ω			
7	2373.35 Ω			
8	928.979 Ω			
9	1337.6 Ω			
10	1017.95 Ω			
11	2350.08 Ω			
12	1288.86 Ω			
13	6582.77 Ω			
14	390.95 Ω			
15	2519.48 Ω			
16	7787.22 Ω			
17	2715.73 Ω			
18	3476.15 Ω			
19	1685.51 Ω			
20	44340.2 Ω			

A.5. ECG Test Results

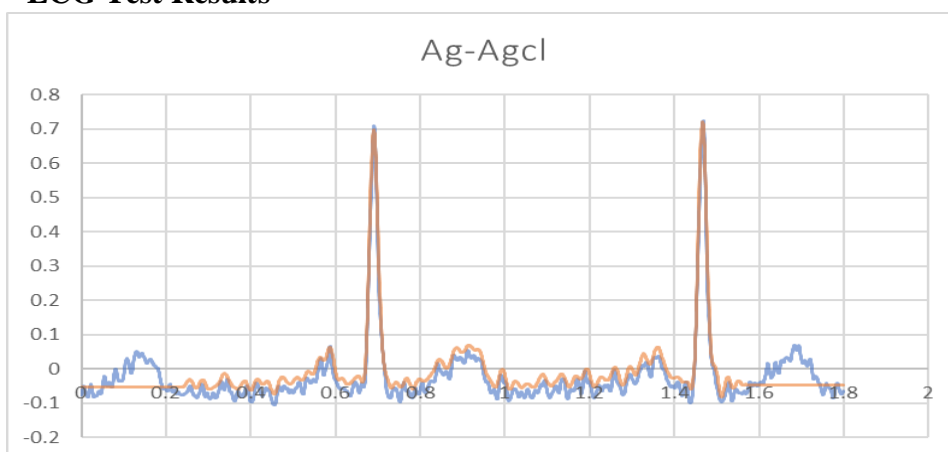


Figure A.22: ECG result using the standard Ag-AgCl Electrodes.

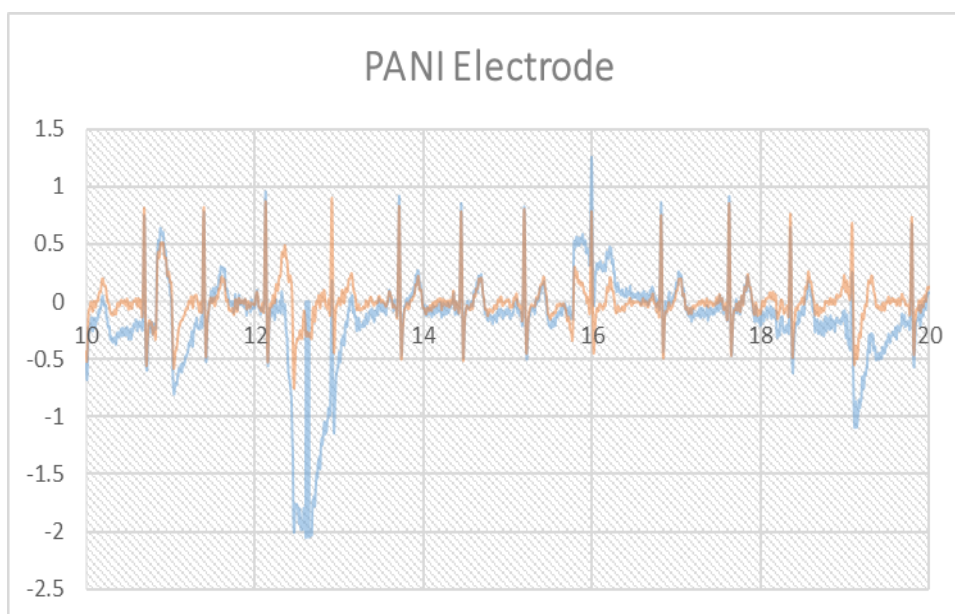


Figure A.23: ECG result using the fabricated Electrodes.

A.6. MATLAB code for calculating the Charge Storage Capacity (CSC)

```

clc;close all;clear all;
j=1;
y1Range='B2:B4001';
filename = 'Book1.xlsx';
ImA=xlsread(filename,y1Range);
i=ImA; %Saving the current from the imported data
x1Range='A2:A4001';
Time=xlsread(filename,x1Range);
t=Time; %Saving the time from the imported data

for z=1: numel(i)
i(z)=i(z)*0.785; %To divide the current by the area to find current density
end
for z=1: numel(i)
if i(z)<0 %To identify the negative (cathodal) current values

x(j)=Time(z); %Save their corresponding time in a new matrix
y(j)=i(z); %Save the values of current density in a new matrix
j=j+1;
end
end
c=abs(trapz(x,y)) %Using the function to calculate the area under the curve
c=c/0.1 %Dividing by the square root of the scanning rate

```

Figure A.24: MATLAB code for calculating CSC

Vita

Nader Almufleh was born in 1996, in Amman, Jordan. He received his primary and secondary education in Ajman, UAE. He received his B.Sc. degree in Biomedical Engineering from Ajman University in 2018.

In January 2019, he joined the Biomedical Engineering master's program at the American University of Sharjah as a graduate teaching assistant.